

POLITEHNICA UNIVERSITY TIMIȘOARA
Civil Engineering Faculty
Department of Steel Structures and Structural Mechanics

APPLICATION OF CORRUGATED WEB BEAMS FOR PEDESTRIAN STEEL BRIDGES

Author: Rem KIPARISOV, BSc(Eng)

Supervisor: Prof. dr. ing. Viorel UNGUREANU, Ph.D.



Universitatea Politehnica Timișoara, Romania

Study Program: SUSCOS_M

Academic year: 2014/2015

Table of contents

List of pictures	5
Acknowledgement	9
Members of the Jury	10
Abstract	11
1. Introduction to girders with corrugated webs	12
1.1. Girders with corrugated webs and application of the concept	12
1.2. Theoretical and experimental researches of the structures with corrugated webs	17
1.3. Manufacturing and materials.....	19
1.4. Advantages and disadvantages of the SIN-beam systems.....	19
2. Research works done in the Politehnica University of Timisoara.....	21
2.1. Introduction.....	21
2.2. The peculiarities of the new solution	21
3. Pedestrian bridges design.....	22
3.1. Conceptual design of a pedestrian bridge	22
3.2. Bridge accidents and breakdowns.....	26
4. Application of the SIN-beam for the pedestrian bridge	28
4.1. Introduction.....	28
4.2. Geometric conditions	30
4.3. Grade	32
4.4. Stairways	32
4.5. Loads.....	34
4.5.1. Introduction.....	34
4.5.2. Loads as Function of Deck Length.....	35
4.5.3. Asymmetric Loading	35
4.5.4. Wind Loads.....	36
4.6. Dynamics	37
4.6.1. Introduction.....	37
4.6.2. Pedestrian Traffic and Action.....	37

4.6.3.	Comfort Criteria and Limit Values	38
4.6.4.	Design Procedure	39
4.7.	Deck surfacing	44
4.8.	Railings	46
4.9.	Illumination	47
5.	Numerical simulations	49
5.1.	Introduction.....	49
5.2.	Simulations in SAP2000	49
5.2.1.	Introduction.....	49
5.2.2.	Axis criteria.....	51
5.2.3.	Materials.....	51
5.2.4.	Loads.....	51
5.2.5.	Load combinations.....	58
5.2.6.	Main beam with steel plates as a web.....	59
5.2.7.	Main beams with linear elements.....	62
5.2.8.	Truss main beams	63
5.3.	Simulations in ABAQUS	65
5.3.1.	Introduction.....	65
5.3.2.	Elements and assembly.....	65
5.3.3.	Materials.....	67
5.3.4.	Loads.....	67
5.3.5.	Interaction	68
5.3.6.	Mesh	70
5.3.7.	Restraints and boundary conditions.....	71
5.3.8.	Results of analysis	72
6.	3D Model of the bridge. Technical detailing.....	78
7.	Economic effect	87
8.	Conclusions	91
9.	References	92

ANNEX 1. The calculation of the steel plate thickness for the Plate model in SAP2000.....	99
ANNEX 2. Results of section design.....	101
ANNEX 3. Verification of the most loaded cross-section.....	106
ANNEX 4. The verification for the reversible serviceability.....	109

List of pictures

Figure 1. Girder with corrugated web (SIN-beam)	12
Figure 2. Possible configurations of the corrugated sheeting	12
Figure 3. Application of SIN-beams for industrial buildings.....	14
Figure 4. Application for the first 15 floor residential building with the seismicity of 9, Kazakhstan 2005 (The Medvedev–Sponheuer–Karnik scale)	15
Figure 5. Pedestrian bridge with curved SIN-beam and the span of 42 meters and width 2.25m, Almaty, Kazakhstan.....	15
Figure 6. Yahagigawa composite cable-stayed bridge with the span of 235 meters, Japan.....	16
Figure 7. Hangar made with using of corrugated sheets	16
Figure 8. Arch made from corrugated sheeting for a tunnel.....	16
Figure 9. The cold-forming production	19
Figure 10. Out-of-plane stiffness of the corrugated web.....	20
Figure 11. Zeman fully-automated SIN-beam production.	20
Figure 12. The diagram of the pedestrian bridges collapses through the history.	26
Figure 13. Distribution of the collapses in reference to the human on the deck during the collapse	27
Figure 14. The location of the Eiffel Bridge on the map of the city center of Timișoara.	29
Figure 15. Photographs of the Eiffel bridge.	30
Figure 16. Capacity of pedestrian walkway dependent on traffic type and pedestrian density	31
Figure 17. Chosen configuration of the pedestrian walkway.....	31
Figure 18. Existing stairs with poor accessibility for wheel chaired people and bicyclists.....	32
Figure 19. Combined stairs solution applied in Vancouver, Canada.....	33
Figure 20. Combined solution applied in Aachen, Belgium.....	33
Figure 21. Ramps on a bridge over a canal in Venice.....	34
Figure 22. Antisliding solutions for the ramps.	34

Figure 23. Live load (nominal) as a function of span length for spans of 0-200 m, service load.....	35
Figure 24. Proposed treatment of one-sided live loads.	36
Figure 25. Force coefficient $c_{fx,0}$ for bridges	37
Figure 26. Different types of pedestrian densities	38
Figure 27. Methods for calculating the maximum acceleration.	43
Figure 28. Fiber-glass panel cross-section.	45
Figure 29. Connection of the fiberglass panel to the structure.....	45
Figure 30. Construction of the safety barrier for a pedestrian bridge in Nurnberg, Germany.....	46
Figure 31. LED handrail illumination.....	47
Figure 32. Chosen lighting systems for the pedestrian bridge.	48
Figure 33. Plate model for SAP2000.....	49
Figure 34. Linear elements model for SAP2000.....	50
Figure 35. Truss model for SAP2000	50
Figure 36. The labelling of the axis in SAP models.....	51
Figure 37. Dead load D on the structure.....	52
Figure 38. Wind load W_x in X direction	52
Figure 39. Wind load W_y in Y direction	52
Figure 40. Wind load W_z in Z direction	53
Figure 41. Live load L_1 with 100% of the live load distributed along the secondary beams.....	53
Figure 42. Live load L_2 with asymmetric loading	53
Figure 43. Live load L_3 with asymmetric loading	54
Figure 44. Assigning of the actions on handrails - L_r	54
Figure 45. Definition of Mass Source for seismic analysis.....	55
Figure 46. Horizontal and vertical response spectrums for seismic loading	57
Figure 47. Load case data for seismic loading.....	57
Figure 48. The cross-section of the main beam with plate web.....	59
Figure 49. Deflection at the midspan in the shell structure (COMB1).....	60

Figure 50.	Results of modal analysis of the plate model.....	62
Figure 51.	The linear elements model	62
Figure 52.	Deflection at the midspan in linear elements model (COMB1) ...	63
Figure 53.	Deformed shape of the truss model under COMB1	64
Figure 54.	Trapezoidal sheets T50-250 – 0.7 mm	65
Figure 55.	C250x3mm cold-formed profiles as flanges	66
Figure 56.	Shear plates and V-shape intermediate connecting profile	66
Figure 57.	Supporting and I-shape intermediate connecting profiles.....	66
Figure 58.	Main views of the CWB.....	66
Figure 59.	Load application scheme.....	67
Figure 60.	Detailed scheme of the connections at the support.....	68
Figure 61.	Detailed scheme of the connections at the midspan of the CWB	69
Figure 62.	Force-displacement curves for the tested connections	70
Figure 63.	Mesh for the CWB.....	70
Figure 64.	Restraints.....	71
Figure 65.	The Anti-LTB boundary condition	71
Figure 66.	Von Mises stress distribution at the support.....	72
Figure 67.	Von Mises stress distribution of the beam	72
Figure 68.	Von Mises stress distribution at the midspan	73
Figure 69.	Von Mises stress distribution at the support.....	73
Figure 70.	Local plasticity	74
Figure 71.	Force-displacement curve for CWB.....	74
Figure 72.	Stress distribution in corrugated webs and flanges	75
Figure 73.	Stress distribution in shear plates	76
Figure 74.	Deformed shape of the beam end shear panel and distortion of the web corrugation (Model and results of tests).....	77
Figure 75.	Main views of the CWB pedestrian bridge.....	78
Figure 76.	Overview of the pedestrian CWB bridge without decking	79
Figure 77.	Cross-section of the deck	79
Figure 78.	Transversal bracing system	80

Figure 79.	Longitudinal bracing system	80
Figure 80.	Connection of the main and secondary beams in assembly with bracings	81
Figure 81.	Cross-section of the midspan connection	81
Figure 82.	Connection of the bracings to the top flange	82
Figure 83.	Connection of the transversal bracing element and bottom flange	82
Figure 84.	Connection of the secondary beam to the top flange at the support	83
Figure 85.	Connection of the bottom flanges at the midspan.....	84
Figure 86.	Connection of the top flanges at the midspan	85
Figure 87.	Handrail connection to the secondary beams and safety barriers	86
Figure 88.	The comparison in steel consumption	87
Figure 89.	Comparison of the costs for materials depending on a type of bridge	88
Figure 90.	Economical comparison of CWB and truss beams with the prices indicated in Euro	89
Figure 91.	Geometrical characteristics for the flange.....	99

Acknowledgement

This dissertation work would not been possible without the support of many people. I am deeply indebted to my supervisor, Prof. dr. ing. Viorel UNGUREANU, for his guidance, encouragement and support throughout this research work.

My sincere thanks to Prof. dr. ing. František WALD, Prof. dr. ing. Dan DUBINA, Prof. dr. ing. Luís Simões da Silva, Prof. dr. ing. Jean-Pierre JASPART, Prof. dr. ing. Raffaele Landolfo and Prof. dr. ing. Milan Veljkovic as coordinators of our SUSCOS_M European Erasmus Mundus Master program (Sustainable Constructions under natural hazards and catastrophic events 520121-1-2011-1-CZ-ERA MUNDUS-EMMC), for organizing this excellent master degree program and for their assistance and guidance in Liege and Timisoara. Without their help, this program would not have been possible.

I would like to take this opportunity to express my profound gratitude to my mother, Neonika and my girlfriend Ioana Dicu, for their moral support, patience, advising and motivation during my studies within this master degree program and especially in the beginning, in Liege.

Finally, I would like to acknowledge the European Union, namely the Consortium Grant, as without this funding I would not have the opportunity to participate in this master degree course and meet the above-mentioned excellent people. I would like to express my apologies that I could not mention each one personally, who was involved in the successful elaboration of this thesis.

Members of the Jury

President: **Prof. dr. ing. Dan DUBINA, Ph.D.**
 C. M. of the Romanian Academy

Politehnica University Timișoara Str. Ion Curea, Nr. 1
300224, Timisoara – Romania

Members: **Assoc. Prof. dr. ing. Adrian CIUTINA, Ph.D.**

Politehnica University Timișoara Str. Ion Curea, Nr. 1
300224, Timisoara – Romania

Prof. dr. ing. Viorel UNGUREANU, Ph.D.
(Thesis Supervisor)

Politehnica University Timișoara Str. Ion Curea, Nr. 1
300224, Timisoara – Romania

Prof. dr. ing. Raul ZAHARIA, Ph.D.

Politehnica University Timișoara Str. Ion Curea, Nr. 1
300224, Timisoara – Romania

Secretary: **Assoc. Prof. Adrian DOGARIU, Ph.D.**

Politehnica University Timișoara Str. Ion Curea, Nr. 1
300224, Timisoara – Romania

Abstract

Modern civilization is using more and more complex structures, ensuring durability and reliability with the high efficiency as a paramount importance. Design of such structures should be primarily based on modern methods of calculation, satisfying all the requirements.

Corrugated web girders represent a relatively new structural system emerged in the past two decades especially in Germany and Austria, used in a large number of applications. Increased interest of this solution was observed for the main frames of single-storey steel buildings and in steel bridges.

The main benefits of this type of beams are that the corrugated webs increase the beam's stability against buckling, which may result in a very economical design via the reduction of web stiffeners. Due to improvements of the automatic fabrication process, corrugated webs up to 6 mm thickness became possible. Furthermore, the use of thinner webs results in lower material cost, with an estimated cost savings of 10-30% in comparison with conventional fabricated sections and more than 30% compared with standard hot-rolled beams. The buckling resistance of used sinusoidal corrugated sheet used for webs is comparable with plane webs of 12 mm thickness or more.

In the existing solutions the flanges are flat plates, welded to the sinusoidal web sheet, requiring a specific welding technology and highly automated manufacturing process. The flanges mainly provide flexural strength to the beam with low contribution from the corrugated web, which provides the shear capacity. Failure of the web occurs by steel yielding or web buckling. Lateral-torsional buckling of the girder and local flange buckling, separately or in interaction, represents other possible failure modes.

In this work, I tried to highlight the importance of the widening of the corrugated web beams concept that has significant advantages in front of the welded profiles and trusses. A new technological solution of such a system, composed by webs made of trapezoidal cold-formed steel sheets and flanges of built-up back-to-back lipped channels steel members have been used for the main beams of a pedestrian bridge. The connections between flanges and web are made with self-drilling screws. It is easy to be observed that the new solution, as a whole, is 100% composed by cold-formed steel elements, avoiding the combination of two types of products, i.e. cold-formed for webs and hot-rolled for flanges. High protection to corrosion due to the fact that all components are galvanized is a major advantage.

1. Introduction to girders with corrugated webs

1.1. Girders with corrugated webs and application of the concept

Girder with corrugated web (SIN-beam) – is a construction that includes flanges with arbitrary profiles and thin-walled web, which is laterally bent (corrugated). The webs of the girders can be corrugated into different ways. Figure 1 shows the most popular types of profiles: arc-and-tangent-type (sinusoidal type), trapezoidal-type and triangle-type. Possible configurations of the profiles are presented at the Figure 2.

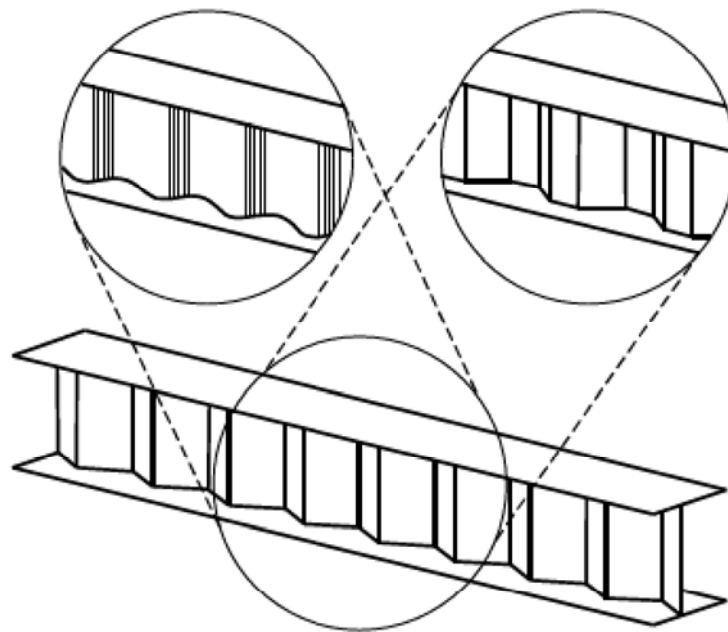


Figure 1. Girder with corrugated web (SIN-beam)

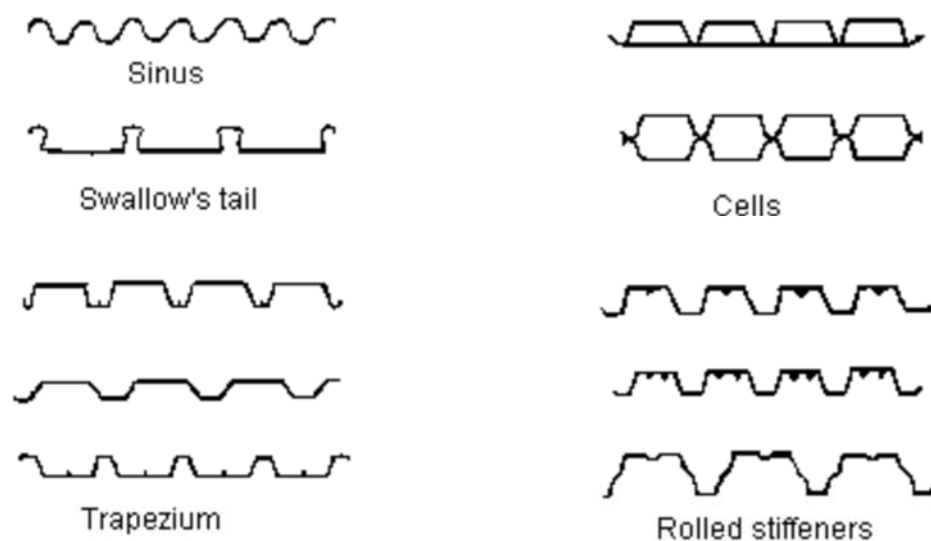


Figure 2. Possible configurations of the corrugated sheeting

The choice of the type is dictated by the application, mechanical behavior of the section, fabrication and economical aspects. Aesthetic view is also a very important factor that should be taken into account while choosing the configuration of the Elements.

Corrugated plates nowadays as load-bearing structural elements are widely used in construction sphere (columns, arches, beams and girders, girth rails, span superstructures with corrugated girders for bridge construction), in shipbuilding (corrugated bulkheads, corrugated body panels, hatches with a corrugated cover), in the aircraft industry (corrugated wall of aircraft wing spar).

One of the first constructions with corrugated web was a bulkhead with rectangular corrugations made for Russian battleships type “Borodino” in the year of 1901. The edges of the flutes were connected by two rows of rivets with overlapping. Tests under water pressure shown sufficient strength and rigidity and 20% material economy of the concept.

For the beginning of the XXth century there were a lot of application attempts concerning using corrugated plates for tankers. The ease of surface cleaning was the most important task. The material economy these days was defined as a minor factor. The need to perform riveted connections caused considerable technical difficulties in manufacturing. That apparently explains the small amount of application.

In the period of 1920-1930 the welding becomes more widespread and the amount started to grow. The shipbuilding industry is still the major consumer.

Soon, the application was applied in the sphere of aeronautics. A.F. Fraiser published a work, where the advantage of the corrugated plates over plane webs for the plane wing was proved.

The widespread of the concept was observed in the 80s with the construction of a variety of the bridges: Cognac Bridge (1986), Val de Maupre Viaduct (1987) and Parc Asterix Bridge (1989). Corrugated sheeting was used with the concrete chords. In 90s, the trend was kept at the high level.

Starting from 1996 fundamental research works and experiments of R. Hamilton, M. Elgaaly and A. Seshadri concerning the corrugated web beams as a structural element the school of SIN-beams obtained solid knowledge in

questions of stability, shear capacity and as a result – recommendations for design.

Nowadays with the availability of the modern technical approaches and powerful FEM-systems, application is even more flexible. Some examples are presented on Figures 3-8.



Figure 3. Application of SIN-beams for industrial buildings



Figure 4. Application for the first 15 floor residential building with the seismicity of 9, Kazakhstan 2005 (The Medvedev–Sponheuer–Karnik scale)



Figure 5. Pedestrian bridge with curved SIN-beam and the span of 42 meters and width 2.25m, Almaty, Kazakhstan





Figure 6. Yahagigawa composite cable-stayed bridge with the span of 235 meters, Japan



Figure 7. Hangar made with using of corrugated sheets



Figure 8. Arch made from corrugated sheeting for a tunnel

1.2. Theoretical and experimental researches of the structures with corrugated webs

At the first time the concept of corrugated sheeting application for beams appeared in the research works related to aerospace domain.

The NASA engineer Fraiser A. in 1956 published the work, dedicated to practical determination of multi-web beams with corrugated webs strength. This approach models the wing of the plane. Author finds out that this construction has a significant strength over the traditional at that time classic plane wings with multiple flat partitions. Fraiser predicts the wide usage of such construction in future not only in aeronautics, but in other domains as well, instead of beams with flat webs.

Similar research work had been done in the United Kingdom. In 1963, McKenzie K.I. in the article presented the results of theoretical determination of the corrugated web stiffness and the relationship between geometry and stiffness.

Up to 1990-s the concept of corrugated webs was continuously connected to aircraft construction. Theoretical researches of the CWB started to gain speed after implementation of CWB in some bridges.

D. Smith tested in 1992 two types of CWB and considered that from the point of view of the shear strength, interrupted weld for web is not acceptable for the concept.

R. Hamilton in 1993 put into practice 42 tests on 21 types of CWB and concluded, that within the web with high step loses its stability faster. In the work of Elgaaly M., Hamilton R.W., Seshadri A. in 1996 the formulas for the critical tangent stresses for local and global loss of stability were published. Formulae for the local loss of stability was obtained as a result of considering the corrugated web as a plate with constant thickness. The results of calculations were very close to the observed behavior of the tested beams.

In the work of Elgaaly M., Seshadri A., Hamilton R.W. "Bending Strength of Steel Beams with Corrugated Webs" in 1997 after the full-scale tests of beams the results were compared with FEM results. It was concluded, that the corrugated web almost does not participate in bending and for practical calculations it can be neglected.

The optimal geometrical parameters for corrugated webs were offered in works of Zhang W., Zhou Q., Li Y., Cai Z., Wedera in 1998.

Rem Kiparisov, Master Thesis

In 2000 Elgaaly M., Sheshadri A., Rodriquez R., Ibrahim S. published the article “Bridge girders with corrugated webs” with the results of cycle loading of CWB.

In the year of 2003, Wang X. in his PhD dissertation “Behavior of Steel Members with Trapezoidally Corrugated Webs and Tubular Flanges under Static Loading” studied beams with flanges made from tubular profiles and trapezoidal webs describing the behavior of the beams under shear and bending loading and stability aspects.

Dissertation of Abbas H.H. in 2003 is dedicated to high steel grade CWB for bridge construction. The aspects of cycle loading, local and global instability are highlighted, the practical advises for CWB calculations were given.

The “accordion effect” of the corrugated web, when the normal stresses in the web are propagated at the short distance from the flanges and come to naught very fast, was studied in the work “Simulation of accordion effect in corrugated steel web with concrete flanges” of Huang L., Hikosaka H. and Komine K. in 2004. The simulation in FEM software was presented.

The cyclic durability of the CWB beams was the result of the research made by Ibrahim S.A., El-Dakhakhni W.W. and Elgaaly M. in 2006. The corrugated web had an edge on plate webs of about 49-78%.

Abbas H.H., Sause R. and Driver R.G. in 2006 in the work “Behavior of Corrugated Web I-Girders under In-Plane Loads” came to the conclusion, that because of the displacement of the corrugated web from the central axis in the cross-section flexure-torsion stresses appear. The calculation method is presented in the paper.

1.3. Manufacturing and materials

The cold-formed steel member can be manufactured using the roll forming technology (Figure 9).

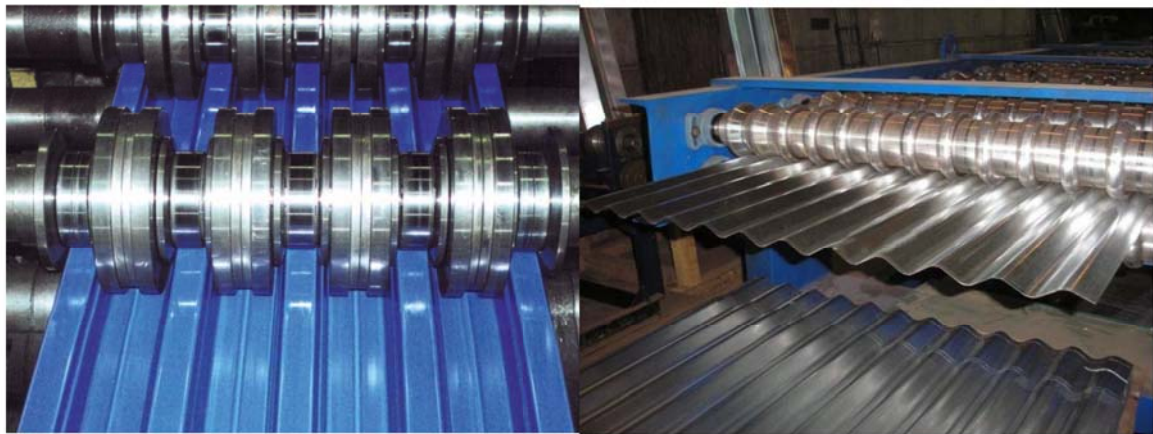


Figure 9. The cold-forming production

Cold forming has the effect of increasing the yield strength of steel, the increase being the consequence of cold working well into the strain-hardening range. These increases are predominant in zones where the metal is bent by folding. The effect of cold working is thus to enhance the mean yield stress by 15% - 30%. For purposes of design, the yield stress may be regarded as having been enhanced by a minimum of 15%. The mechanical properties are dependent on the rolling direction so that yield strength is higher transversally to the rolling direction.

The most common material is structural steel. For corrosion protection, the corrugated webs can be treated with:

- Metal coating (Zink or Aluminum-Zink hot-dip galvanization)
- and/or Paint coating.

1.4. Advantages and disadvantages of the SIN-beam systems

In the construction of engineering structures, industrial and transport facilities the concept of SIN-beams takes a well-deserved place due to its significant advantages.

- Lower dead load of the structure;
- Possibility to use thinner webs results in saving of 10–30% in comparison with conventional fabricated sections and more than 30% compared with standard hot-rolled beams;
- Plate girder with trapezoidal corrugated web has a higher load carrying capacity, compared with plate girders with stiffened flat web. The capacity is higher with the smaller corrugation wave length;

- Decrease of necessary transverse and longitudinal stiffeners, because of the high out-of-plane stiffness of the web (Figure 10) leads to the economy of the material;



Figure 10. Out-of-plane stiffness of the corrugated web

- Once we use corrosion protection (galvanization and/or painting), the construction have high corrosion resistance;
- High automation of the production process is possible due to using robots;
- Improved buckling behavior;
- Reduced cost of erection due to high resistance against bending about the weak axis, none of the auxiliary lifting equipment normally needed is required.

Among the disadvantages, we can highlight:

- Lack of available software that can help with the calculation;
- The manufacturing process needs complicated equipment with precise settings (for example, robots for welding);



Figure 11. Zeman fully-automated SIN-beam production.

- Combination of hot-rolled and cold-formed profiles causes sometimes difficulties.

2. Research works done in the Politehnica University of Timisoara

2.1. Introduction

In the solutions developed previously, the flanges were flat plates welded to the sinusoidal web sheet, which required a specific welding technology. It is the flanges that are mainly responsible for the flexural strength of the beam, with only a low contribution from the corrugated web, which provides the shear capacity. Failure of the web occurs by steel yielding or web buckling. Lateral-torsional buckling of the girder and local flange buckling represent other possible failure modes.

The experimental and numerical investigations carried out at the CEMSIG Research Centre (<http://cemsig.ct.upt.ro>), Politehnica University of Timisoara evaluate and validate a new technological solution – SIN-beams fully made from cold-formed profiles (for the details see references 12 and 29).

2.2. The peculiarities of the new solution

The main difference that is applied is a usage of the cold-formed profiles without combinations with hot-rolled products for flanges. That provides all the advantages of the traditional SIN-beams, but gives more flexibility in the production process. Thus, bolts, screws or spot welds can be used for the flange-to-web connection providing a reduction of the manufacturing costs.

Variations in connections arrangement and types of fasteners make it possible to optimize the structure according to the distribution of stresses, reduce the material consumption in the zones of low stresses, and improve the behavior of corrugated web beam in the critical zones that work in shear bending increasing the capacity of the structure.

3. Pedestrian bridges design

3.1. Conceptual design of a pedestrian bridge

Footbridges are walked upon, touched and looked at by the slow moving pedestrian. This means that they are more directly experienced than road and railroad bridges, a fact that certainly influences their design as a whole and even more so in detail. They must be on a human scale.

In comparison to road bridges (and, largely, railroad bridges), which must usually connect two points in the most direct way; footbridges offer a multitude of possibilities to escape this one-dimensionality. Pedestrian 'desire lines' can be reflected in the design and heavily influence the layout of the bridge. Movable bridges, curved and cable supported decks or the intersection of several decks can generate a spatial experience.

Contrary to road and railway bridges, in footbridge design location, length and elevation of the bridge are not usually given parameters. The designer should instead carefully investigate them. Furthermore, bridges can prevent or foster future urban or environmental developments by the way they are inserted in existing surroundings. Concerning such aspects, the contribution of architects can be very helpful.

Footbridges therefore offer the designer a wide variety of design choices. This freedom is due to the following characteristics of footbridges:

- In plan, the deck shape can be formed more freely and with stronger curvature than the deck of road bridges. The deck of a footbridge is also narrow. A width of 3 to 4 m is usually sufficient.
- There are fewer restrictions to the deck inclination (relative to highway/railway bridges), which permits unusual structural types such as stress-ribbons or arches that can be walked upon.
- Besides the usual spectrum of asphalt and concrete surfacing, wood, steel, plastics, aluminum or even glass can sometimes be used as pavement.
- The shape and the materials for railings can be chosen more freely.
- The footbridge can be treated differently concerning loading. Even if local codes specify high live loads, deformations are not usually as limited as they are for bridges that support fast moving vehicles. This allows the design of a much more slender and elegant structure. However, slenderness leads to liveliness and dynamics must be considered.

- New materials and structural types may be easily introduced in footbridges due to their relatively low cost.

Considering the human scale of footbridges, it is important to take into account the needs of the users, passers-by and nearby residents to the design. These may include able-bodied people, the physically handicapped, the elderly, infants and pregnant women. Some issues addressing the relationship between footbridge structures and the users and nearby residents are provided below:

- The effects of vibrations should be considered taking into account the type of user (elderly, handicapped, etc.)
- Users walking on a narrow elevated pathway may feel uncomfortable when seeing vehicles passing below. Special consideration should thus be paid to the perspective of users.
- Rest stations (benches, etc.) can be set up on an elevated pathway when an open space is available.
- Spiral staircases may interfere with the passage of the elderly and physically handicapped.
- Gently sloping stairs are preferable, though steep stairs are generally adopted in congested cities. For very busy urban footbridges, the use of escalators or elevators may be considered.
- Footbridges, when constructed across narrow roads, leave little space in the areas around their entrances. In such cases, alternative plans should be developed – e.g., exploitation of neighboring alleys or elimination of the entrances by linking footbridges to adjacent buildings.
- When housing is located near footbridges, specific measures should be adopted to avoid overlooking. Likewise, users may feel the eyes of someone below when going up and down the stairs or walking on footbridges. Board screens are commonly used in Japan, but there are many problems to be solved with such a system.

The approach to the design of a footbridge depends on the location and the surroundings of the bridge. Each site and each task is different and rarely can the same design fit different contexts. For a bridge in an unspoiled natural environment, the designer will generally attempt to create a light and transparent design. If the designer chooses to create a bolder structure, he wants to create a symbol or landmark in these natural surroundings. In an urban environment, it is often necessary to counteract the mass of the surrounding buildings with a strong and dominant design. On other occasions,

it might be advisable to humbly adjust the design to conform to the adjacent cityscape.

Heavily congested urban areas, such as in East Asia, may provide more difficult constraints. Special considerations for this type of setting are provided below:

- At large intersections, horizontal and vertical travel distance should be reduced as much as possible through measures such as installation of multiple 'entrances' and links to adjacent buildings.
- During rush hours, a large number of users pass through from mass transit systems (trains) to smaller transit systems (buses, taxis, etc.). Widening pathways, reducing vertical travel distances and creating networks of elevated pathways, can prevent the congestion due to this type of traffic.
- Current urban redevelopment projects may be based on a long-term perspective. It is therefore desirable that the aisles of the upper floors of buildings be linked to footbridges to minimize vertical travel distance.
- There is generally a high incidence of traffic accidents at large intersections in densely populated areas. To avoid this, footbridges are often constructed. During the planning of footbridges in such areas thorough consideration should be given to the location of the bridge piers and entrances. Alternative access positions may also be provided.
- The locations of entrances are particularly important when constructing footbridges across narrow intersections. In this case, the entrances of adjacent buildings could be used as entrances to footbridge, if the structure is linked to the buildings.
- Extension of pedestrian malls is a preferred option when linking footbridges to adjacent parks.

Footbridges show a larger diversity in materials than other bridge types. The superstructure may be made of steel, concrete, timber, masonry, stainless steel, aluminum alloy or fiber-reinforced plastics among others, or as a composite or hybrid structure, that uses a combination of those materials. Materials with which there is little experience or newly developed materials are often tested in the footbridge. Such materials can be introduced more easily for footbridges being that it is easier to convince a client if the structure, and thus related cost, is small. However, all materials to be used must conform to the requirements of the appropriate international standards or the relevant national standards, unless sufficient test results and/or analytical results have already been obtained.

In the choice of materials, the close relationship between the structure and its users as well as the large impact on its surroundings must be taken into account. In the design, the idea of proposing a new regional character or harmony with the existing regional character may be considered, and the aesthetics of individual materials should be utilized sufficiently. For example, appropriate materials should be chosen for different types of structures whether they are free forms with soft curved surfaces, or structural forms in which lightness and slenderness are emphasized. By considering texture, color and lustre, it is also possible to produce designs with warmth and grace. Designs with an historic atmosphere can also be created through the aging of the materials and surfaces.

Also for footbridges, sustainability is an important issue. The responsible designer should try to use materials of low environmental impact. The application of a highly recyclable material, or the quantitative reductions caused by high-performance materials requires consideration.

The superstructure materials should suit the materials of the substructure and nonstructural members. In examining the suitability of a superstructure material with substructure materials, the effect of the structure on the landscape should also be considered. In addition, the suitability of all non-structural materials needs to be studied carefully considering the users of the bridge.

Bridges are structures that require profound knowledge of the pertinent engineering concepts. Therefore, it should be a team lead by the engineer and, depending on the case, with the support and advice of an architect. The engineers and architects should start working together at an early stage and try to find a carefully detailed solution that satisfies structural as well as formal requirements. If the engineer or architect works alone and knows nothing of his partner's field, one risks creating a:

- Bridge design based solely on formal 'visions' without consideration of structural function. The structural engineer is called in later to make structural sense of an essentially sculptural design. This leads to changes in form and the necessity of additional structural elements not to mention higher costs.
- Bridge design based solely on utilitarian and cost considerations. The architect is called in later to 'apply beauty' to an essentially unimaginative design. Neither approach can lead to a harmonious whole.

Footbridges are permanent structures that, in addition to providing a necessary path connecting two points, may positively contribute to their environment or create a symbol for a place. They may therefore provide structural, social, aesthetic and visual value. These opportunities must be taken into account during the design or one risks creating a structure devoid of inspiration where the only value taken into consideration is minimizing construction cost. The most successful designs arise from the understanding that the true value of a bridge consists of a combination of positive assets in addition to cost.

3.2. Bridge accidents and breakdowns

In last 180 years people encountered considerable amount of bridge collapses that were caused by pedestrian load. If we do not consider military involvements or natural hazards, those accidents claimed more deaths than any kind of constructions ever. Let us see in details, what generally caused those tragic cases, analyze some regularities and influences of the shape, structure, loading and behavior of the crowd.

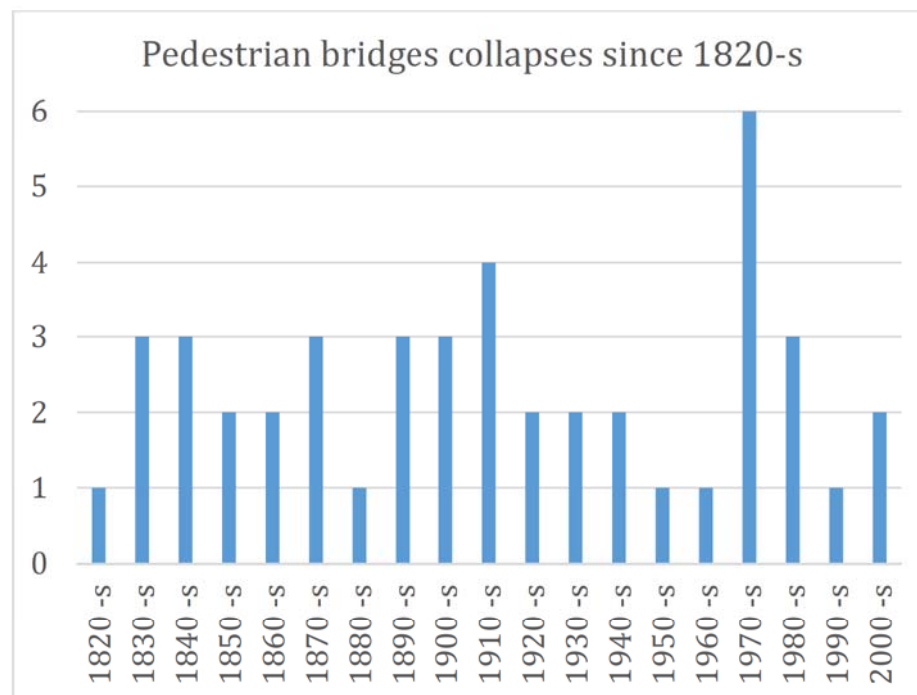


Figure 12. The diagram of the pedestrian bridges collapses through the history.

Due to the fact that the collapse information and statistics is scant, registered cases represent only the part of all accidents happened all over the world. The character of the appearance governable to the law of randomness increased the degree of ignorance. However, the available data (Figure 12) proves that engineers must take into account the probability of the overloading of the bridge with the extremely high-density crowd. The loading can be not only

static, but dynamic as well. The behavior of the crowd should also be taken into consideration.

Analysis of the available reports and data represents the high percentage of the timber bridges collapses due to pedestrian overload – almost half of the accidents. Steel and cast-iron bridges are backward – one third of the entire amount. Meantime concrete, reinforced concrete and stone bridges are not so sensible to the crowd. In case of steel and iron bridges, the maintenance was subject-related reason, corrosion of the elements together with human imposed vibrations caused tragedy. Moreover, it is clear, that improper maintenance of concrete structures can change our positive confidence in future.

Amount of people on the deck	Accidental cases
< 26	6
26 – 150	21
151 – 250	7
251 – 500	6
501 – 750	3
> 750	2

Figure 13. *Distribution of the collapses in reference to the human on the deck during the collapse*

The approximate statistics of the amount of people that was on the bridge during the accidents is presented at Figure 13. Obviously, the behavior of the crowd has to be considered. For this purpose, we should use as an addition the distribution of accidents in reference to crowd behavior.

Crowd behavior	Accidental cases
Traffic along the bridge	2
Procession	4
Public gathering along one side of the bridge	5
Traffic from one side of the bridge to another one	2
Queueing	6
Passage of cavalry, infantry or other types of corps	6

4. Application of the SIN-beam for the pedestrian bridge

4.1. Introduction

The project takes into account the current focus on the renovation of the Bega Canal to become navigable and modern solutions obtained by the collective of Politehnica University of Timișoara.

[Wikimapia](#) says:

One of the most beautiful bridges in the city, the bridge still withholds a romantic taste. Legend says that the plans for this metal bridge, whose construction elements are kept untouched, were sketched using an original design made by the famous Gustave Eiffel, the famous architect who designed the well-known Eiffel Tower in Paris. According to Árpád Jancso, "the bridge was more of a recycling scheme by incorporating metallic parts of what used to be the Hunyadi Bridge". The bridge was completed in 1917, however, its over scaled size condemned it to be used only by pedestrians, as building access ramps for cars involved demolishing several houses nearby. This fact determined Franz Engelmann (one of Banat's famous historians) to name it "die Irrtumsbrücke" - "The Bridge of Mistakes".

Qualified historians claim that there are not any suggestive or clear evidences in order to certify without doubt that, "The Eiffel Bridge" was indeed built by any of Eiffel's plans or drawings. Despite this uncertainty, the legend is still being passed on from generation to generation, thus keeping alive the mystery surrounding the most charming bridge in Timișoara.

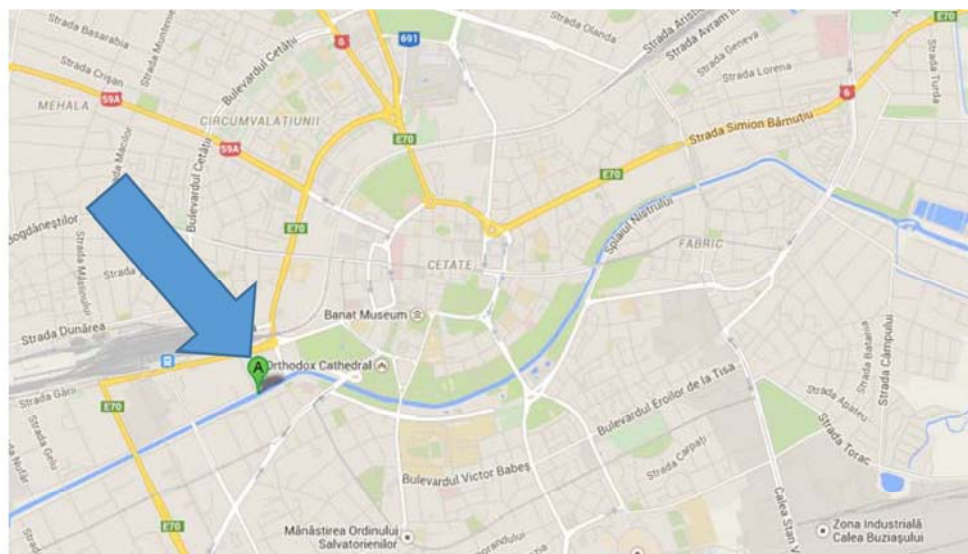


Figure 14. The location of the Eiffel Bridge on the map of the city center of Timișoara.





Figure 15. Photographs of the Eiffel bridge.

I will perform the possible solution for the bridge replacing the Iron Bridge.

4.2. Geometric conditions

One of the first decisions to be made when designing a bridge for pedestrians is the deck width, i.e. the capacity of the bridge. The width is dependent on local conditions and the expected density of pedestrians. It may also depend on the location of the footbridge, be it on a trail, in a park or in an urban setting. Cultural setting may also play a role, as the width of Japanese footbridges is usually narrower than bridges built in North America or Europe. The information given in the table below that has been prepared for pedestrian walkways and has proved helpful for the determination of deck width. The sketches in Figure 16 define pedestrian density and the corresponding live load.

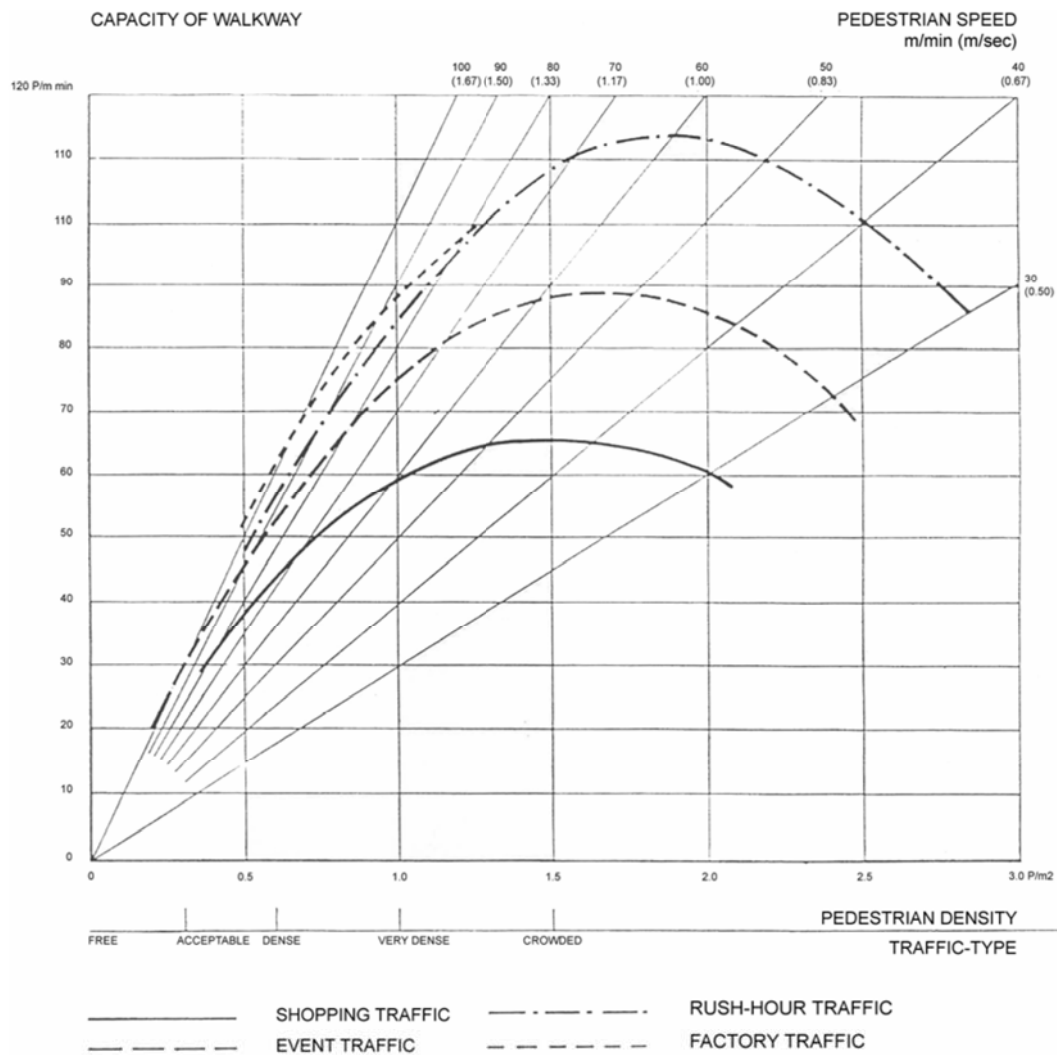


Figure 16. Capacity of pedestrian walkway dependent on traffic type and pedestrian density

According to the location and given requirements specification, the width of the designed bridge is 3.5 meters and banisters handrails height is 1.15 meters. The configuration is given on the Figure 17.

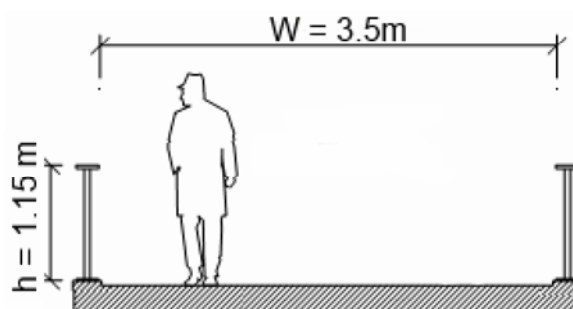


Figure 17. Chosen configuration of the pedestrian walkway.

4.3. Grade

In general, the grade of the bridge deck can be freely chosen. Bridge grade requirements depend on the location of the footbridge. Bearing in mind that for wheelchair users grades of more than 6% are difficult to handle, I have chosen the slope of 5% (or 3 degrees) along the half-span.

The span of the bridge is 22 meters.

For the design and simulations has been chosen the following configuration of the structural elements:

4.4. Stairways

According to the necessity to perform the accessibility to handicapped people, the adjacent territory should be reorganized.



Figure 18. Existing stairs with poor accessibility for wheel chaired people and bicyclists.

The solutions can be performed either in structural way (see Figure 19) or as an additional element (see Figure 20). For safety reasons any solution must guarantee high coefficient of friction in order to avoid sliding of the wheelchairs (see Figure 21 and 22).



more awesome pictures at THEMETAPICTURE.COM

Figure 19. Combined stairs solution applied in Vancouver, Canada.

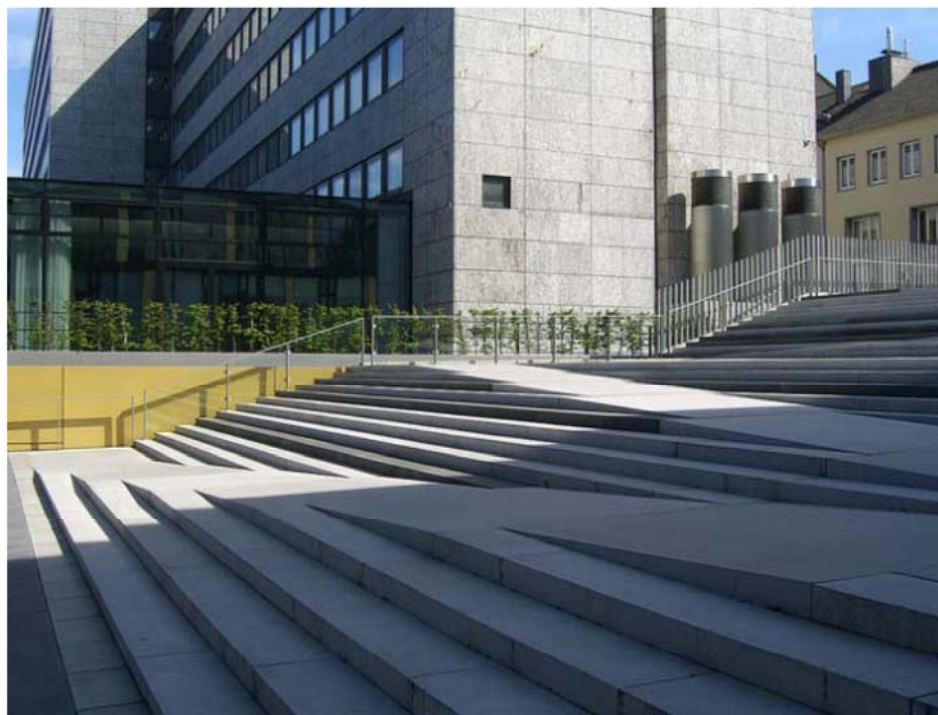


Figure 20. Combined solution applied in Aachen, Belgium.



Figure 21. Ramps on a bridge over a canal in Venice.



Figure 22. Antisliding solutions for the ramps.

4.5. Loads

4.5.1. Introduction

Footbridges are subject to different loads than highway or railroad bridges. Although appropriate loading would seem instinctively lower for footbridges, most codes call for a live load that is comparable to the values for highway bridges. Nevertheless, high wheel loads need not be considered in footbridge design, although consideration should be made to the use of the structure by maintenance or emergency vehicles. The 'hands-on' nature of footbridges should also be taken into account and is important for railing loads and vandalism considerations.

Rem Kiparisov, Master Thesis

4.5.2. Loads as Function of Deck Length

Depends on a code, live loads can vary according to the span. (see Figure 23)

For the design, it is assumed to have not more than 4,5 kN/m².

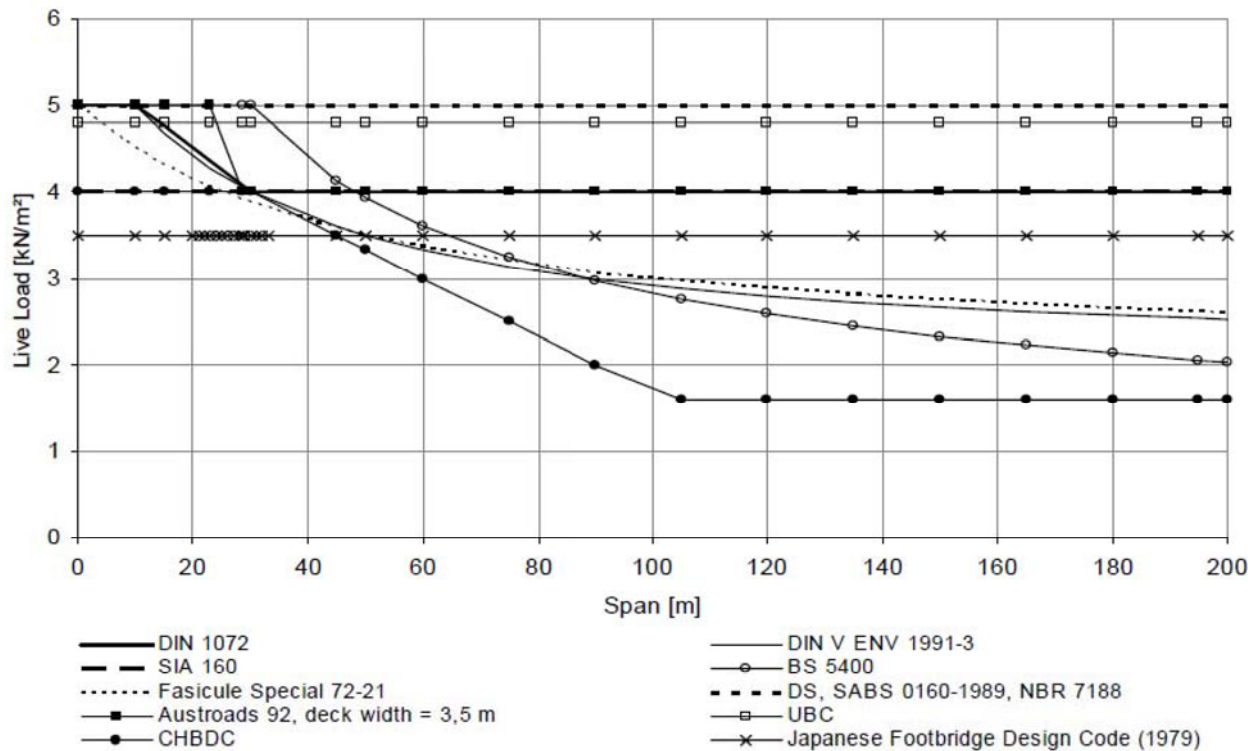


Figure 23. Live load (nominal) as a function of span length for spans of 0-200 m, service load.

4.5.3. Asymmetric Loading

One-sided live loads are of special concern in footbridge design. Unbalanced loads can occur when numerous spectators stand at the railing to one side of a narrow footbridge during an event. Common practice may lead the designer to apply the full live load to one-half of the bridge deck while applying only one-half of this value to the other half of the bridge deck. (see Figure 24)

This depends on how, for a given task, the designer interprets codes like the Eurocode 1 which state that 'for each individual application, the models of vertical loads should be applied anywhere within the relevant areas so that the most adverse effect is obtained'. For railing loads see chapter Figure 40.

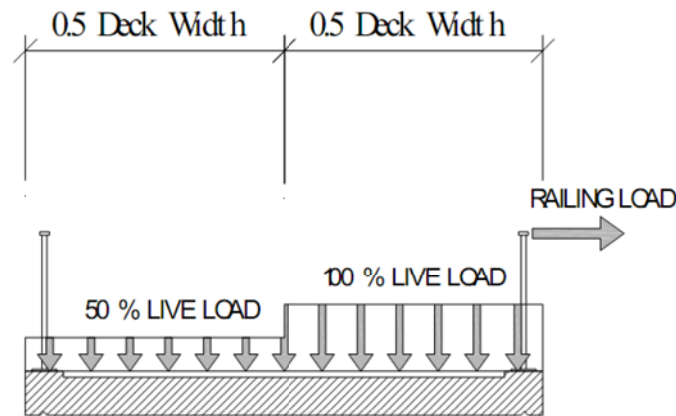


Figure 24. Proposed treatment of one-sided live loads.

4.5.4. Wind Loads

Footbridges are subjected to wind actions. Wind loads are very important for movable and covered footbridges. In many countries in which wind gusts are a particular problem, a detailed analysis of wind loads is required. Wind occurrence must be examined carefully as it varies greatly from location to location. Flexible, long-span suspended structures may also be subject to wind-induced phenomena such as flutter and galloping.

The DIN V ENV 1991-2-4; Eurocode 1, Part 2-4 considers forces due to wind pressures laterally (y), transversely (x), and vertically (z). The ratio of structure width to height and the height of the construction above the ground determine the wind pressure values, which range from 1.2 kN/m^2 to 4.1 kN/m^2 . These values are to be found in Table N.1 in Appendix N of the code. This basis value of wind pressure is multiplied by a coefficient of force c_f . This coefficient of force consists of a basis coefficient $c_{f,x,0}$, which takes into account the shape of the bridge section and a factor $\psi_{\lambda,x}$ takes into account the slenderness of the structure l/b . The coefficients of force in the z direction $c_{f,z}$ and y direction $c_{f,y}$ are to be taken from diagrams in the code.

$$h_w = 1.4 \text{ m}; b = 3.5 \text{ m}; d_{\text{tot}} = h_w + 0.6 \text{ m} = 2 \text{ m}; b/d_{\text{tot}} = 1.75;$$

$$\text{Wind pressure } P_w = 4 \text{ kN/m}^2$$

According to Figure 25 $c_{f,x,0} = 2$. The wind load is $W_x = 2 \times 4 \text{ kN/m}^2 = 8 \text{ kN/m}^2$. For plated bridges the coefficient $c_{f,y}$ is 25% of wind forces in X direction, $W_y = 0.25 \times 8 \text{ kN/m}^2 = 2 \text{ kN/m}^2$. The $c_{f,z}$ coefficient is 0.7, $W_z = 0.7 \times 4 \text{ kN/m}^2 = 2.8 \text{ kN/m}^2$

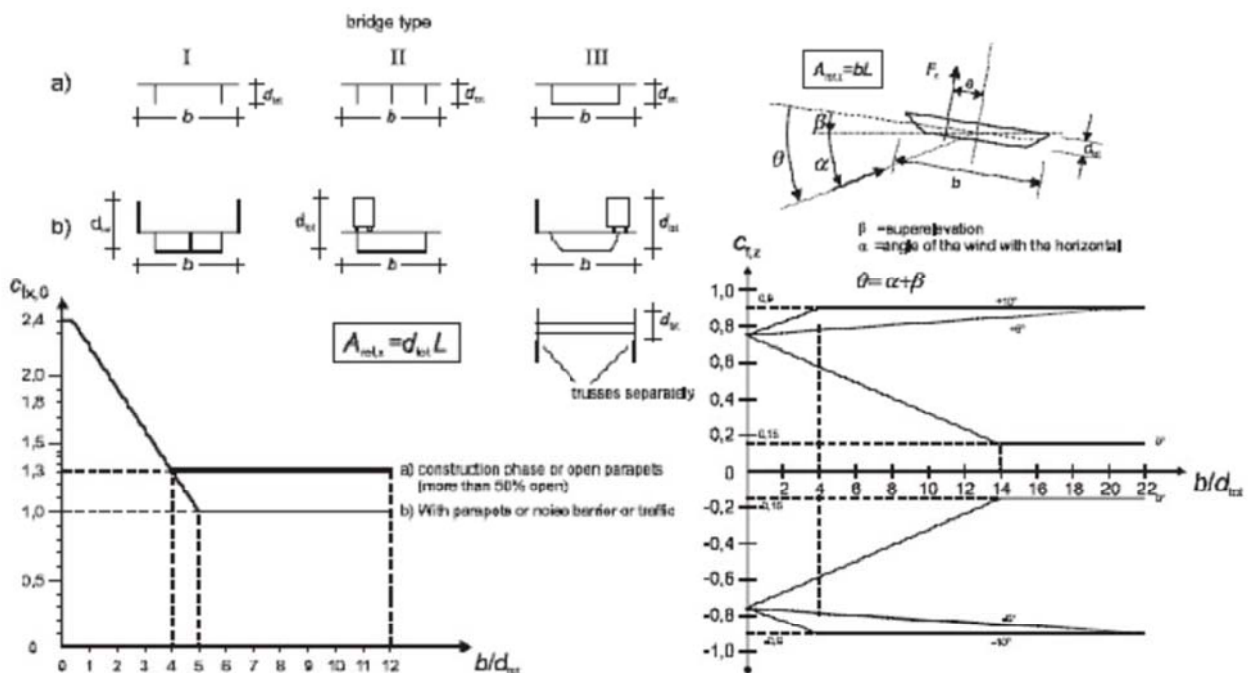


Figure 25. Force coefficient $c_{fx,0}$ for bridges

4.6. Dynamics

4.6.1. Introduction

The footbridge should no longer be designed for static loads only, but also for the dynamic actions and vibration behavior of the bridge due to pedestrian loading characteristics. It is very important to predict and take into consideration all possible scenarios of pedestrian traffic at the design stage of the project and guarantee a required comfort level for pedestrians verifying the serviceability.

4.6.2. Pedestrian Traffic and Action

The pedestrian density greatly influences the speed of the individual and is therefore important for the dynamic analysis. If the pedestrian density increases, the single pedestrian is no longer able to walk with his individual step frequency and walking velocity. The synchronization of pedestrians regarding step frequency, phase and velocity takes place that can also occur in combination with the bridge movement.

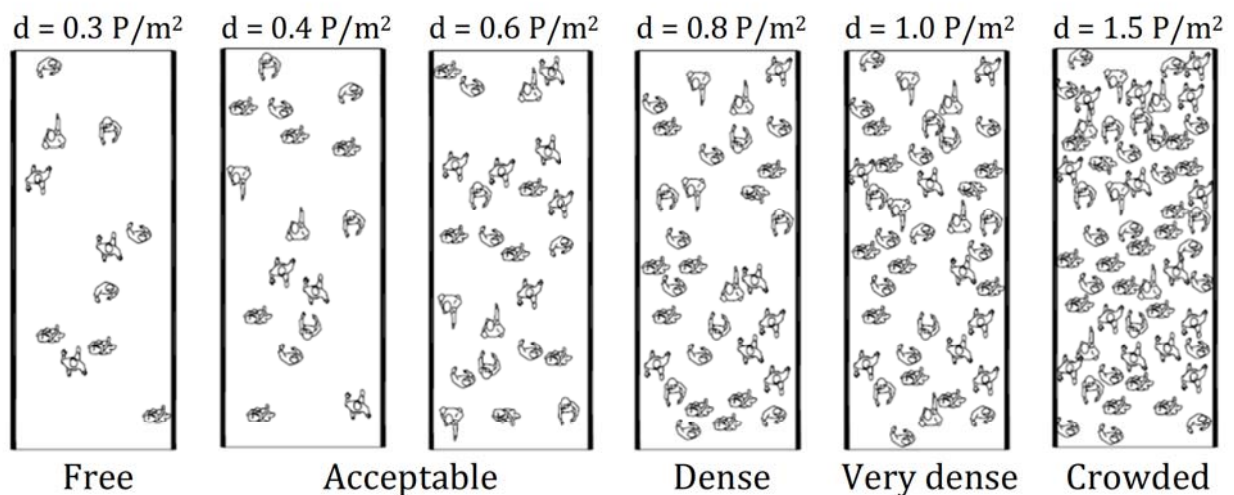


Figure 26. Different types of pedestrian densities

In general the walking velocity reduces with increasing traffic density. The single pedestrian has to adjust his walking velocity to the movement of the mass. First restrictions occur at a pedestrian density of 0.6 pers./m² as passing becomes more difficult. From a pedestrian density of 1.0 pers./m² the freedom of movement is greatly inhibited. The pedestrians must adjust their velocities and step frequencies to each other. If the density is about 1.5 pers./m², columns dependent on the direction of walking with a very low velocity develop. 2.0 pers./m² result in a very crowded stream where only a sliding movement with very small steps is possible. The pedestrian is not able to move on his own.

It should also be noted that by dense pedestrian traffic, the modal characteristics of the structure might be changed due to an increase in mass and an increase in damping caused by their vertical movements. Horizontal movements may experience negative damping with the presences of large numbers of pedestrians.

4.6.3. Comfort Criteria and Limit Values

The human perception of vibrations is subjective and depends on individual characteristics and psychological influences. The perception is influenced by the physical factors vibration frequency, acceleration and the time period of exposure. The discomfort depends much on the environmental conditions and the attitude towards the vibration cause. Sound caused by rattling or resonating of bridge equipment as well as visual influences may provoke discomfort. The height above ground of the bridge or the traffic below the bridge may influence the perception also. However, over the time, pedestrians get used to the vibrations and the acceptance with regard to the vibrations can

rise. Stochastic vibration in general induces more discomfort than periodic ones.

Comfort requirements in Eurocode are subdivided in two parts:

- Limit values for structural frequencies: Pedestrian induced loading falls within certain frequencies. Structures whose natural frequencies fall outside these pedestrian loading frequencies will generally not be at risk of resonance loading.
- Limit values of accelerations: Should the natural frequency of a structure fall within the range of pedestrian induced loading frequencies. The resulting structural accelerations are then limited to ensure pedestrian comfort.

4.6.4. Design Procedure

Step 1: Evaluation of natural frequencies

There are several ways to calculate the natural frequency of a footbridge during design, especially for the preliminary check of the bridge vibration, e.g.:

- By the finite element (FE) method
- Using hand formulas derived e.g. from closed-form solutions for beams, cables and plates.

For the design we will take the value obtained from the finite element model analysis.

$$f = 6.23 \text{ Hz}$$

Step 2: Check of critical range of natural frequencies

The critical ranges for natural frequencies f_i of footbridges with pedestrian excitation are:

- for vertical and longitudinal vibrations:

$$1.25 \text{ Hz} \leq f_i \leq 2.3 \text{ Hz}$$

- for lateral vibrations:

$$0.5 \text{ Hz} \leq f_i \leq 1.2 \text{ Hz}$$

Footbridges with frequencies for vertical or longitudinal vibrations in the range of

$$2.5 \text{ Hz} \leq f_i \leq 4.6 \text{ Hz}$$

might be excited to resonance by the 2nd harmonic of pedestrian loads. In that case, the critical frequency range for vertical and longitudinal vibrations expands to:

$$1.25 \text{ Hz} \leq f_i \leq 4.6 \text{ Hz}$$

Lateral vibrations are not affected by the 2nd harmonic of pedestrian loads.

Footbridges, which have natural frequencies f_i in the critical range, should be subject to a dynamic assessment to pedestrian excitation.

Step 3: Assessment of Design Situation

The design of a footbridge starts with specifying several significant design situations - sets of physical conditions representing the real conditions occurring during a certain time interval. An expected traffic class (Table 1) and a chosen comfort level (Table 2) define each design situation.

There are design situations, which might occur once in the lifetime of a footbridge, like the inauguration of the bridge, and others that will occur daily, such as commuter traffic. Table 1 gives an overview of some typical traffic situations, which may occur on footbridges. The expected type of pedestrian traffic and the traffic density, together with the comfort requirements, has a significant effect on the required dynamic behavior of the bridge.

Table 1. Pedestrian traffic classes and densities.

Traffic Class	Density d $d = \frac{15P}{B \cdot L}$	Description	Characteristics
TC1	$d = 0.1 P/m^2$	Very weak traffic	B – width of deck, L – length of deck
TC2	$d = 0.3 P/m^2$	Weak traffic	Comfortable and free walking Overtaking is possible Single pedestrians can freely choose pace
TC3	$d = 0.5 P/m^2$	Dense traffic	Still unrestricted walking Overtaking can intermittently be inhibited
TC4	$d = 1.0 P/m^2$	Very dense traffic	Freedom of movement is restricted Obstructed walking Overtaking is no longer possible
TC5	$d = 1.5 P/m^2$	Exceptionally dense traffic	Unpleasant walking Crowding begins One can no longer freely choose pace

Table 2. Defined comfort classes with common acceleration ranges.

Comfort Class	Degree of Comfort	Vertical a_{lim}	Lateral a_{lim}
CL1	Maximum	$< 0.5 \text{ m/s}^2$	$< 0.1 \text{ m/s}^2$
CL2	Medium	$0.5 - 1.0 \text{ m/s}^2$	$0.1 - 0.3 \text{ m/s}^2$
CL3	Minimum	$1.0 - 2.5 \text{ m/s}^2$	$0.3 - 0.8 \text{ m/s}^2$
CL4	Unacceptable discomfort	$> 2.5 \text{ m/s}^2$	$> 0.8 \text{ m/s}^2$

Step 4: Assessment of structural damping

The amount of damping present is very significant in the evaluation of the amplitude of oscillations induced by pedestrians. The attenuation of vibrations, i.e., the energy dissipation within the structure, depends both on the intrinsic damping of construction materials, which is of distributed nature and on the local effect of bearings or other control devices. Additional damping is also provided by non-structural elements, like handrails and surfacing.

The logarithmic damping of different materials, structural systems, and bearing conditions according to Petersen is given in Table 3 – 5.

The total damping of the structure can be calculated according to the following formula:

$$\Lambda = \Lambda_1 + \Lambda_2 + \Lambda_3$$

where $\Lambda = 2 \cdot \pi \cdot \xi$ – logarithmic decrement
 ξ – damping ratio, in percent of critical damping
 Λ_1 – logarithmic decrement of material damping (Table 3)
 Λ_2 – logarithmic decrement of structural damping (Table 4)
 Λ_3 – logarithmic decrement of bearing conditions (Table 5)

Table 3. Material damping.

Material Damping Λ_1 (logarithmic decrement)	Range	Mean Value
Ferritic Steel	0,005...0,012	0,008
Austenitic Steel	0,008...0,018	0,013
Aluminium alloys	0,010...0,025	0,015
Hardwoods	0,030...0,040	0,035
Softwoods	0,040...0,050	0,045
Laminated wood	0,025...0,035	0,030
Fibre glass	0,035...0,045	0,040
Reinforced Concrete Uncracked	0,025...0,040	0,030
Reinforced Concrete Cracked	0,035...0,055	0,045
Prestressed Concrete	0,020...0,030	0,025
Lightweight Concrete	0,035...0,055	0,045

Table 4. Structural damping.

Material Damping Λ_2 (logarithmic decrement)	Range	Mean Value
Steel Bridges		
Steel and asphalt deck	0,020...0,030	0,025
Concrete and composite deck	0,025...0,040	0,035
Wooden deck	0,030...0,050	0,050
Wooden Bridges		
Laminated	0,015...0,025	0,020
Mechanical connections – nails, bolts, and pegs	0,035...0,050	0,040
Concrete bridges	0,015...0,025	0,020
Cable stayed bridges	0,030...0,050	0,040
Suspension bridges	0,025...0,035	0,030

Table 5. Damping due to bearing conditions.

Material Damping Λ_3 (logarithmic decrement)	Range	Mean Value
Steel sliding bearings	0,012...0,018	0,015
Roller bearing	0,004...0,006	0,005
Pot bearings	0,008...0,012	0,010
Elastomeric	0,010...0,025	0,015

The total damping of the bridge calculated according to the following formula:

$$\Lambda = \Lambda_1 + \Lambda_2 + \Lambda_3 = 0,18 + 0,03 + 0,025 = 0,235$$

Damping ratio $\xi = \frac{\Lambda}{2 \cdot \pi} = 0,037$ or 3.7%

Step 5: Determination of maximum acceleration

When one or several design situations are defined and the values for damping are determined, the next step is to calculate the maximum acceleration a_{\max} for each design situation.

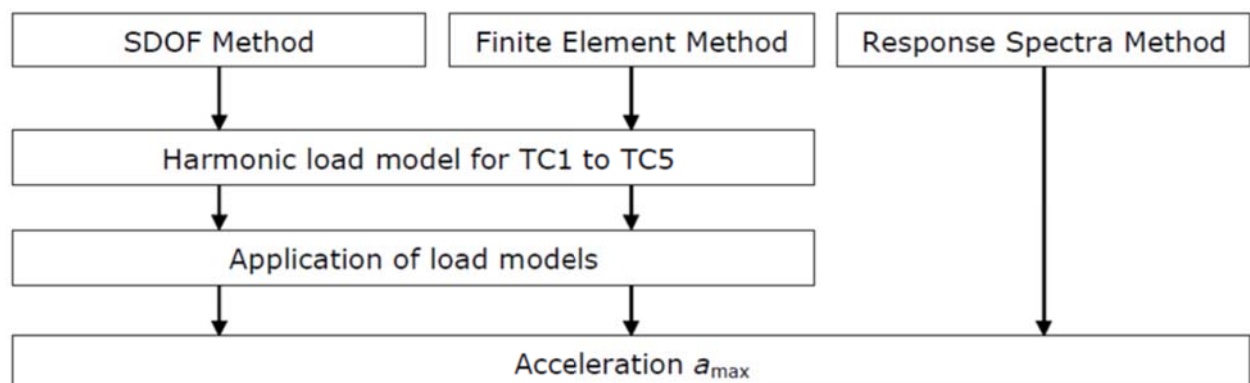


Figure 27. Methods for calculating the maximum acceleration.

I will apply the Finite Element Method. The aim of a spectral design method is to find a simple way to describe the stochastic loading and system response that provide design values with a specific confidence level.

The verification for the reversible serviceability of the pedestrian bridge is presented in ANNEX 4.

4.7. Deck surfacing

The primary functions of a deck surface are to define the traffic surface and provide suitable traction for the user. Applied surfaces may also act to protect the structural deck from weathering and wearing. Segregation, for instance between pedestrians and cyclists, can be facilitated by a change of surface specification. The choice of surface decking may have a dramatic effect on aesthetic criteria and issues such as lighting.

Deck surfaces must provide adequate traction to inhibit slipping. Note that cyclists and horses display different characteristics in terms of speed, stability and area of surface contact to pedestrians and should be considered accordingly. Where the pedestrian is concerned, traction is influenced by factors including the type of user and footwear, environmental conditions and the condition of the deck surface. A broad range of issues contribute to the technical condition of the traffic surface, including the gradient of the bridge deck, system porosity, drainage strategy, surface texture, continuity of surface and so on. The surface material should provide adequate friction and be sufficiently resistant to polishing through use. Whilst a level deck is less prone to cause slipping, good drainage must also be provided in order to prevent deterioration of the wearing surface or ponding, leading to 'aquaplaning' through reduced friction.

Traction is not only an objective characteristic but subjective as well, with perception playing a key role. Pedestrians tend to change their pace and gait if they are aware that a surface is slippery and tend towards parapets and handrails for support. Lighting, color and pattern may additionally affect the confidence of the pedestrian and should be considered accordingly.

There are many possible solutions for decking materials with a variety of advantages:

- asphalt paving
- open grating decks
- concrete surfacing
- wood surfaces
- synthetic materials
- glass

For the application, it was decided to use FRP decking system FiberSpan™. It is a molded sandwich construction, which consists of thick fiberglass face sheets on top and bottom with fiberglass shear webs. A key component of FiberSpan™

is the fiberglass reinforced core. The closely spaced webs provide good crushing resistance to concentrated loads. There is no local skin deflection since the skins are so well supported by the webs. The redundancy of the multiple webs provides improved damage tolerance over thick, wider-spaced webs (see the Figure 28).

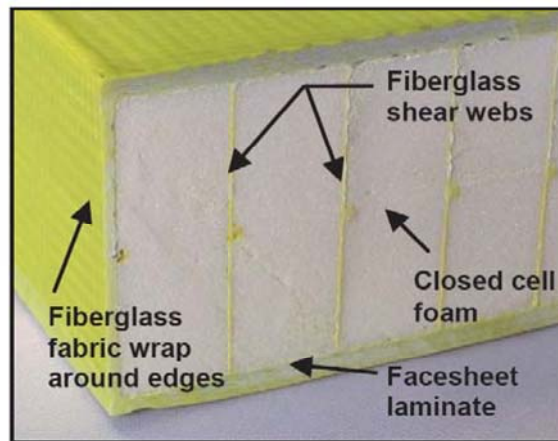


Figure 28. Fiber-glass panel cross-section.

Easy transportation, movement, quick placement and simple connection (Figure 29) make the using of FiberSpan™ very efficient for our bridge.



Figure 29. Connection of the fiberglass panel to the structure.

4.8. Railings

For the railings, I used tubular cross-section with diameter of 76mm with the steel horizontal cables for safety reasons.



Figure 30. Construction of the safety barrier for a pedestrian bridge in Nurnberg, Germany

4.9. Illumination

Footbridges have no set point or direction of view, unlike the roadway bridge with its set lanes. This leads to footbridge lighting facilities to be graded according to their illumination as opposed to their luminous intensity.

The lighting must ensure that cyclists and pedestrians are able to recognize the continuation of their path. Curves and path intersections must be clearly marked and may call for additional lighting in these areas. This is also the case for interfaces between stairways and bridge access routes and the bridge itself.

Colors of light can also be used to increase visibility or create an architectural effect. The choice of lighting color should not be confusing for traffic passing below the bridge. Recognizing color contrast is also affected by the lighting color. For increased visibility warm-white or neutral-white is often used on footbridges. The warm-white and neutral-white light permits good color contrast.

Lamps must meet several criteria. They must provide good contrast and lighting color should blend in with the surrounding area. Warm white lights are therefore recommended. Maintenance costs must also be considered. Lamps with high luminous efficiency have lower energy costs. In addition, the life span of lamps is a large factor in choosing a lamp. Maintenance costs for lamps often outweigh the initial investment cost for an economic design.

For the design, it was considered to have lamps at ground level and lighting elements in railings. (see Figures 31 and 32)



Figure 31. LED handrail illumination.

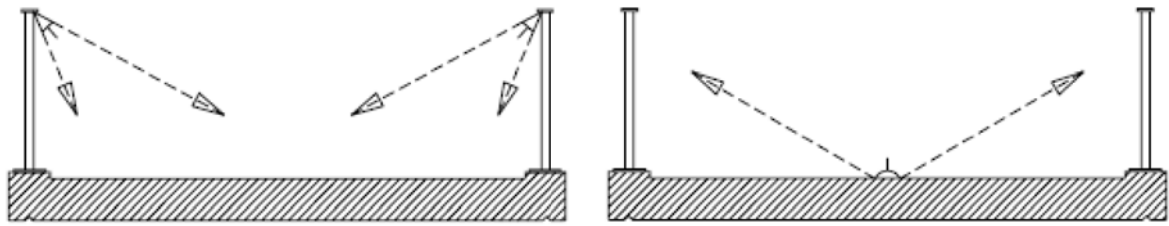


Figure 32. Chosen lighting systems for the pedestrian bridge.

Lighting fixtures are exposed to the environment and vandalism. This affects the choice of materials. Lighting fixtures must not corrode easily and be robust to avoid damage due to vandalism. This leads to the recommendation that plastics be used in place of glass fixtures where vandalism is a particular problem. Compact lamp designs are also less prone to vandalism.

5. Numerical simulations

5.1. Introduction

Section 6 is dedicated to numerical modelling of three types of constructions – bridge with plate web configuration of the main beams (modelled as linear elements and with using of thin shell elements) and bridge with truss structure of the main beams.

For the introduction of connections behavior, the results of CWB analysis will be presented. The simulation is made with application of the ABAQUS software. The characteristics of the connections, specific interaction and corrugated sheeting are amongst the most significant differences.

5.2. Simulations in SAP2000

5.2.1. Introduction

For the simplification of the models, it was decided to use two equivalent models of the pedestrian bridge. The first one is presented on a Figure 33. This is the pedestrian bridge with two main beams with plates as webs and cold-formed C250×3mm profiles as flanges.

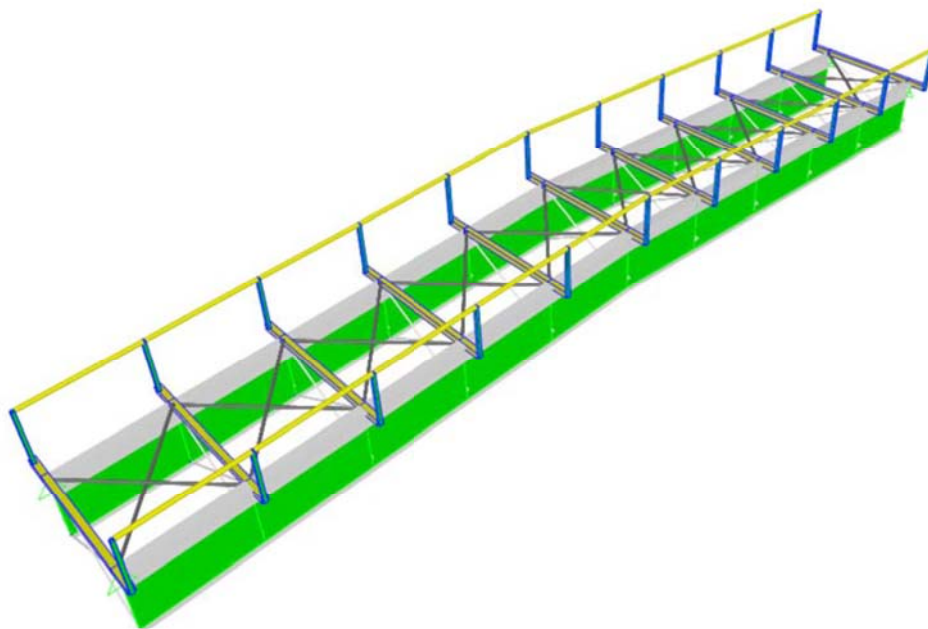


Figure 33. Plate model for SAP2000

The thickness of the steel sheet is governed by the equivalence calculation (See ANNEX 1).

The second model is a bridge with two main beams modelled as linear elements with assigned in the Section Builder cross-sections (Figure 34).

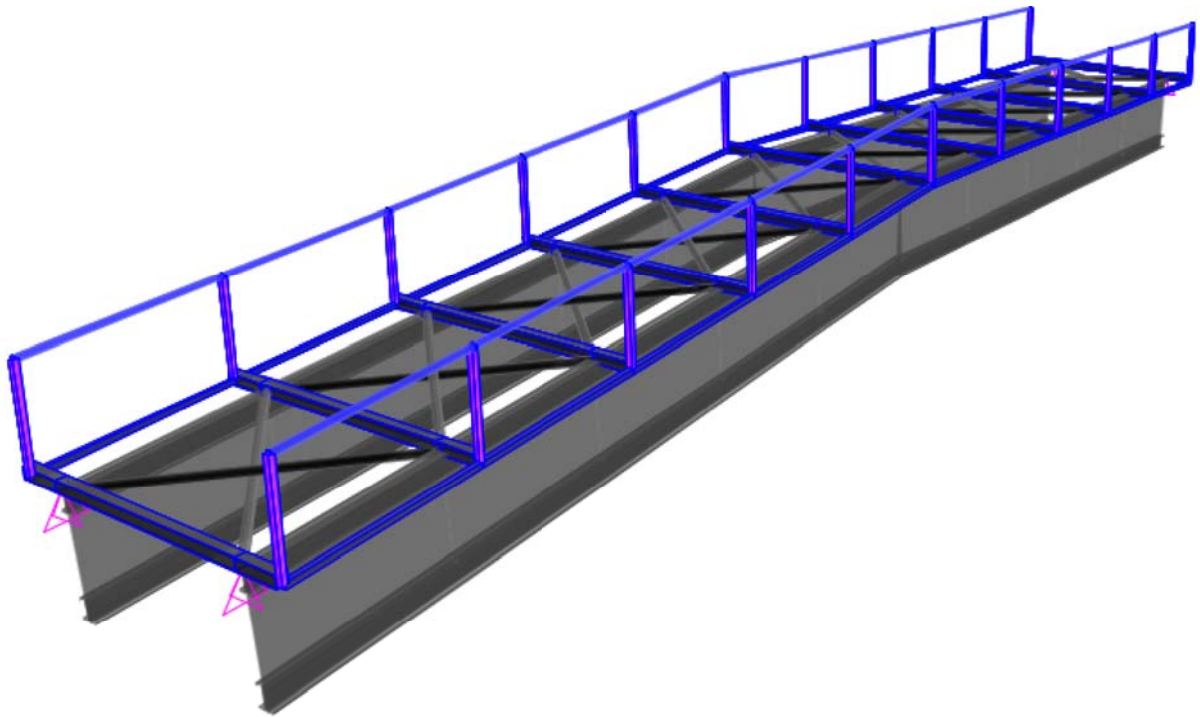


Figure 34. Linear elements model for SAP2000

For the estimation of economic effect it was used the third concept – truss beams made from rectangular hollow-sections (Figure 35).



Figure 35. Truss model for SAP2000

In this part, I will try to model the pedestrian truss bridge with the similar structural response in the deflection domain and establish the economical comparison between truss structure and CWB pedestrian bridge referencing to the price for the steel and labor costs (See Section 7).

5.2.2. Axis criteria

The labelling of the axis followed in this project is represented in Figure 36.

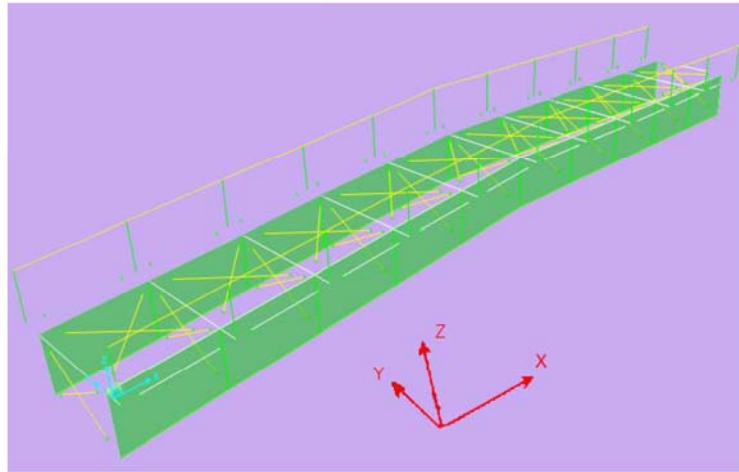


Figure 36. The labelling of the axis in SAP models

5.2.3. Materials

For the entire model, steel S355 will be used.

5.2.4. Loads

On the structure of bridge acting the following loads:

- Dead load (0.6 kN/m^2);
- Live load from pedestrians on the deck and on the handrails in two directions (4.5 kN/m^2 or $4.5 \text{ kN/m}^2 \times 2.2\text{m} = 10 \text{ kN/m}$ distributed along the secondary beams. Half of this value is distributed along secondary beams at the support) according to the **EN1991-2:2003**;
- Wind loads in three directions (in X direction – along the deck, in Y direction – transversally and uplift wind loading in Z direction). Calculation according to the **EN1991-2:2003** is presented in the Section 4.5.4;
- Seismic load is assigned according to the **EN1998-2:2005**. The structure is non-dissipative (structure is designed for a particular seismic design situation without taking into account the non-linear material behavior, $q = 1$). The response spectra parameters are presented in the Figure 46.

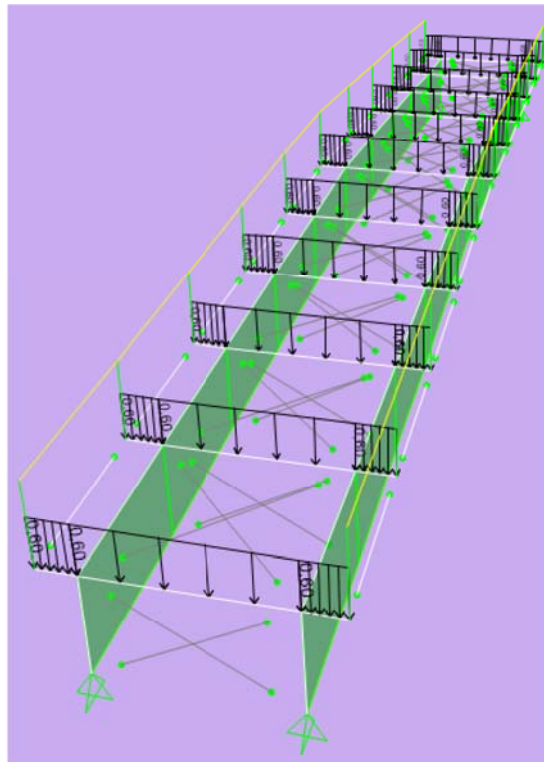


Figure 37. Dead load D on the structure

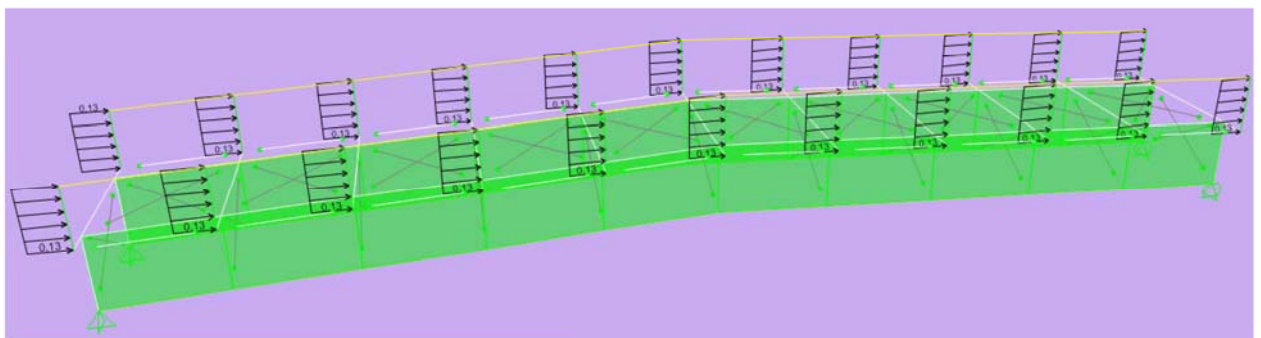


Figure 38. Wind load W_x in X direction

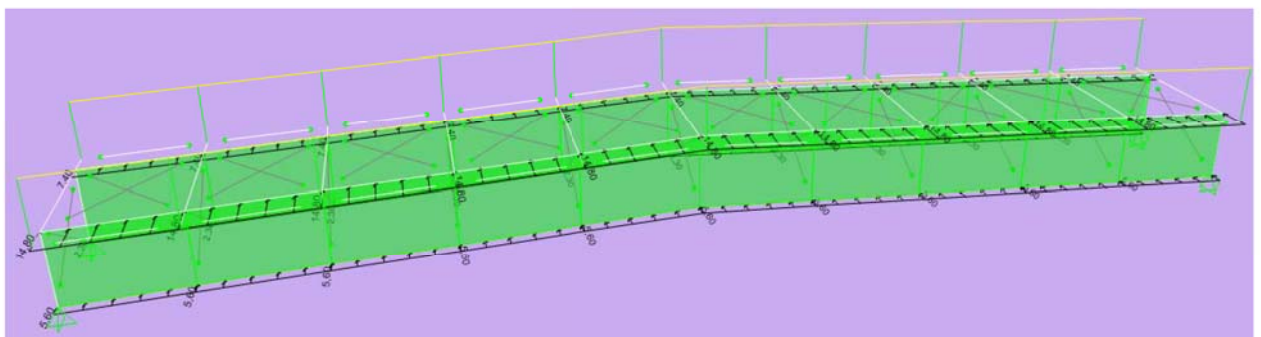


Figure 39. Wind load W_y in Y direction

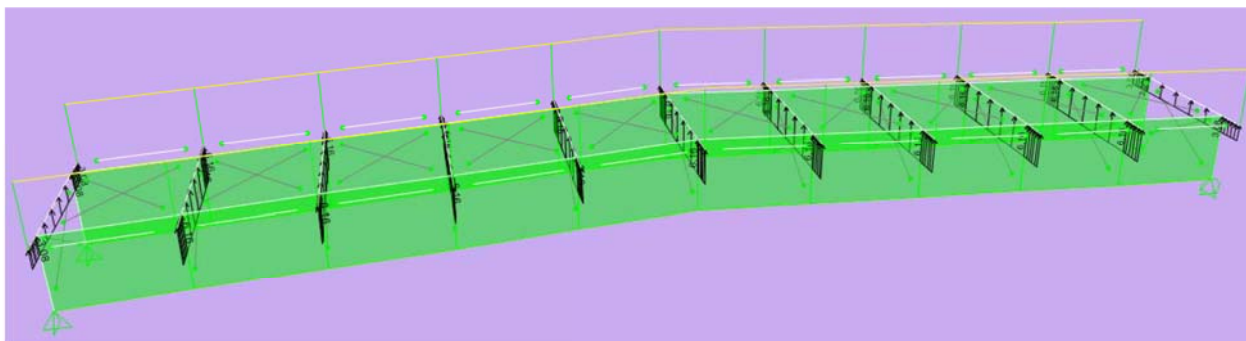


Figure 40. Uplifting wind load W_z in Z direction

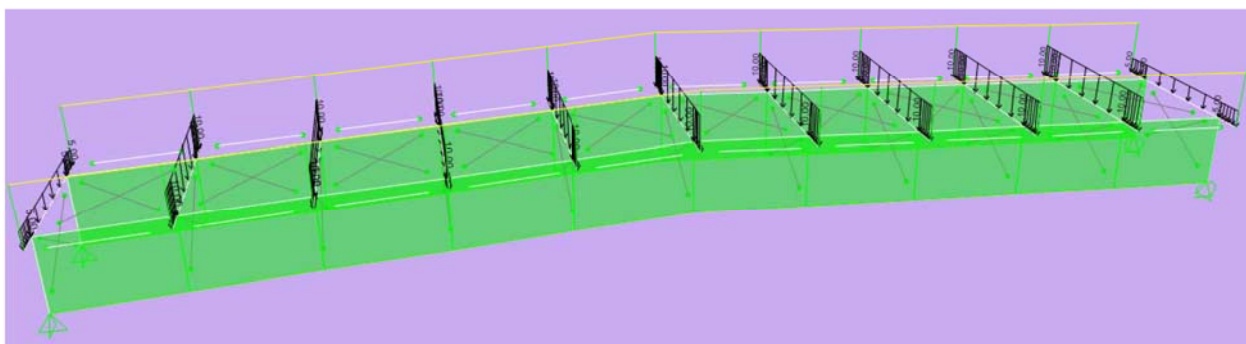


Figure 41. Live load L_1 with 100% of the live load distributed along the secondary beams

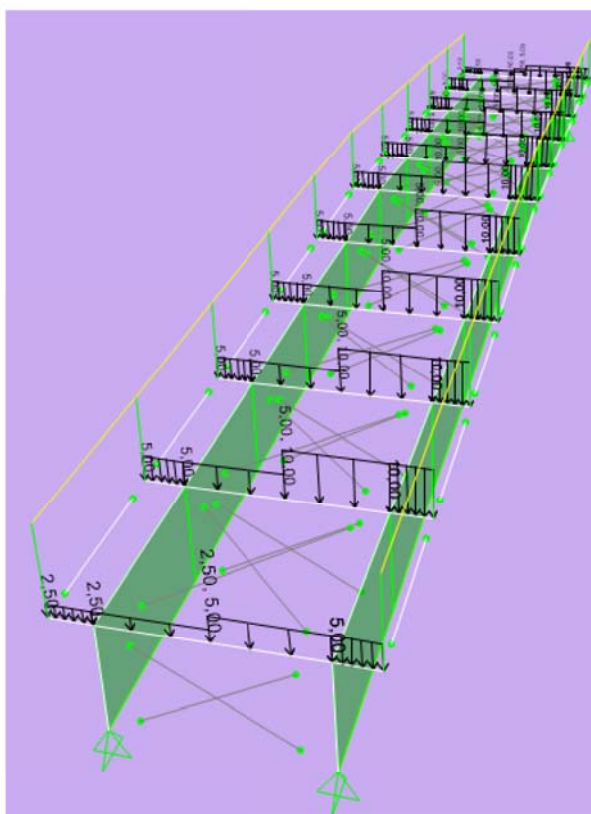


Figure 42. Live load L_2 with asymmetric loading

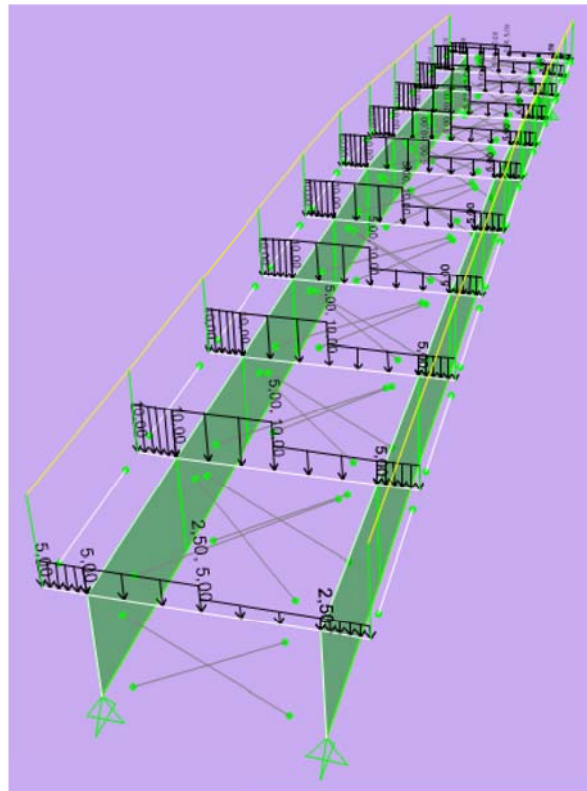


Figure 43. Live load L_3 with asymmetric loading

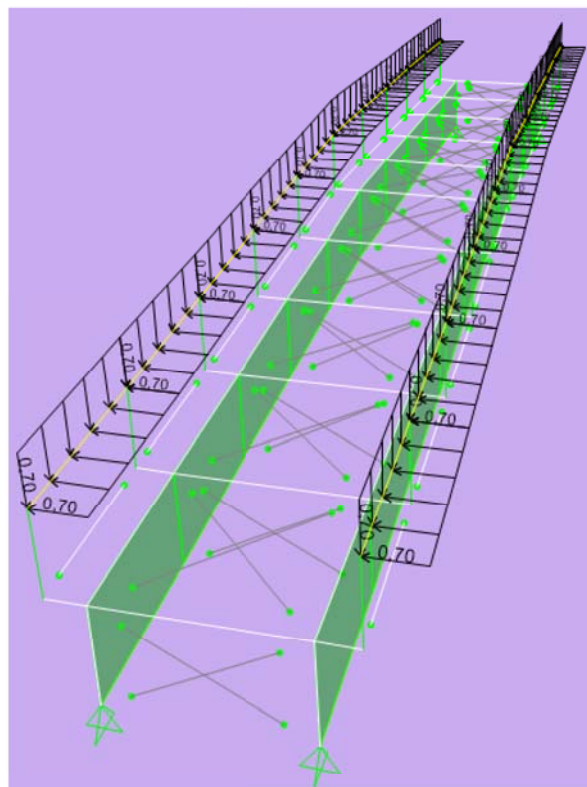


Figure 44. Assigning of the actions on handrails - L_r

Seismic action is assigned using the response spectrum load case type with mass source defined according to the EN1998-2: The quasi-permanent values of variable actions shall be taken as equal to $\psi_{2,1} \cdot Q_{k,1}$, where $Q_{k,1}$ is the characteristic value of traffic load and $\psi_{2,1} = 0$ (according with the recommendation of EN 1990:2002, Annex A2).

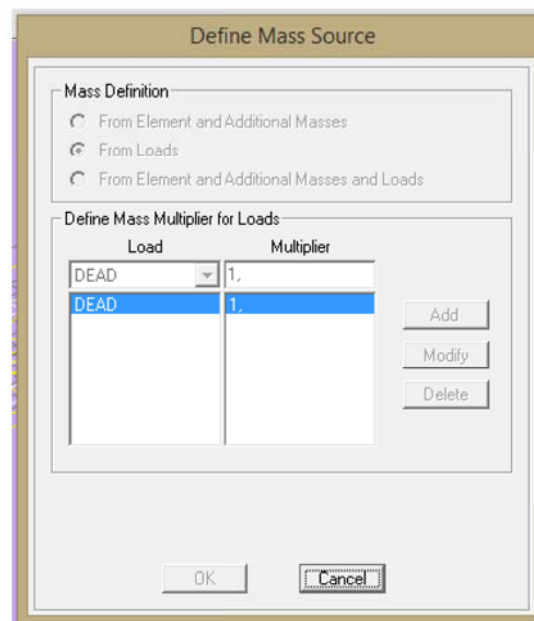


Figure 45. Definition of Mass Source for seismic analysis

The Response Spectrum Definition for Timișoara is based on following data:

For the horizontal action

$$a_g = 0.20 \times g$$

$$T_c = 0.7 \text{ s}$$

$$q = 1$$

$$\beta_0 = 2.5$$

$$\begin{cases} T_B = 0.14 \text{ s} \\ T_c = 0.7 \text{ s} \\ T_D = 3 \text{ s} \end{cases}$$

$$\begin{cases} 0 \leq T \leq T_B & \beta(T) = 1 + \frac{\beta_0 - 1}{T_B} \cdot T \\ T_B \leq T \leq T_c & \beta(T) = \beta_0 \\ T_c \leq T \leq T_D & \beta(T) = \beta_0 \cdot \frac{T_c}{T} \\ T_D \leq T \leq 5 \text{ s} & \beta(T) = \beta_0 \cdot \frac{T_c \cdot T_D}{T^2} \end{cases}$$

For the vertical action

$$a_{vg} = 0.70 \times g$$

$$T_c = 0.7 \text{ s}$$

$$q = 1$$

$$\beta_{0v} = 2.75$$

$$\begin{cases} T_{Bv} = 0.1 \cdot T_{cv} = 0.0315 \text{ s} \\ T_{cv} = 0.45 \cdot T_c = 0.315 \text{ s} \\ T_{Dv} = T_D = 3 \text{ s} \end{cases}$$

$$\begin{cases} 0 \leq T \leq T_{Bv} & \beta(T) = 1 + \frac{\beta_{0v} - 1}{T_{Bv}} \cdot T \\ T_{Bv} \leq T \leq T_{cv} & \beta(T) = \beta_{0v} \\ T_{cv} \leq T \leq T_{Dv} & \beta(T) = \beta_{0v} \cdot \frac{T_{cv}}{T} \\ T_{Dv} \leq T \leq 5 \text{ s} & \beta(T) = \beta_{0v} \cdot \frac{T_{cv} \cdot T_{Dv}}{T^2} \end{cases}$$

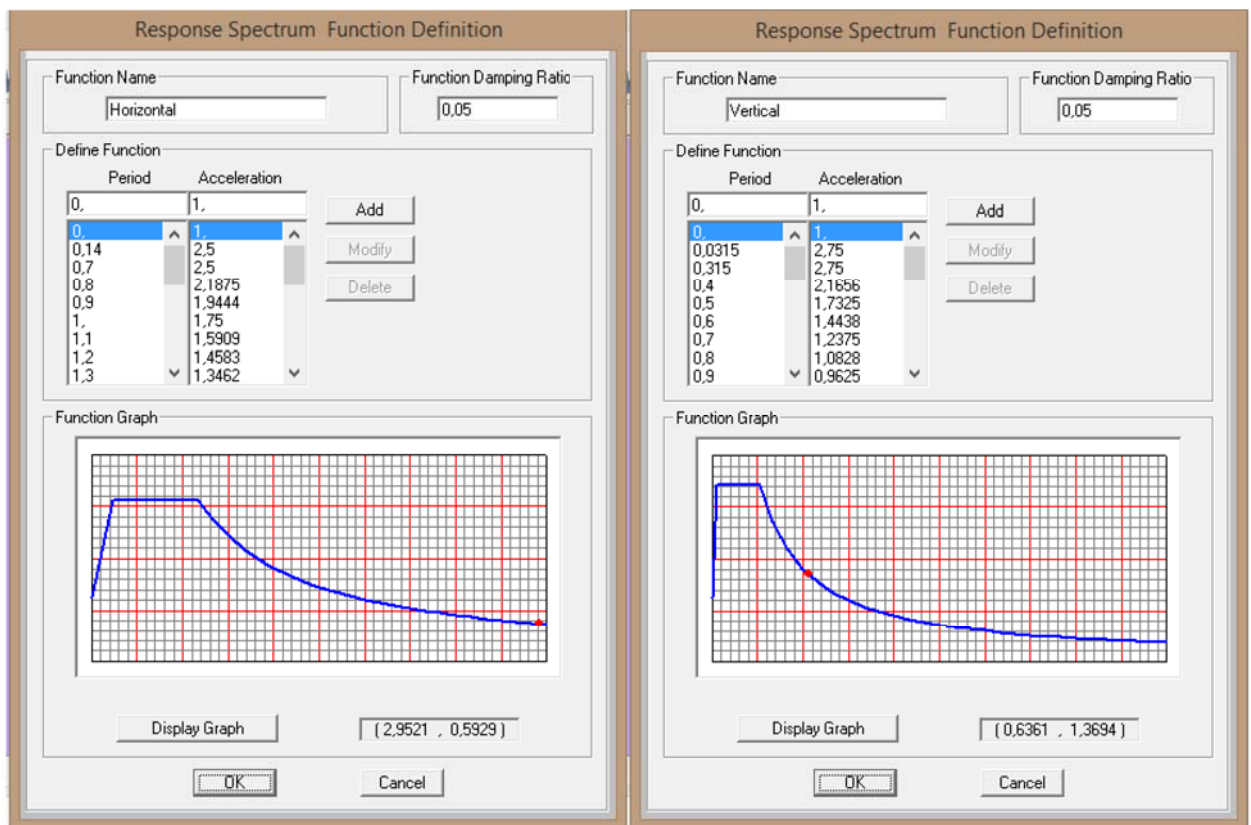
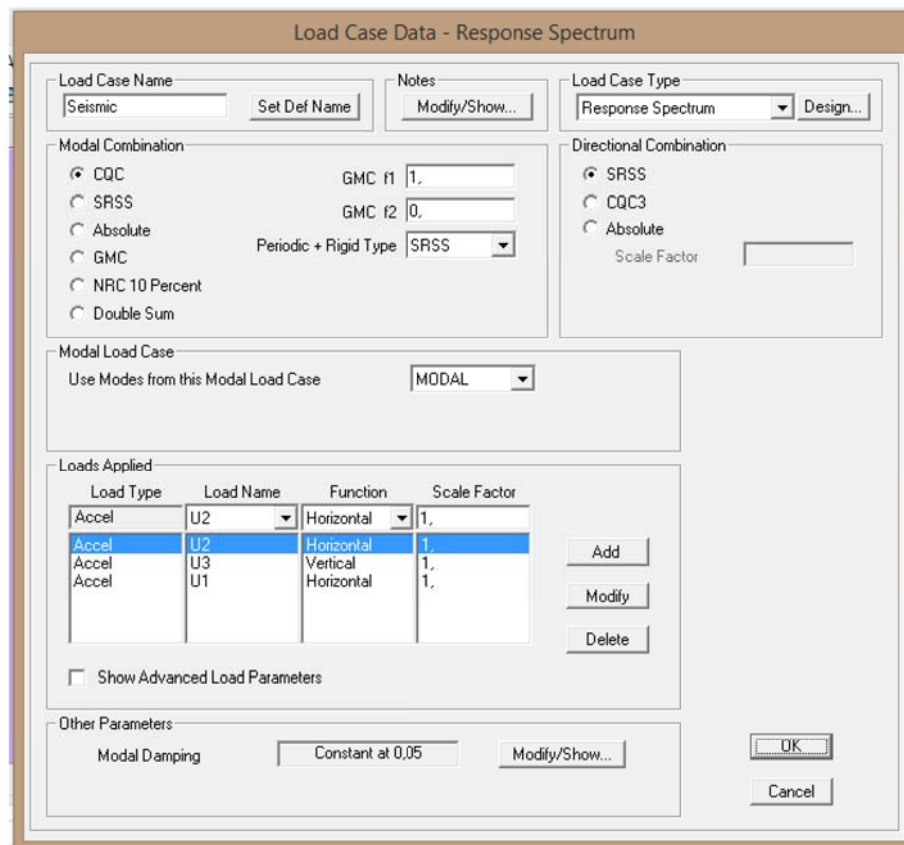


Figure 46. Horizontal and vertical response spectrums for seismic loading



Load Case Data - Response Spectrum

Load Case Name: Seismic | Set Def Name | Notes: Modify/Show... | Load Case Type: Response Spectrum | Design...

Modal Combination: ☒ CQC | GMC f1: 1. | ☐ SRSS | GMC f2: 0. | ☐ Absolute | Periodic + Rigid Type: SRSS | ☐ GMC | ☐ NRC 10 Percent | ☐ Double Sum

Directional Combination: ☒ SRSS | ☐ CQC3 | ☐ Absolute | Scale Factor:

Modal Load Case: Use Modes from this Modal Load Case: MODAL

Load Type	Load Name	Function	Scale Factor
Accel	U2	Horizontal	1.
Accel	U2	Horizontal	1.
Accel	U3	Vertical	1.
Accel	U1	Horizontal	1.

☐ Show Advanced Load Parameters

Other Parameters: Modal Damping: Constant at 0.05 | Modify/Show... | OK | Cancel

Figure 47. Load case data for seismic loading

5.2.5. Load combinations

Load combinations that are used in simulation:

	Combination		Code
ULS	$1.35 \cdot D + 1.5 \cdot L$	$1.35 \cdot D + 1.5 \cdot (L_1 + L_r)$	COMB1
		$1.35 \cdot D + 1.5 \cdot (L_2 + L_r)$	COMB2
		$1.35 \cdot D + 1.5 \cdot (L_3 + L_r)$	COMB3
	$1.35 \cdot D + 1.5 \cdot W$	$1.35 \cdot D + 1.5 \cdot W_x$	COMB4
		$1.35 \cdot D + 1.5 \cdot W_y$	COMB5
		$1.35 \cdot D + 1.5 \cdot W_z$	COMB6
	$1.35 \cdot D + 1.5 \cdot L + 1.05 \cdot W$	$1.35 \cdot D + 1.5 \cdot (L_1 + L_r) + 1.05 \cdot W_x$	COMB7
		$1.35 \cdot D + 1.5 \cdot (L_2 + L_r) + 1.05 \cdot W_x$	COMB8
		$1.35 \cdot D + 1.5 \cdot (L_3 + L_r) + 1.05 \cdot W_x$	COMB9
		$1.35 \cdot D + 1.5 \cdot (L_1 + L_r) + 1.05 \cdot W_y$	COMB10
		$1.35 \cdot D + 1.5 \cdot (L_2 + L_r) + 1.05 \cdot W_y$	COMB11
		$1.35 \cdot D + 1.5 \cdot (L_3 + L_r) + 1.05 \cdot W_y$	COMB12
		$1.35 \cdot D + 1.5 \cdot (L_1 + L_r) + 1.05 \cdot W_z$	COMB13
		$1.35 \cdot D + 1.5 \cdot (L_2 + L_r) + 1.05 \cdot W_z$	COMB14
		$1.35 \cdot D + 1.5 \cdot (L_3 + L_r) + 1.05 \cdot W_z$	COMB15
	$1.35 \cdot D + 1.05 \cdot L + 1.5 \cdot W$	$1.35 \cdot D + 1.05 \cdot (L_1 + L_r) + 1.5 \cdot W_x$	COMB16
		$1.35 \cdot D + 1.05 \cdot (L_2 + L_r) + 1.5 \cdot W_x$	COMB17
		$1.35 \cdot D + 1.05 \cdot (L_3 + L_r) + 1.5 \cdot W_x$	COMB18
		$1.35 \cdot D + 1.05 \cdot (L_1 + L_r) + 1.5 \cdot W_y$	COMB19
		$1.35 \cdot D + 1.05 \cdot (L_2 + L_r) + 1.5 \cdot W_y$	COMB20
		$1.35 \cdot D + 1.05 \cdot (L_3 + L_r) + 1.5 \cdot W_y$	COMB21
		$1.35 \cdot D + 1.05 \cdot (L_1 + L_r) + 1.5 \cdot W_z$	COMB22
		$1.35 \cdot D + 1.05 \cdot (L_2 + L_r) + 1.5 \cdot W_z$	COMB23
		$1.35 \cdot D + 1.05 \cdot (L_3 + L_r) + 1.5 \cdot W_z$	COMB24
SLS	$1.0 \cdot D + 1.0 \cdot L$	$1.0 \cdot D + 1.0 \cdot (L_1 + L_r)$	COMB25
		$1.0 \cdot D + 1.0 \cdot (L_2 + L_r)$	COMB26
		$1.0 \cdot D + 1.0 \cdot (L_3 + L_r)$	COMB27
	$1.0 \cdot D + 1.0 \cdot W$	$1.0 \cdot D + 1.0 \cdot W_x$	COMB28
		$1.0 \cdot D + 1.0 \cdot W_y$	COMB29
		$1.0 \cdot D + 1.0 \cdot W_z$	COMB30
	$1.0 \cdot D + 1.0 \cdot L + 0.7 \cdot W$	$1.0 \cdot D + 1.0 \cdot (L_1 + L_r) + 0.7 \cdot W_x$	COMB31
		$1.0 \cdot D + 1.0 \cdot (L_2 + L_r) + 0.7 \cdot W_x$	COMB32
		$1.0 \cdot D + 1.0 \cdot (L_3 + L_r) + 0.7 \cdot W_x$	COMB33
		$1.0 \cdot D + 1.0 \cdot (L_1 + L_r) + 0.7 \cdot W_y$	COMB34
		$1.0 \cdot D + 1.0 \cdot (L_2 + L_r) + 0.7 \cdot W_y$	COMB35
		$1.0 \cdot D + 1.0 \cdot (L_3 + L_r) + 0.7 \cdot W_y$	COMB36
		$1.0 \cdot D + 1.0 \cdot (L_1 + L_r) + 0.7 \cdot W_z$	COMB37
		$1.0 \cdot D + 1.0 \cdot (L_2 + L_r) + 0.7 \cdot W_z$	COMB38
		$1.0 \cdot D + 1.0 \cdot (L_3 + L_r) + 0.7 \cdot W_z$	COMB39
	$1.0 \cdot D + 0.7 \cdot L + 1.0 \cdot W$	$1.0 \cdot D + 0.7 \cdot (L_1 + L_r) + 1.0 \cdot W_x$	COMB40
		$1.0 \cdot D + 0.7 \cdot (L_2 + L_r) + 1.0 \cdot W_x$	COMB41
		$1.0 \cdot D + 0.7 \cdot (L_3 + L_r) + 1.0 \cdot W_x$	COMB42
		$1.0 \cdot D + 0.7 \cdot (L_1 + L_r) + 1.0 \cdot W_y$	COMB43
		$1.0 \cdot D + 0.7 \cdot (L_2 + L_r) + 1.0 \cdot W_y$	COMB44
		$1.0 \cdot D + 0.7 \cdot (L_3 + L_r) + 1.0 \cdot W_y$	COMB45
		$1.0 \cdot D + 0.7 \cdot (L_1 + L_r) + 1.0 \cdot W_z$	COMB46
		$1.0 \cdot D + 0.7 \cdot (L_2 + L_r) + 1.0 \cdot W_z$	COMB47
		$1.0 \cdot D + 0.7 \cdot (L_3 + L_r) + 1.0 \cdot W_z$	COMB48
Seismic	$1.0 \cdot D + 1.0 \cdot S$	$1.0 \cdot D + 1.0 \cdot S$	COMB49

5.2.6. Main beam with steel plates as a web

As a main model for the simulation of all combinations of loadings, the plate model of the bridge is used. Trapezoidal sheeting acting as a web in main beams is conformed to the plate structure of the beam with the steel plates. The thickness of the steel plates is calculated according to the necessity to have the same geometrical parameters as the CWB cross-section has. The calculation is presented in an Annex 1.

The final cross-section of the main beams is presented on Figure 48:

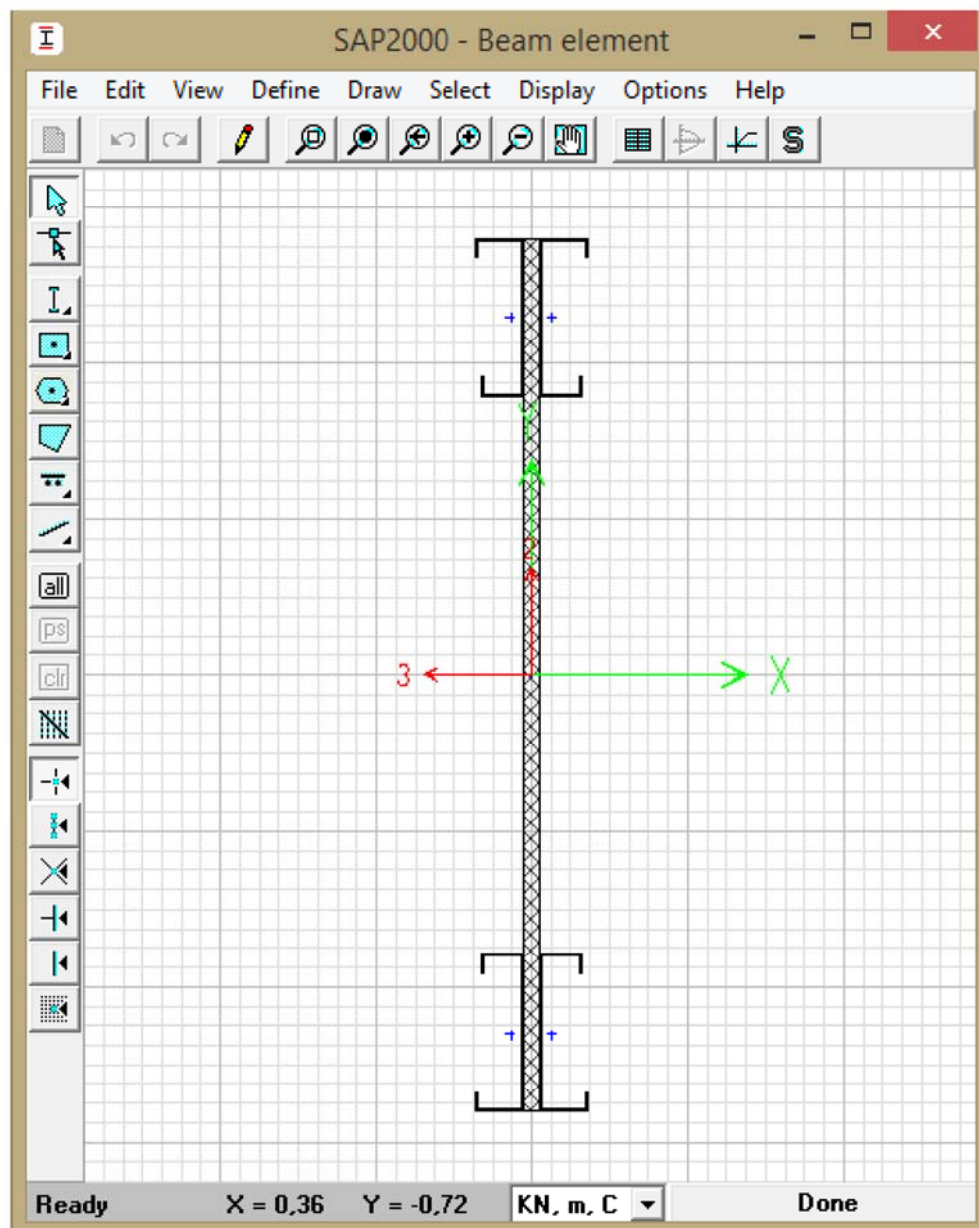


Figure 48. The cross-section of the main beam with plate web

Results of analysis are presented below.

The allowable deflection is $L/500$ or 44 mm. The deflection at the midspan is 35 mm (Figure 49), which is on the safe side.

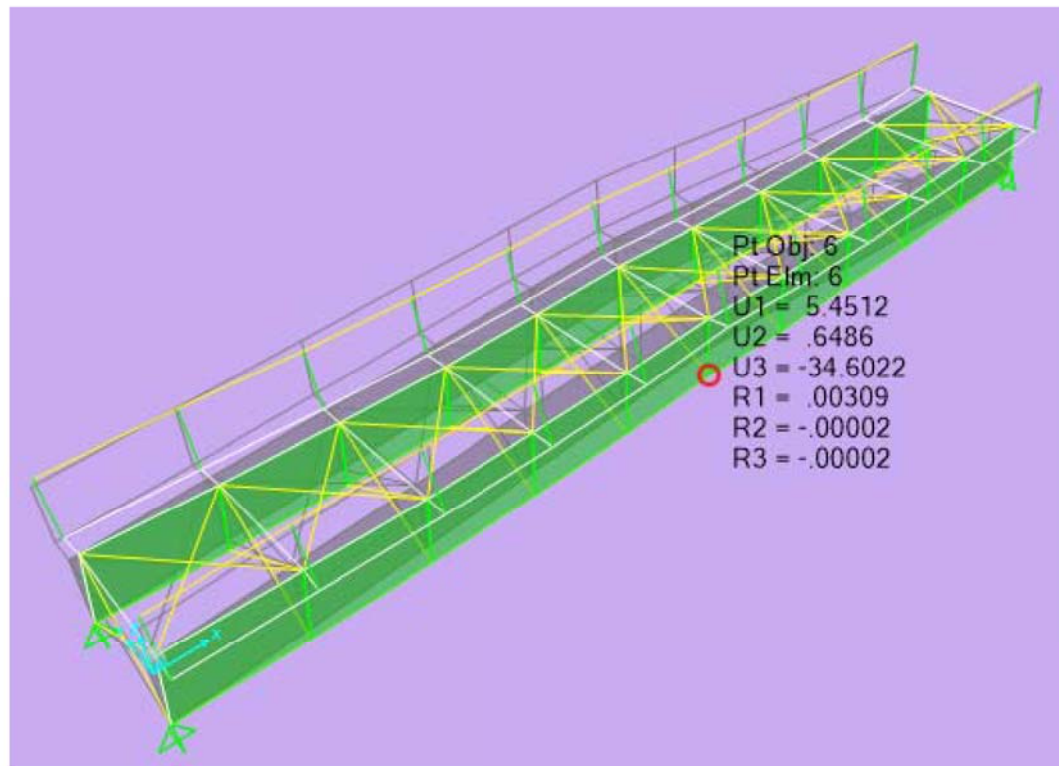
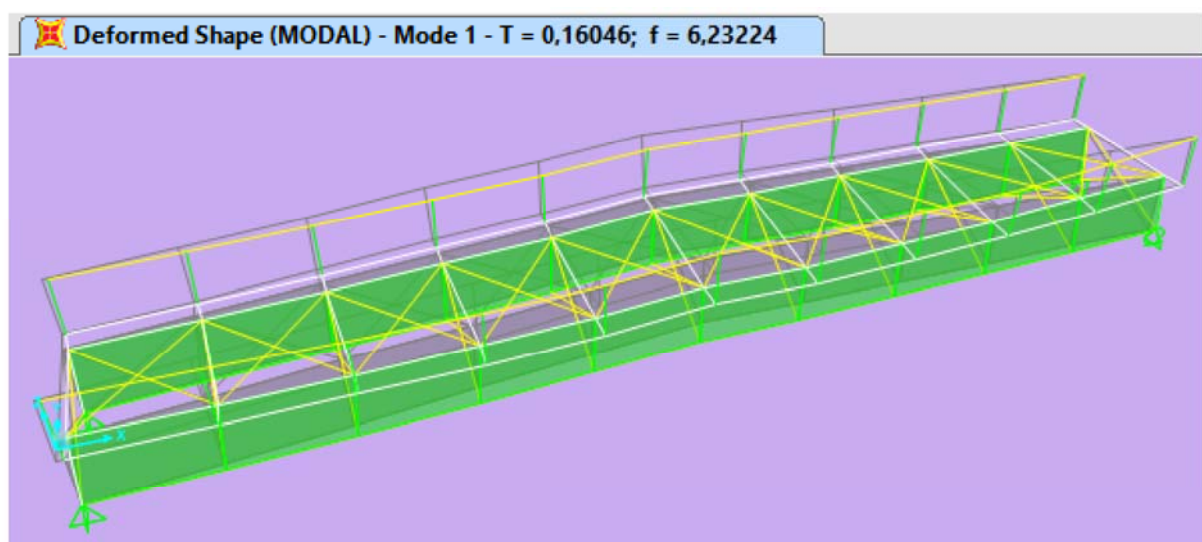
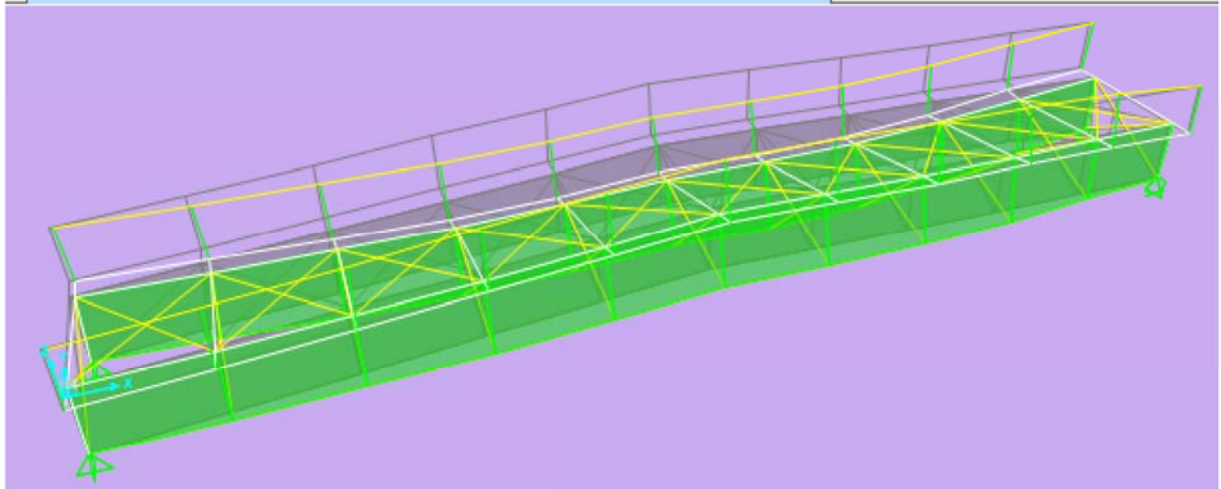


Figure 49. Deflection at the midspan in the shell structure (COMB1)

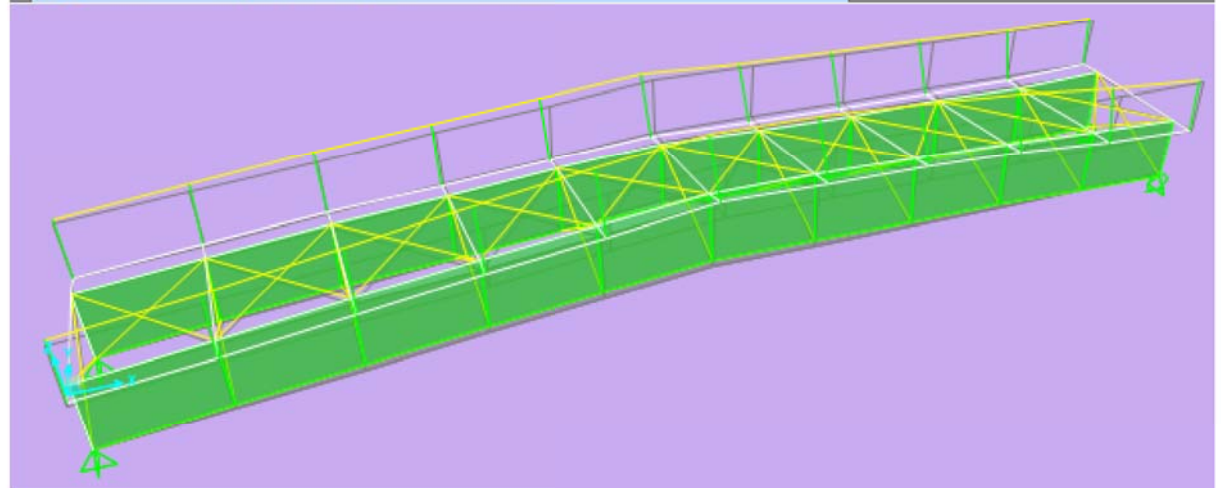
The results of modal analysis



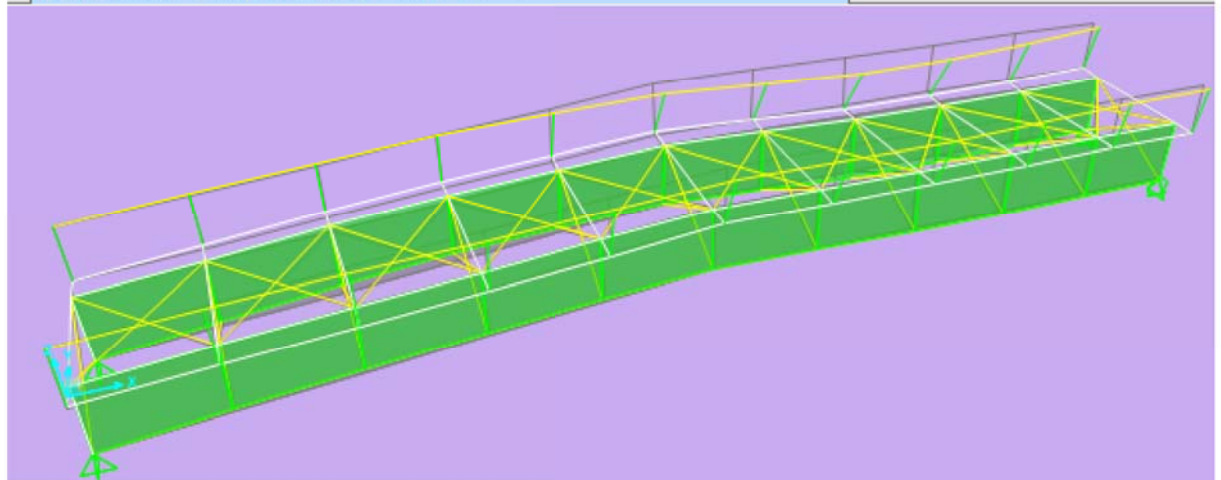
Deformed Shape (MODAL) - Mode 2 - $T = 0,15952$; $f = 6,26897$



Deformed Shape (MODAL) - Mode 3 - $T = 0,08384$; $f = 11,92766$



Deformed Shape (MODAL) - Mode 4 - $T = 0,06492$; $f = 15,40425$



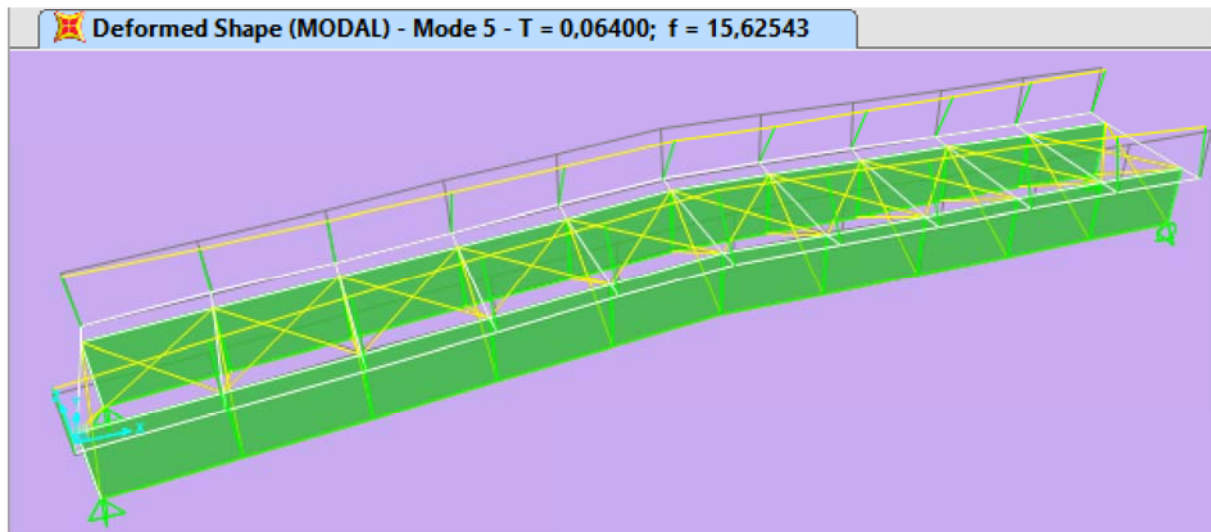


Figure 50. Results of modal analysis of the plate model

As we can see, the minimum natural frequency of the structure is higher than the minimum required natural frequency of 5 Hz.

The results of section design are presented in ANNEX 2.

5.2.7. Main beams with linear elements

It is important to keep in mind that the behavior of the linear model will not reproduce the behavior of the model with plate elements. In order to verify the response of these two structures I make the comparison with the level of stresses in elements.

The model has been changed only in the way of main beams presenting – they are modelled as linear elements with the same (Figure 51) cross-section. Unfortunately, it is not possible to introduce transversal bracings into the structure. In this case, secondary beams are overstressed.

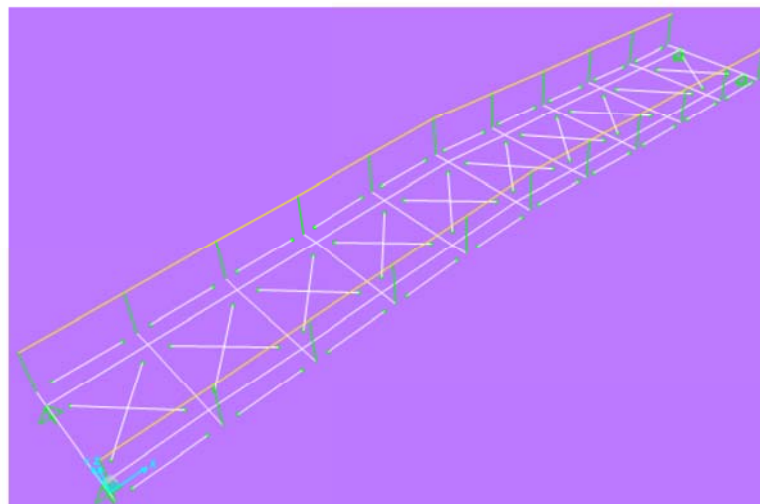


Figure 51. The linear elements model

The allowable deflection is 44 mm. The deflection at the midspan is 35 mm (Figure 52), which is on the safe side.

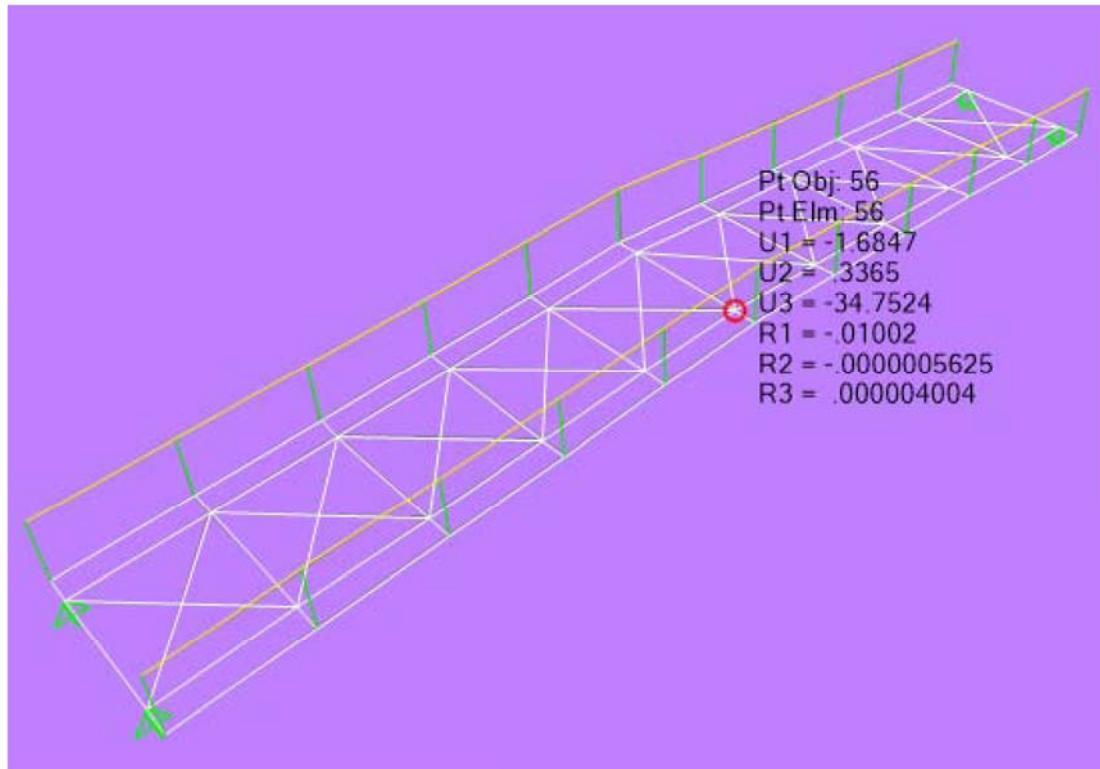


Figure 52. Deflection at the midspan in linear elements model (COMB1)

5.2.8. Truss main beams

It is self-evident that any construction has to be not only acceptable in the domain of resistance, stiffness and durability, but also it must be economically sound. Cost of the production, transportation, mounting, exploitation, maintenance and recycling should be taken into consideration from the beginning, during the phase of decision-making.

In this way, I transform the model changing the type of the main beams – trusses are used for the further analysis. According to the requirements, the height of the main beam is increased up to 2.2 meters as 1/10th part of the span.

The model objective is to achieve the same deflection under the combination COMB1:

$$1.35 \cdot D + 1.5 \cdot (L_1 + L_r)$$

Using the hot-rolled square hollow sections $\square 200 \times 8\text{mm}$ we achieved the midspan vertical deflection of 36.1 mm (Figure 53). The allowable deflection at the midspan is 44 mm, which is higher than the result.

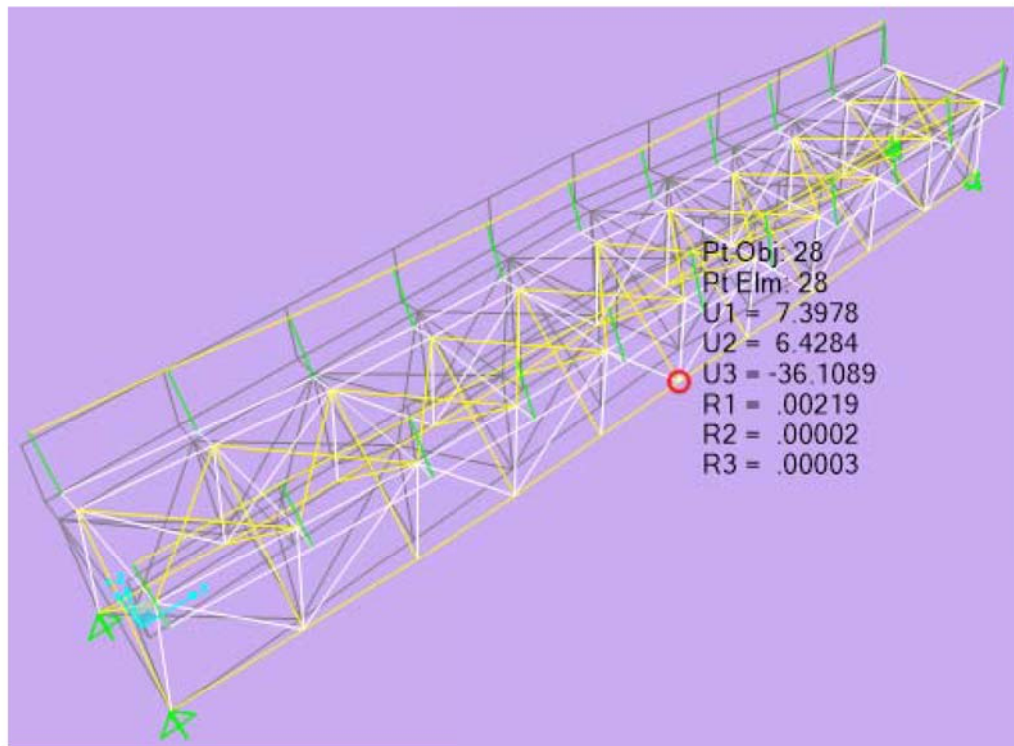


Figure 53. Deformed shape of the truss model under COMB1

For the economical comparison, I will use this model and, based on the quantity of materials and labor costs, I will compare the approximate costs for the bridge with truss main beams and bridge with corrugated web main beams (see Section 7).

5.3. Simulations in ABAQUS

5.3.1. Introduction

Due to the fact that the pedestrian bridge with corrugated web beams modelled in SAP2000 does not take into consideration the behavior of the screw and bolt connections (using fully rigid connections), the advanced numerical simulations have to be done in order to confirm the strength of the main beams and the deflections of the midspan within the allowed limits and prove the solution.

To obtain the behavior of the beam with corrugated webs, I will model one main beam with cambered profile (the slope is 3 degrees or 5 %).

5.3.2. Elements and assembly

The beam consists of following parts:

- 2 Corrugated sheet panels T50-250 – 0.7 mm (Figure 54);
- 4 Cold-formed lipped channels C250×3mm (Figure 55);
- 4 End shear panels made from steel sheets with a thickness of 2 mm (Figure 56);
- 2 Inverted V-shape intermediate connecting panels made from steel sheets with a thickness of 2 mm(Figure 56);
- 2 Supporting profiles (Figure 57);
- 1 I-shape intermediate connecting profile (Figure 57);
- 10 Cold-formed lipped channels U250×4mm;
- 6 Inverted V-shape welded connectors for the flanges made from steel sheets with a thickness of 4 mm.

The assembly of the CWB is presented on Figure 58.

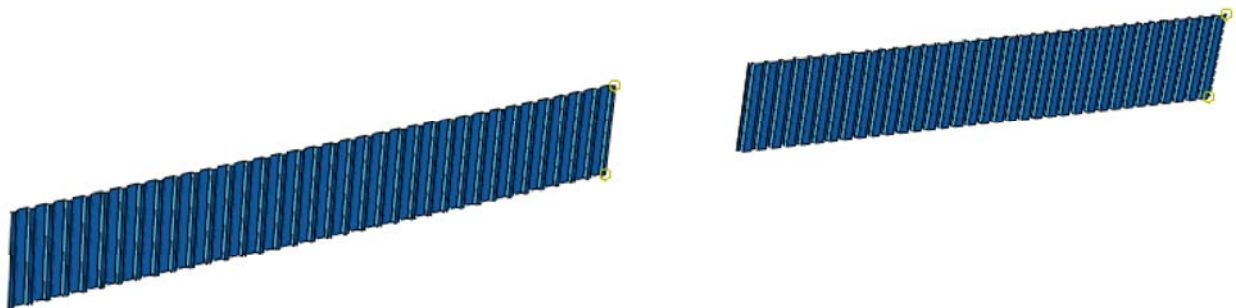


Figure 54. Trapezoidal sheets T50-250 – 0.7 mm

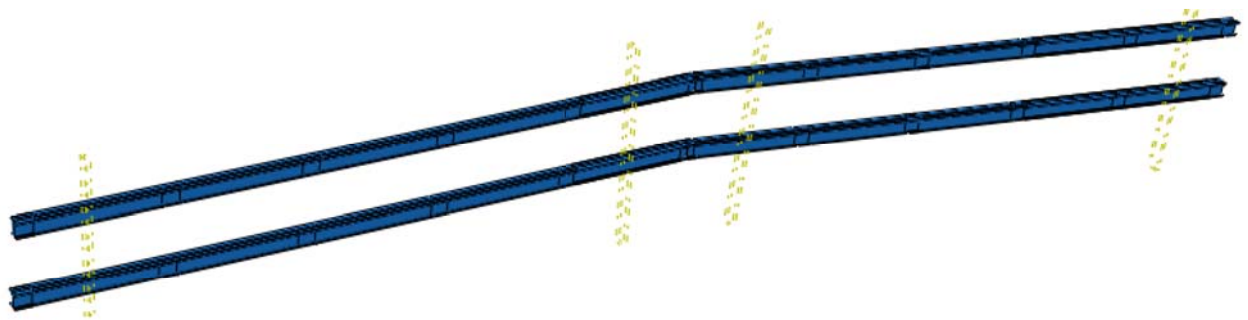


Figure 55. C250x3mm cold-formed profiles as flanges

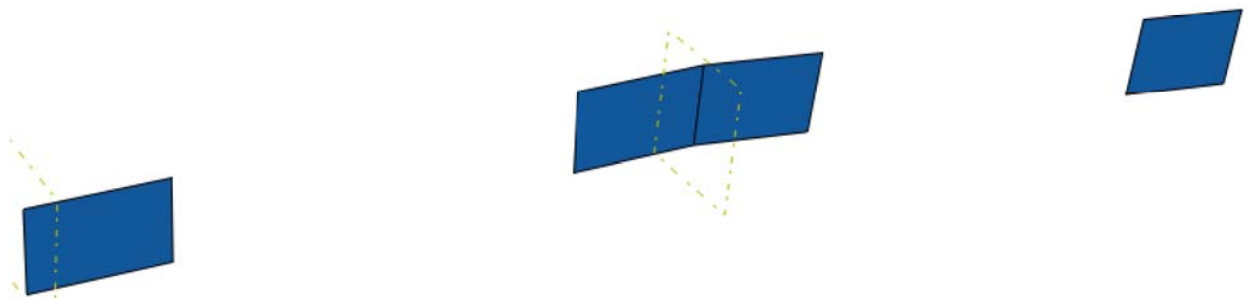


Figure 56. Shear plates and V-shape intermediate connecting profile

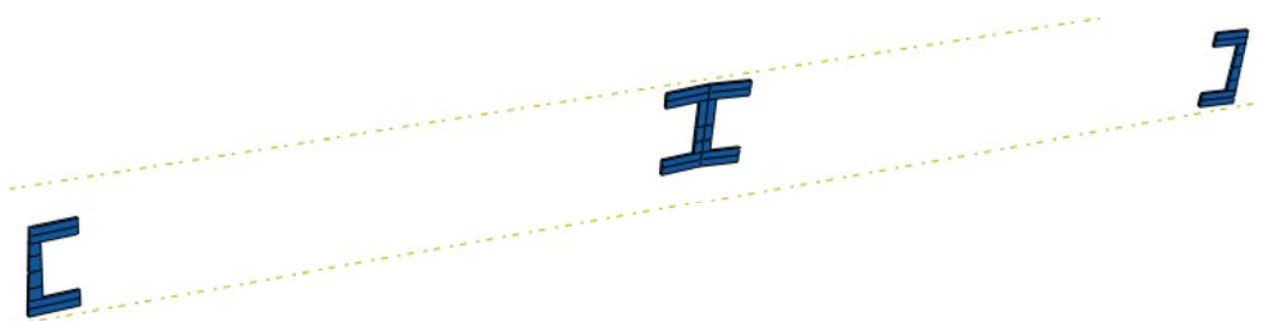


Figure 57. Supporting and I-shape intermediate connecting profiles

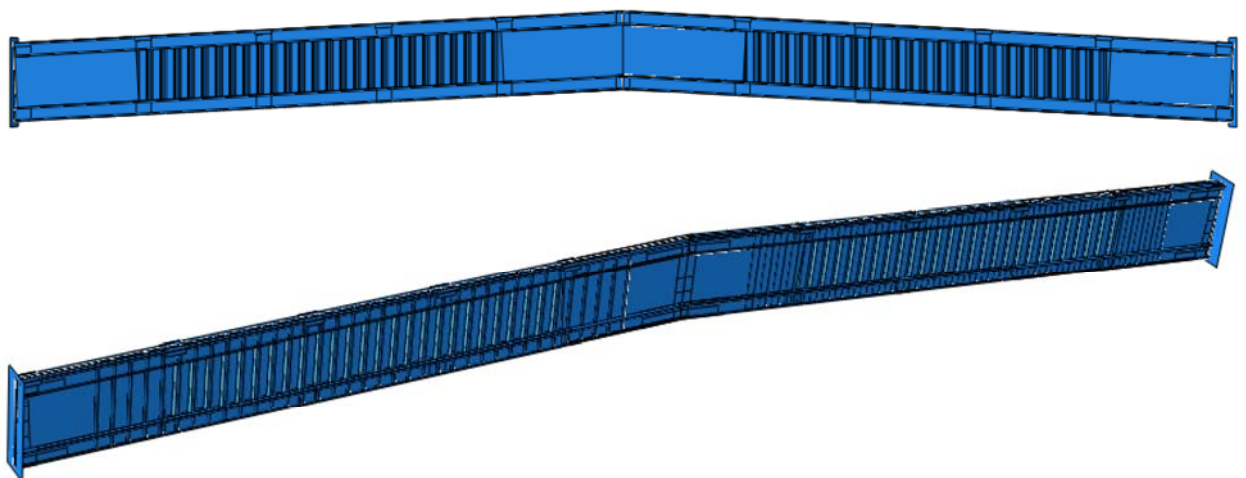


Figure 58. Main views of the CWB

5.3.3. Materials

For the entire beam steel S355 was used.

5.3.4. Loads

For the analysis, I subject the beam to only gravitational loads at the worst combination (see paragraph 5.2.4.). This combination is COMB1:

$$1.35 \cdot D + 1.5 \cdot L = 1.35 \cdot 0.6 \frac{kN}{m^2} + 1.5 \cdot 4.5 \frac{kN}{m^2} = 7.6 \frac{kN}{m^2}$$

Applying this distributed load on one beam, we have the force, acting on the entire beam:

$$R = \frac{1}{2} \left[7.6 \frac{kN}{m^2} \cdot 3.5 m \cdot 22 m \right] = 292.6 kN$$

In respect to the area of the surfaces, which are used for supporting the secondary beams at 11 equally positioned points along the beam, we have the values for pressure:

- for the intermediate supports:

$$p = \frac{292.6 kN}{0.07 m^2} = 0.24 MPa,$$

- for the central support:

$$p = \frac{292.6 kN}{0.154 m^2} = 0.05 MPa,$$

- for the supports at the end of the beam:

$$p = \frac{1}{2} \cdot 0.24 MPa = 0.12 MPa.$$

Load is applied as it is shown on the Figure 59, without following the rotation.

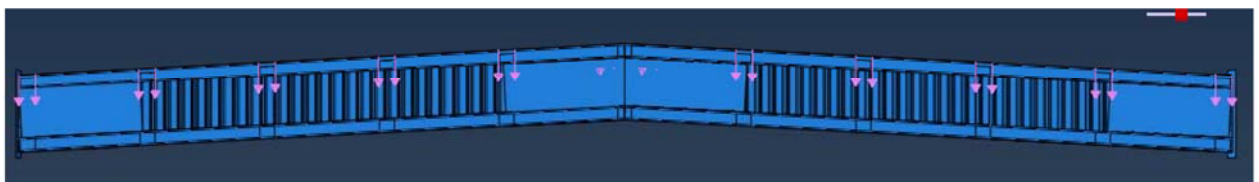


Figure 59. Load application scheme

5.3.5. Interaction

There are several types of interaction used in the model:

- Fasteners
- Couplings

The first type is used for modelling the behavior of the screw connections between elements of the beam:

- Supports with Shear Panels ("SuppShPl" group),
- Supports and Shear Panels with Flanges ("SuppFlange" group),
- Flanges with Corrugated Webs ("WebFlange" group),
- Shear and Intermediate Plates with Corrugated Webs ("WebPlate" group),
- Intermediate Connector with Plates ("SuppShPlate" group),
- Intermediate Connector and Plates with Flanges ("SuppFlange" group).

Detailed schemes of the connections are presented at the Figures 60 and 61 (attachment nodes are in green).

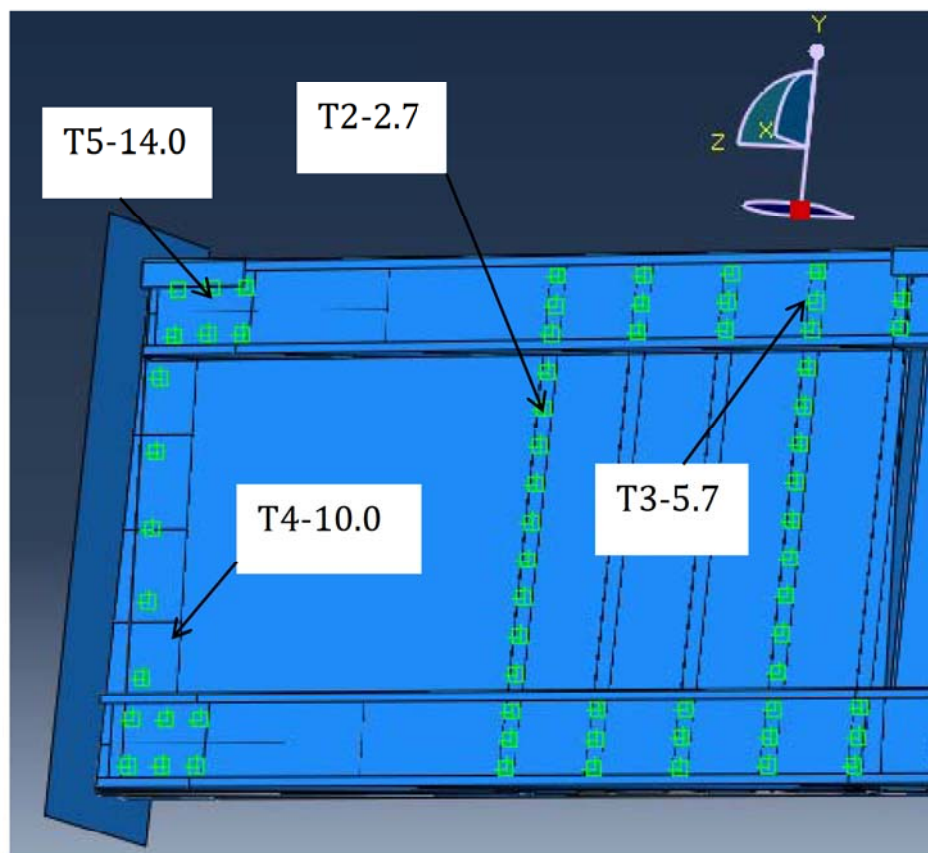


Figure 60. Detailed scheme of the connections at the support

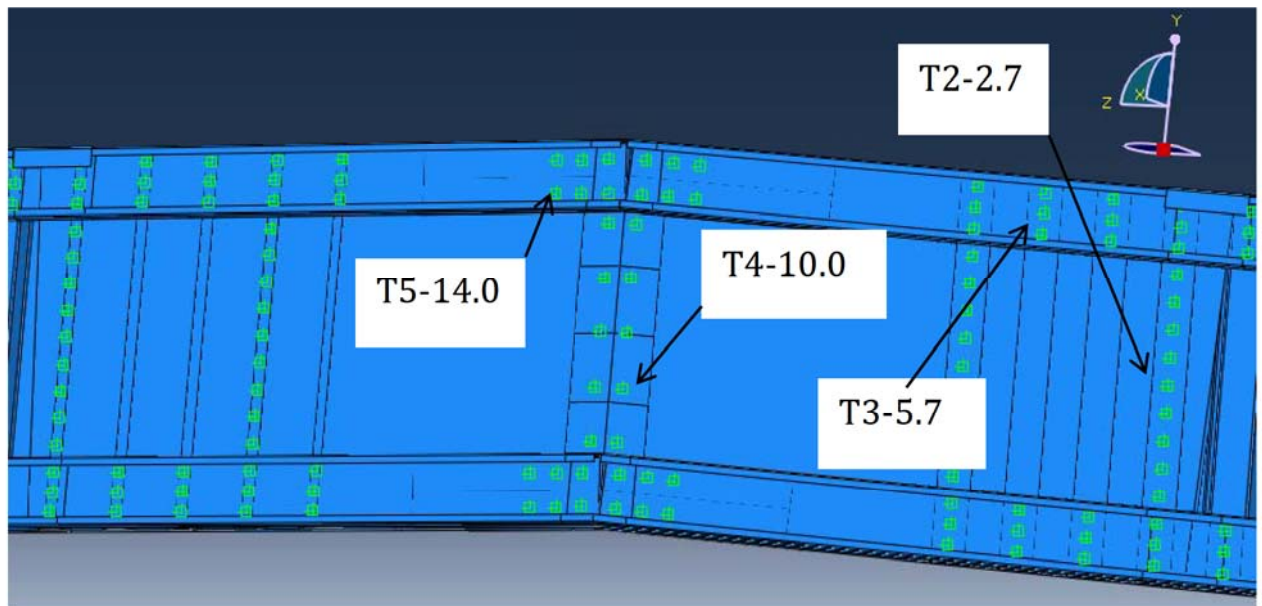


Figure 61. Detailed scheme of the connections at the midspan of the CWB

The characteristics of the connection assigned are based on the research made in “Politehnica” University of Timisoara. Six types of connections were tested according to ECCS publication No. 124 [12] in order to determine their behavior, at a loading velocity of 1 mm/min, and four of them were used:

- (2) T2-2.7, seam fasteners for shear plates and corrugated sheets;
- (3) T3-5.7, self-drilling screws for shear plates and flanges;
- (4) T4-14.0, self-drilling screws for shear plates and end supports;
- (5) T5-11.0, bolts for flanges to end-supports;

in order to determine the behavior of all types of connections found in the beam. Table 6 presents the tested specimens and the number of tests done for each typology, while Figure 62 presents the behavior of connections.

Table 6. Types of tested connections

Name	t_1 [mm]	t_2 [mm]	No. of tests	d_{nom} [mm]
T2-2.7	2.0	0.7	5	4.8
T3-5.7	2.0+3.0	0.7	6	6.3
T4-10.0	2.0	8.0	5	5.5
T5-14.0	2.0+3.0	8.0	5	M12
T6-2.7	2.0	0.7	10	6.3

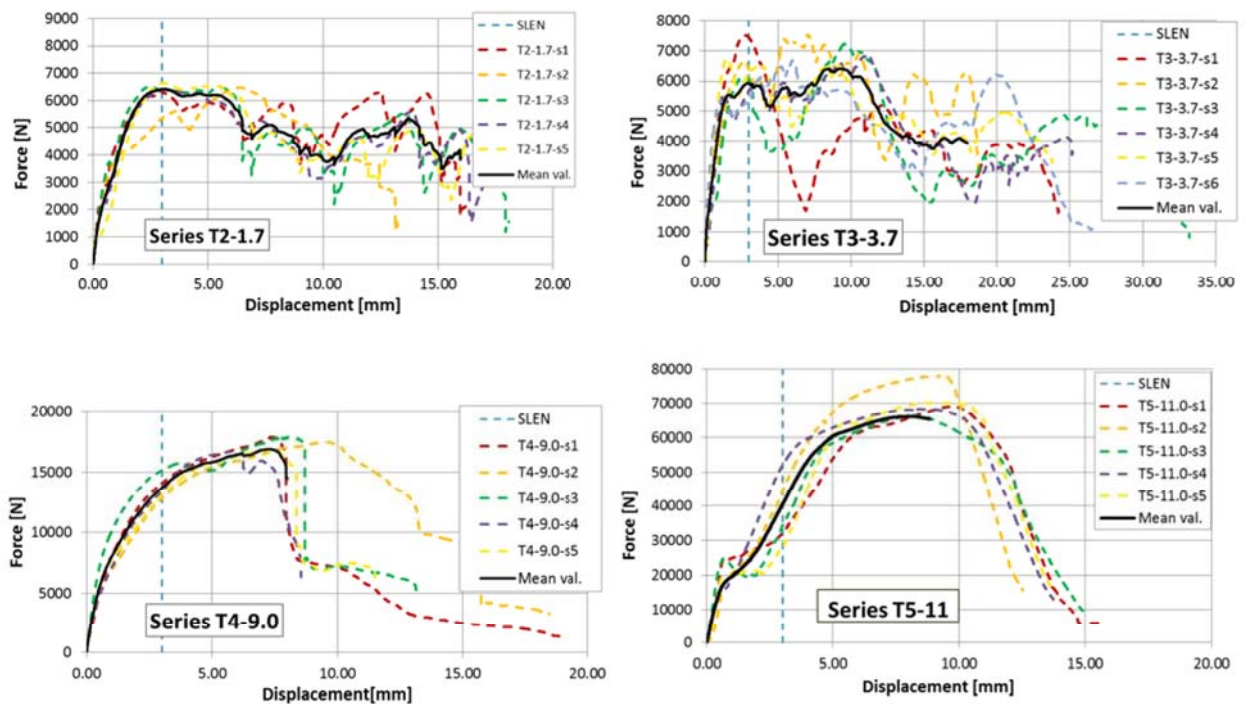


Figure 62. Force-displacement curves for the tested connections

Couplings “RP-101...RP-111” with kinematic type are representing the connection sections and influence of the transversal bracings.

Couplings are used for modelling of the connection of the U250×4 mm profiles below the secondary beams and pressure is set along those panels and for inverted V-shape welded connectors for flanges. Discretization method is “Surface to surface” with adjusting of the slave surface initial positions.

5.3.6. Mesh

Mesh is organized with rectangular elements, radiuses modelled with maximum deviation factor of 0.1, it means that the approximate number of elements per circle is 8 (see Figure 63).

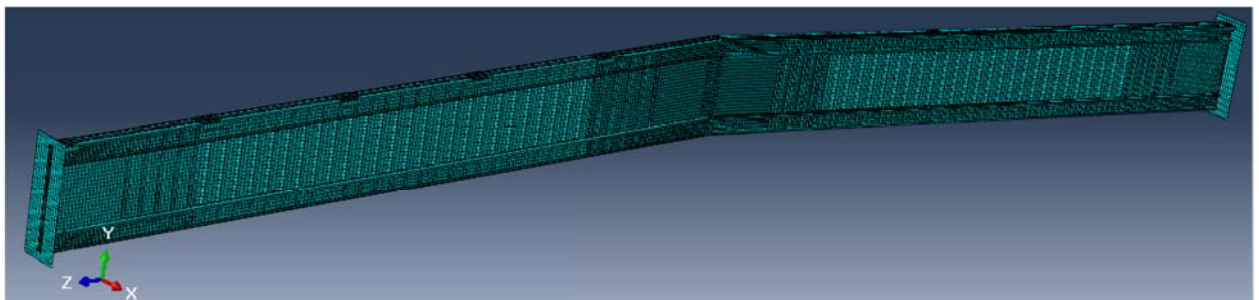


Figure 63. Mesh for the CWB

5.3.7. Restraints and boundary conditions

The beam is simply supported with the entire rotations unrestrained see Figure 64).

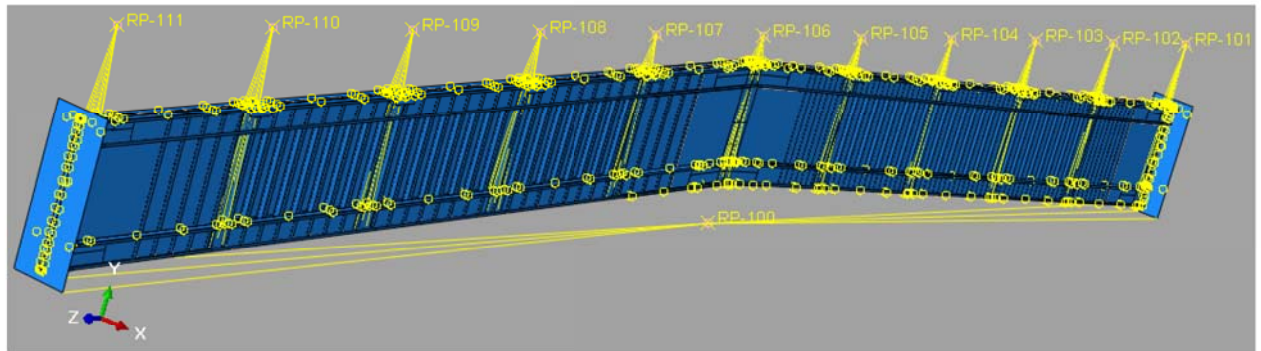


Figure 64. Restraints

For the modelling of the transversal bracings, it was used so called “Anti-LTB” boundary condition created at the first step – Step-1. In the nodal area of the bracing connector, I have:

- restrained the displacements along the X direction – the transversal displacements and along the Z direction – in the real construction two beams act and move in longitudinal direction simultaneously (see Figure 65) – for the top flanges;
- restrained the displacements along the Z direction – the transversal displacements only – for the bottom flanges.



Figure 65. The Anti-LTB boundary condition

As well, I create “ENCASTRE” boundary condition in which using the reference point for the “Support Set” we assign no displacements and no rotations for the reference point RP-100 (see Figure 64). Therefore, we have ENCASTRE ($U_1 = U_2 = U_3 = UR_1 = UR_2 = UR_3 = 0$) created at the initial stage and propagated to the Step-1.

5.3.8. Results of analysis

The results of the dynamic nonlinear analysis of the structure are presented below.

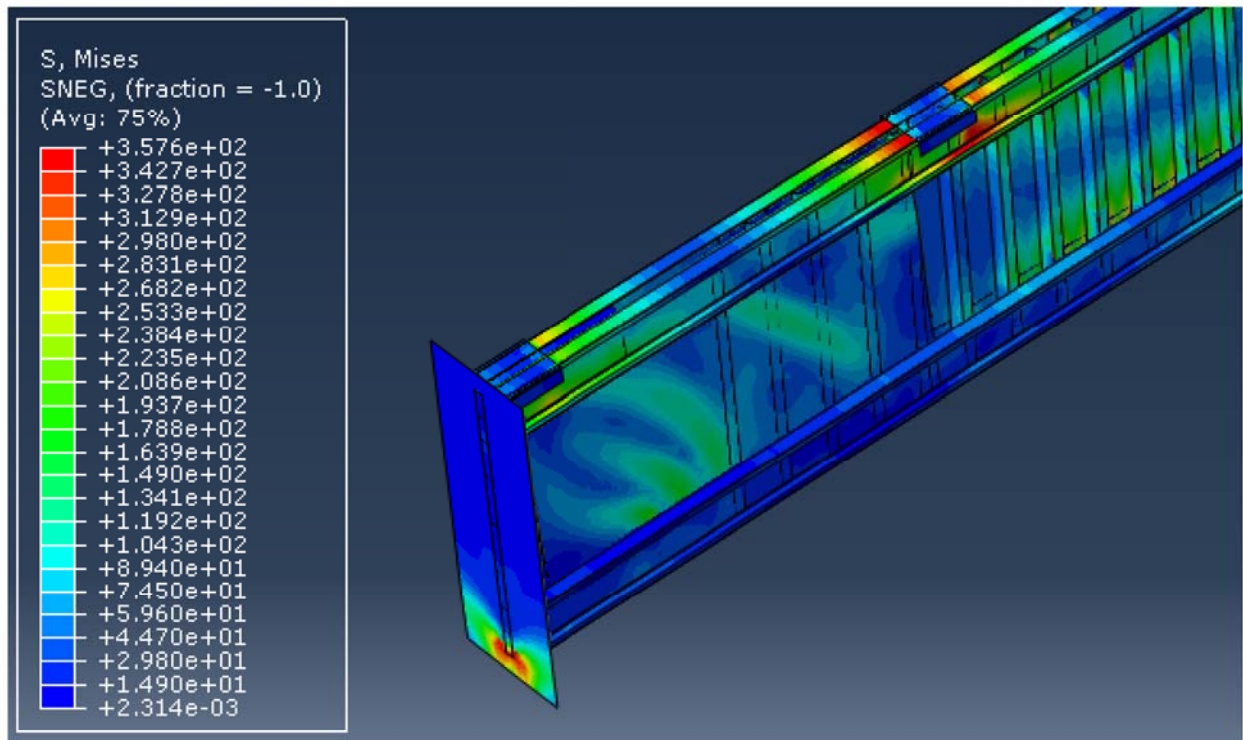


Figure 66. Von Mises stress distribution at the support

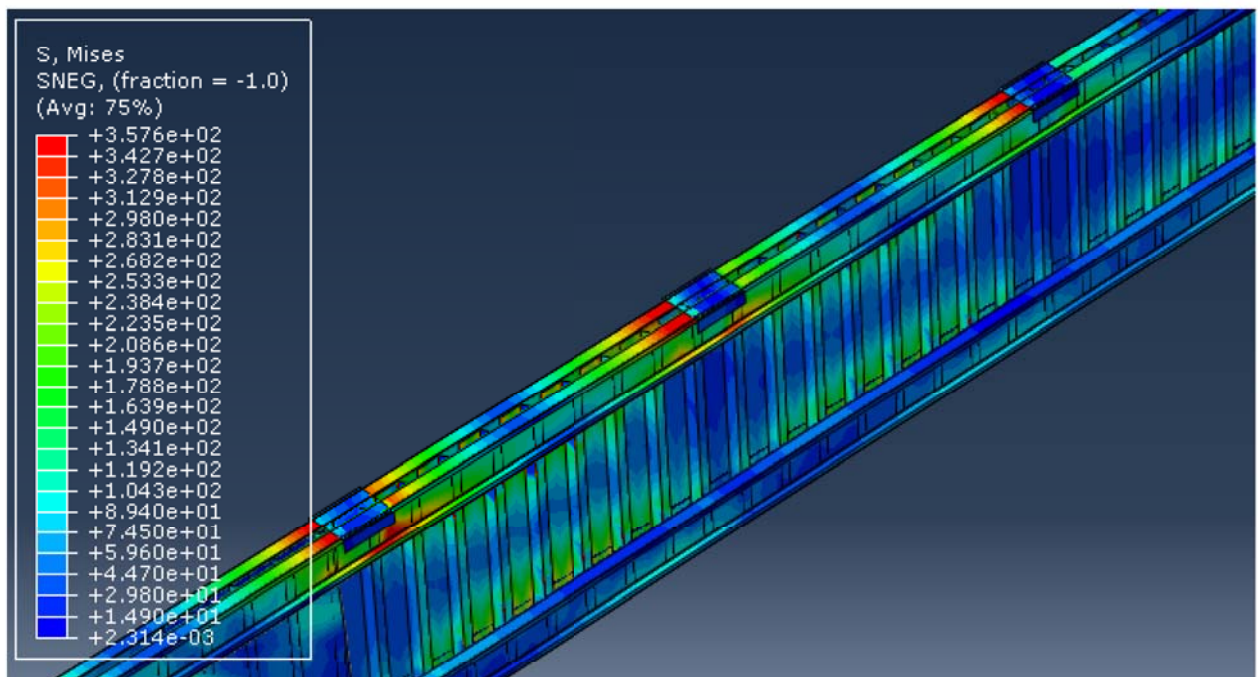


Figure 67. Von Mises stress distribution of the beam

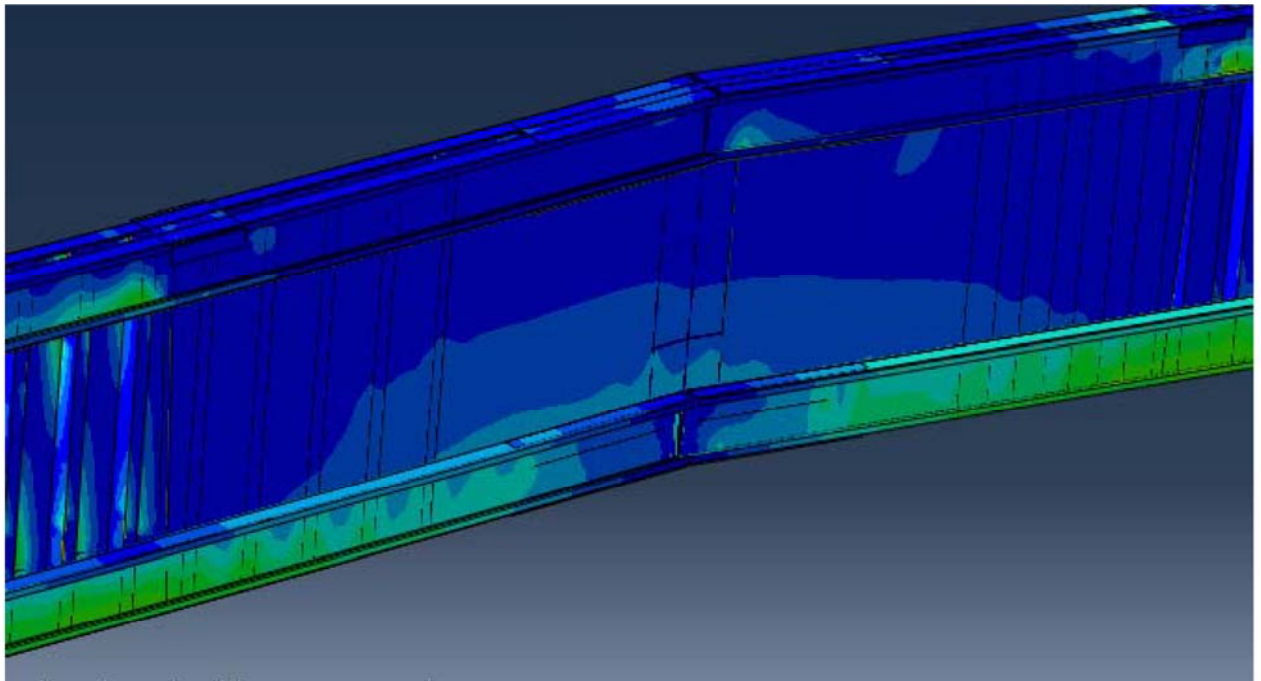


Figure 68. Von Mises stress distribution at the midspan

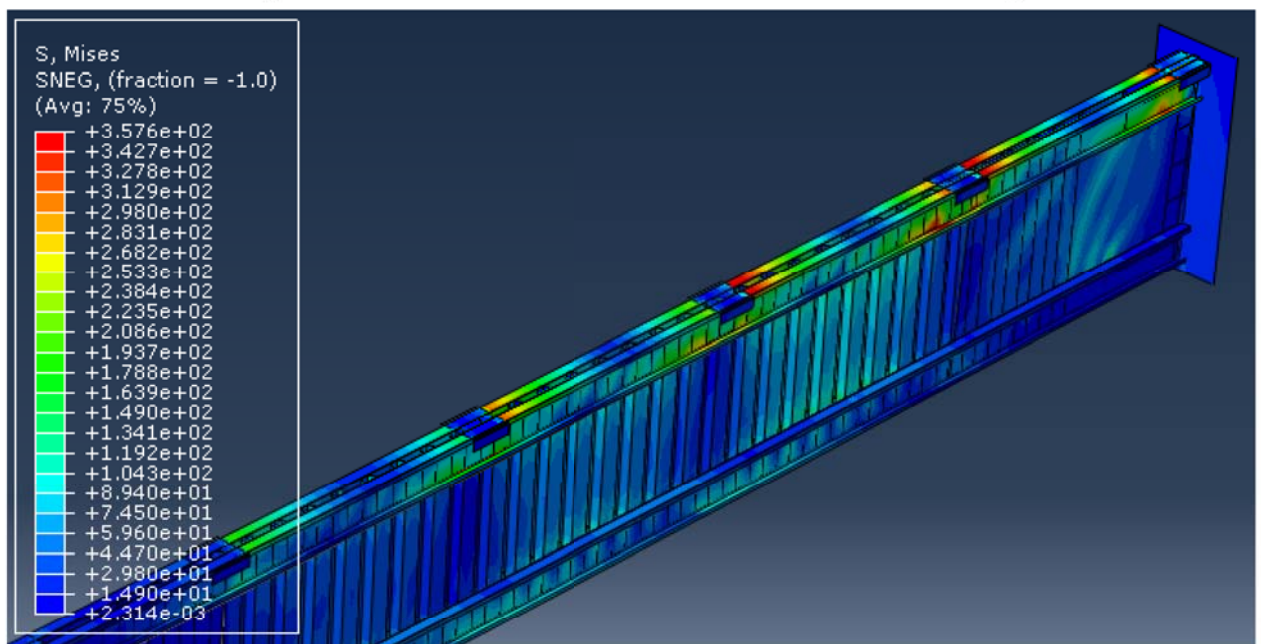


Figure 69. Von Mises stress distribution at the support

There are negligibly small amount of local plastic deformations:

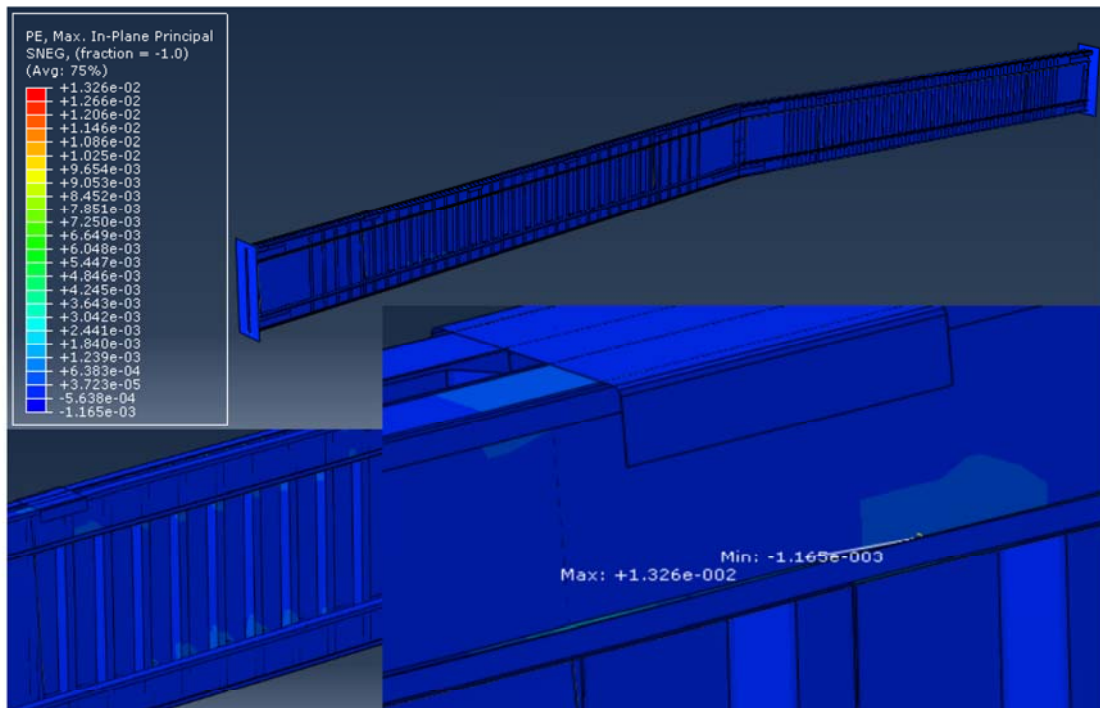


Figure 70. Local plasticity

To obtain the capacity of the beam I applied double load and plotted the Force-Displacement curve (Figure 71). The picture of stresses are presented after.

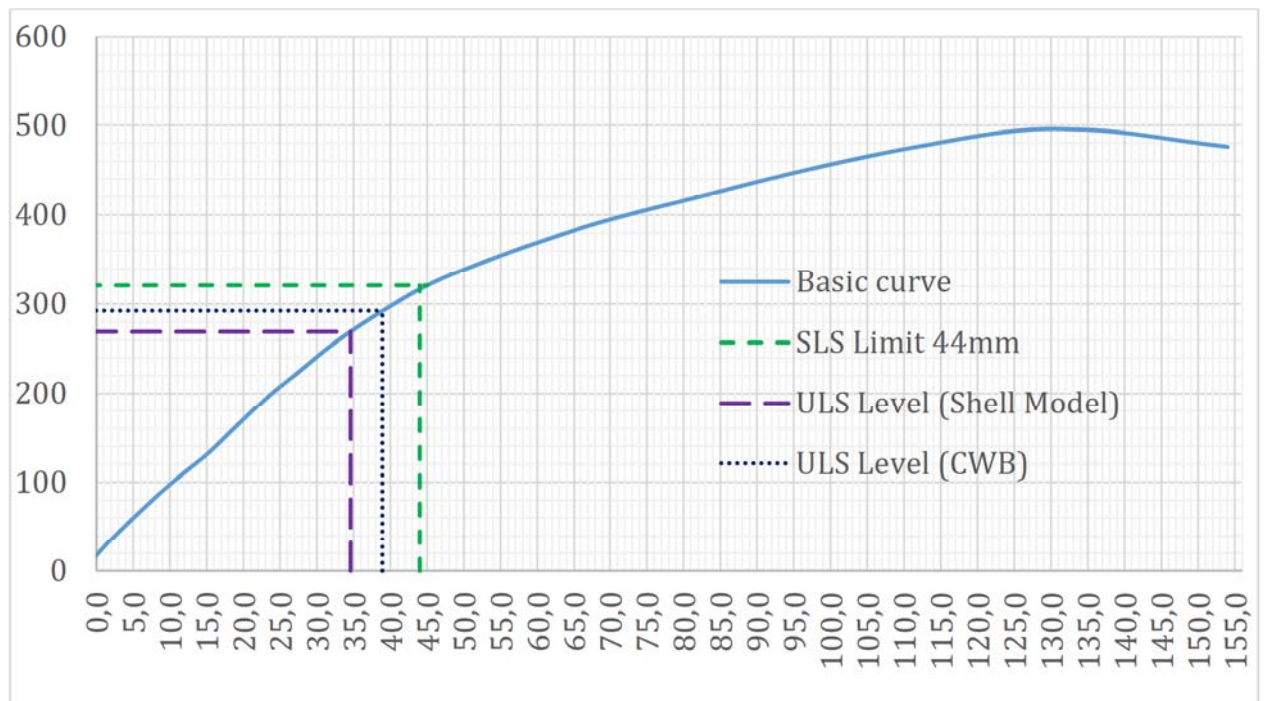


Figure 71. Force-displacement curve for CWB

From the graph we can observe, that introduction of the connection behavior increased the flexibility of the structure. Due to discrete elements, modelling and non-rigid connection the structural response is closer to the reality. Collapse appears at the displacement of 153 mm.

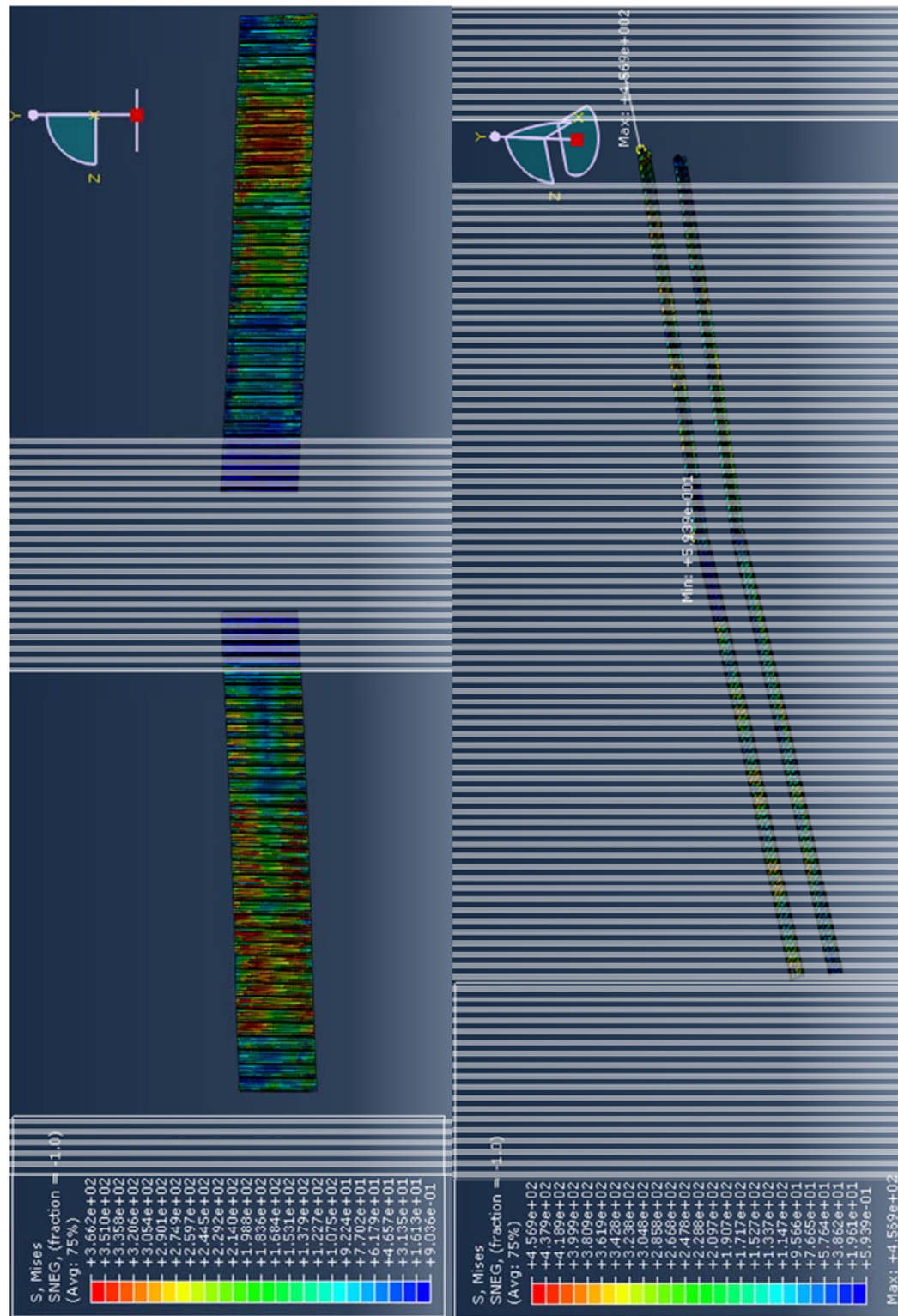


Figure 72. Stress distribution in corrugated webs and flanges

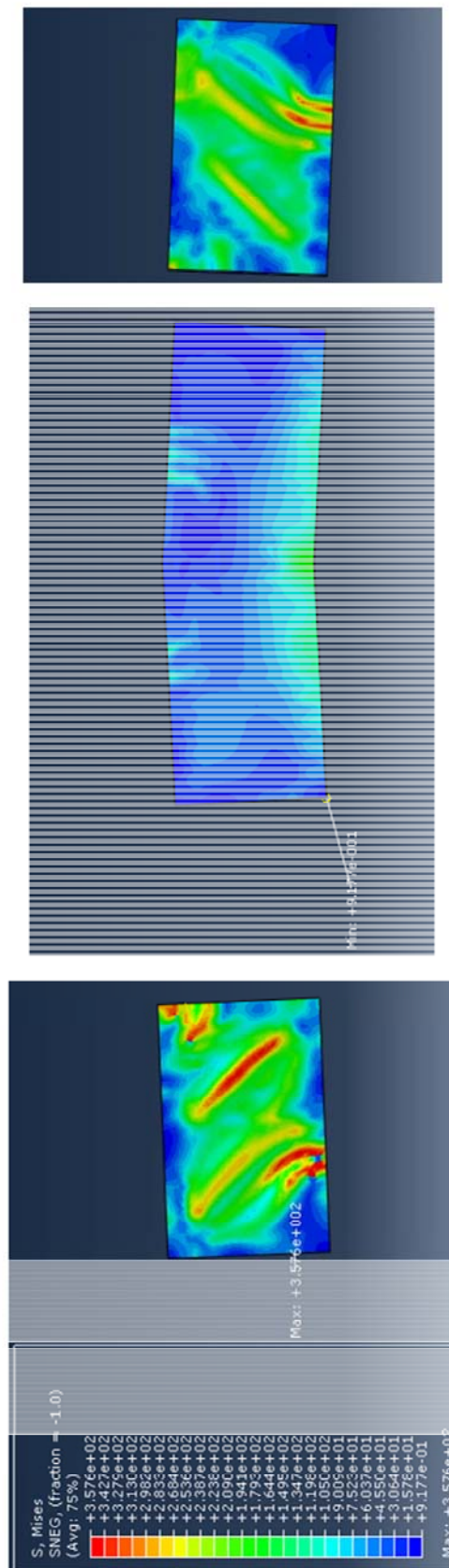


Figure 73. Stress distribution in shear plates

Deformations correspond to the buckling of shear panel combined with the distortion of the corrugated web (Figure 74).

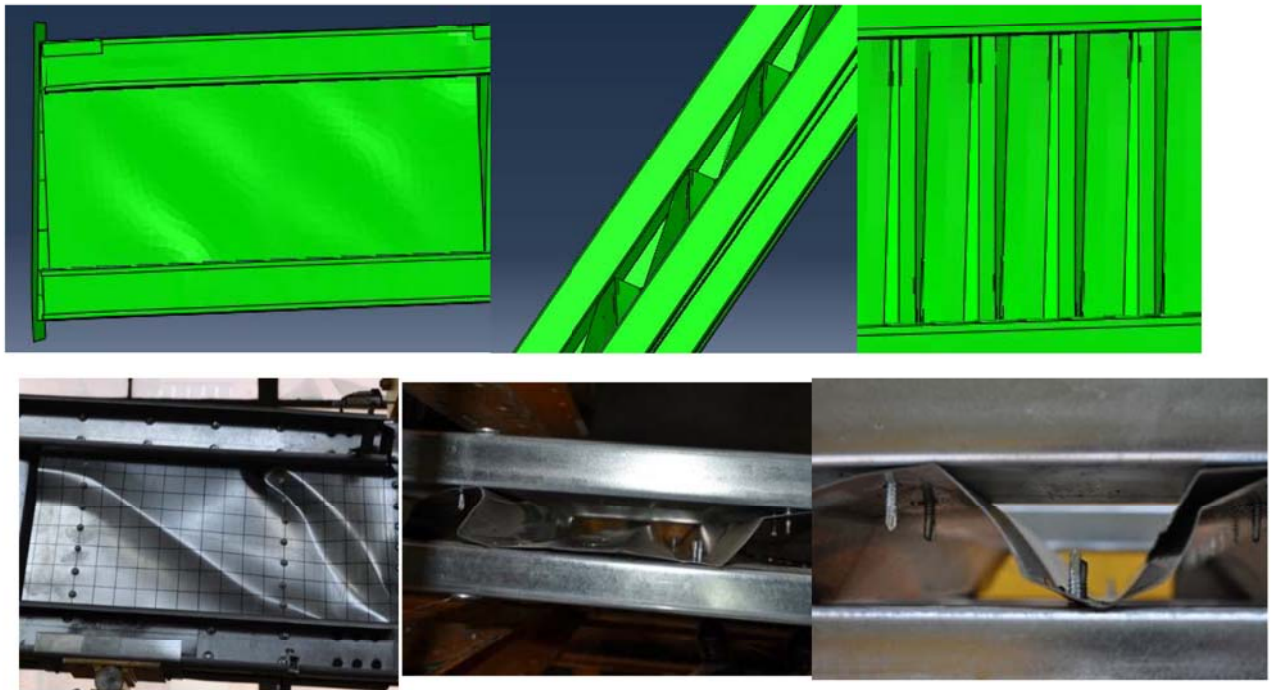


Figure 74. Deformed shape of the beam end shear panel and distortion of the web corrugation (Model and results of tests)

6. 3D Model of the bridge. Technical detailing.

The model is built in AutoCAD and TEKLA software and presented below with detailing of connections, supports and specific components.

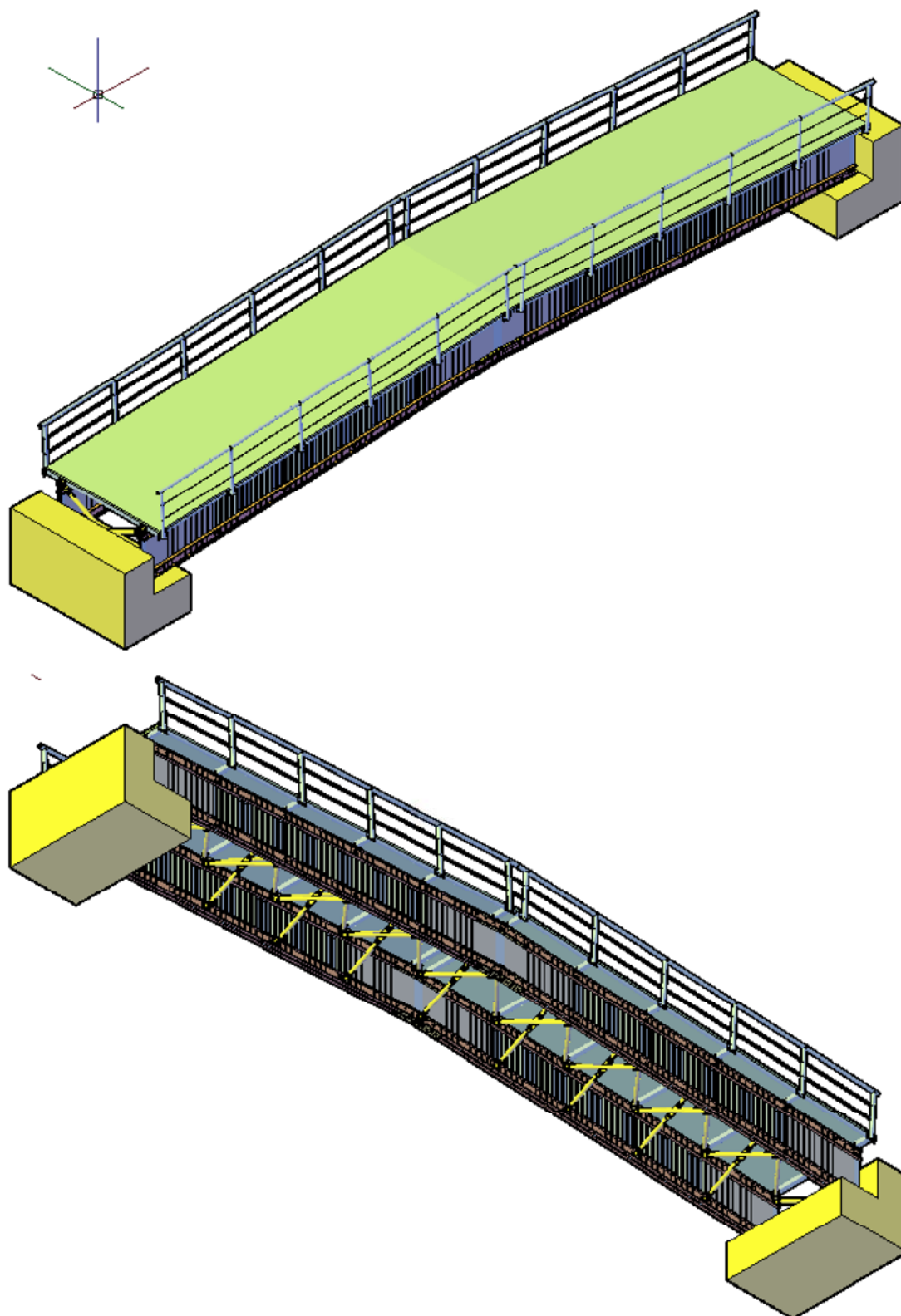


Figure 75. Main views of the CWB pedestrian bridge

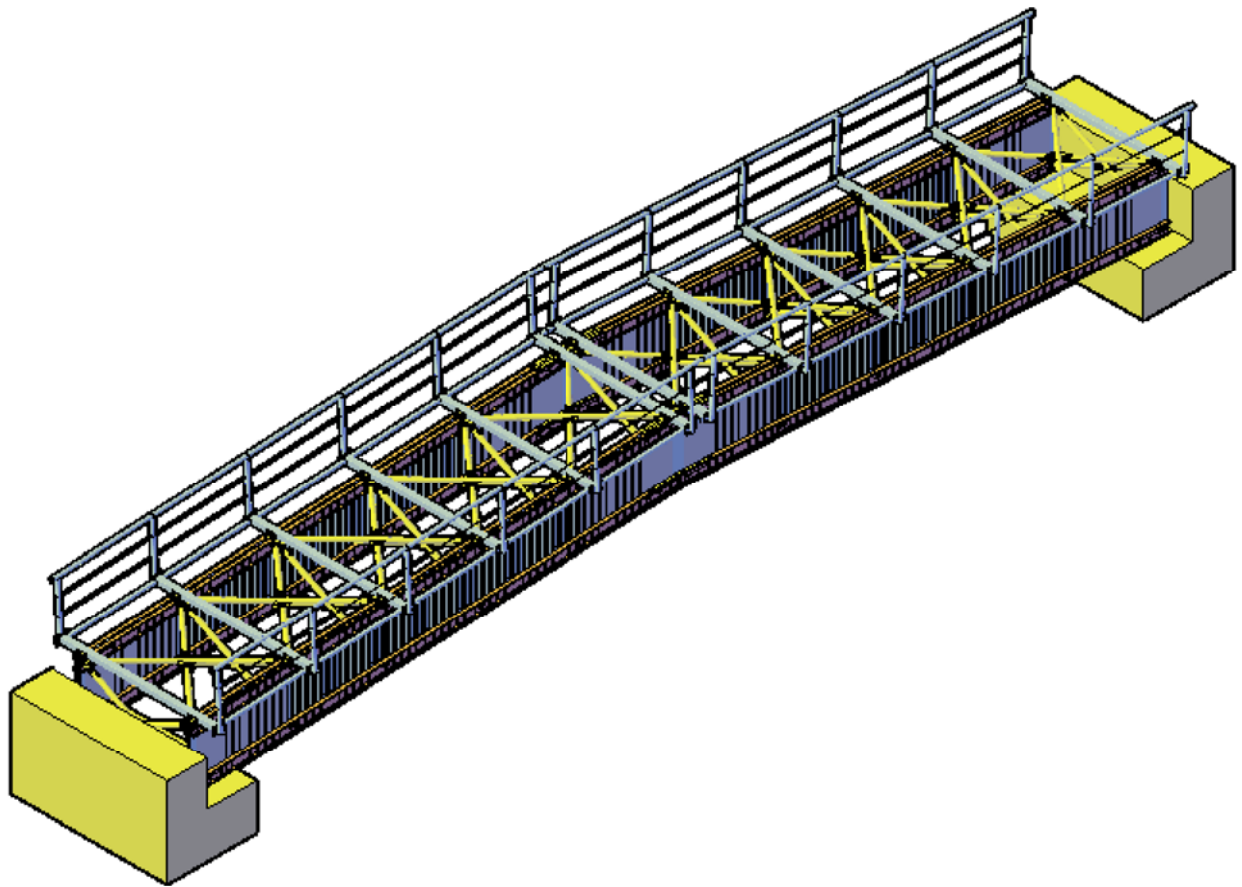


Figure 76. Overview of the pedestrian CWR bridge without decking

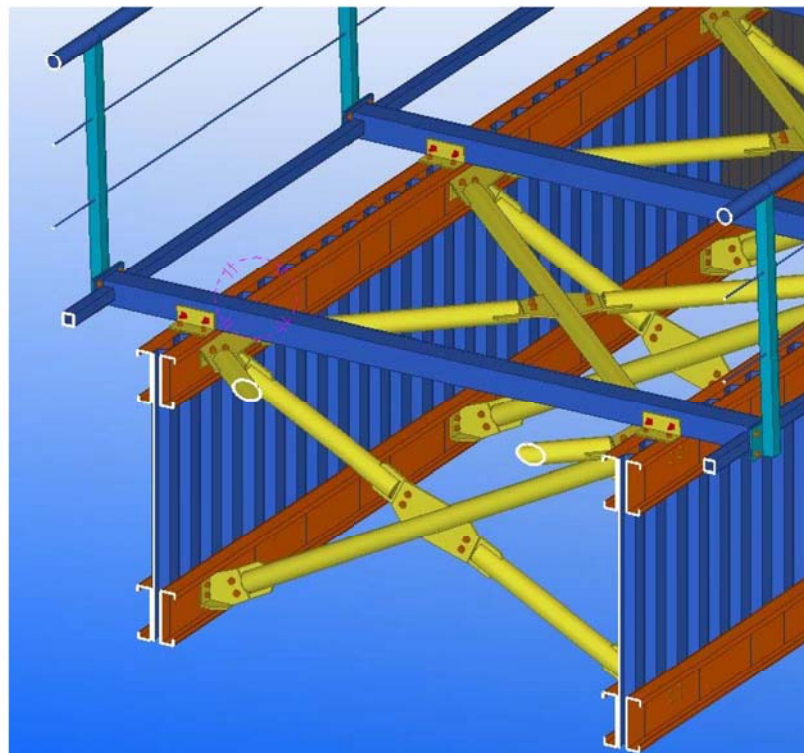


Figure 77. Cross-section of the deck

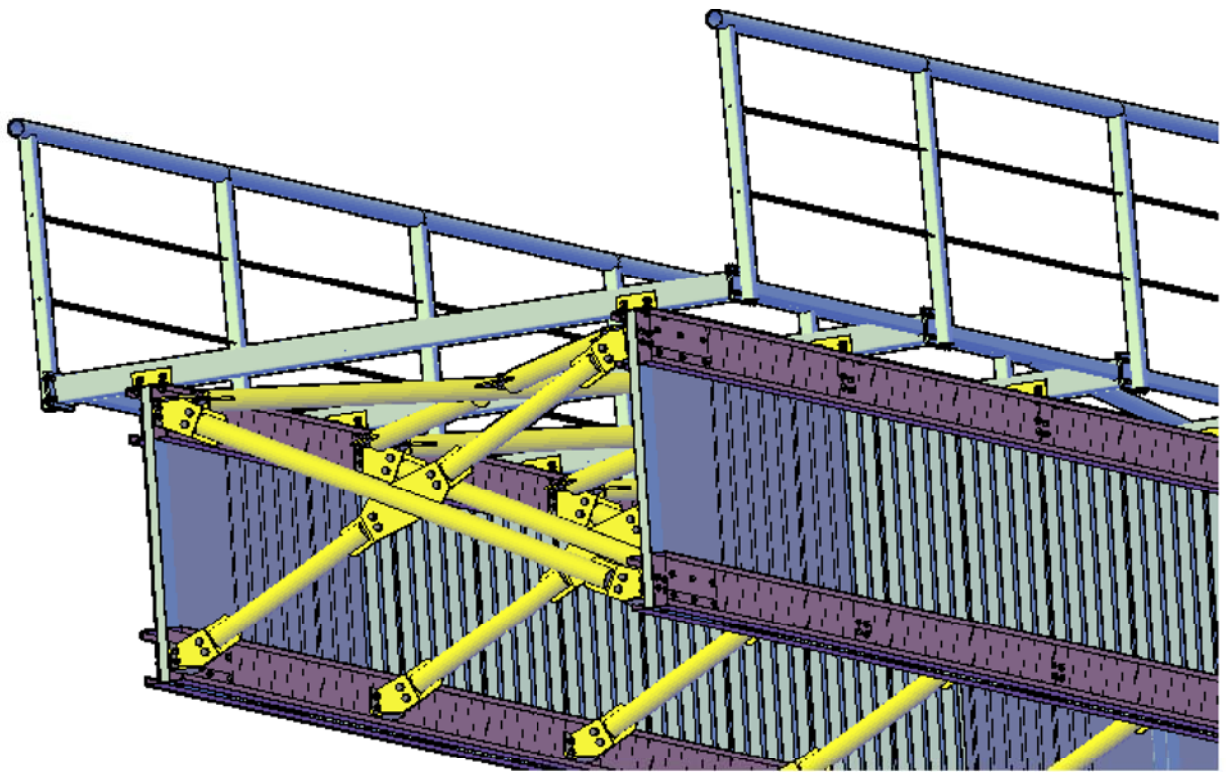


Figure 78. Transversal bracing system

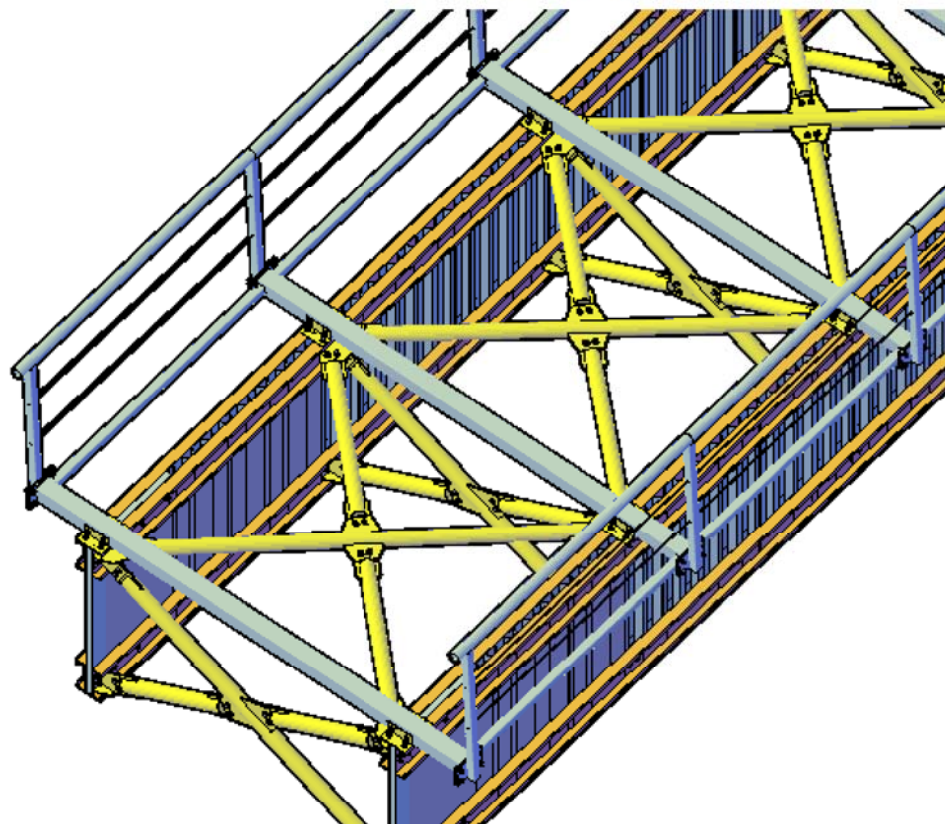


Figure 79. Longitudinal bracing system

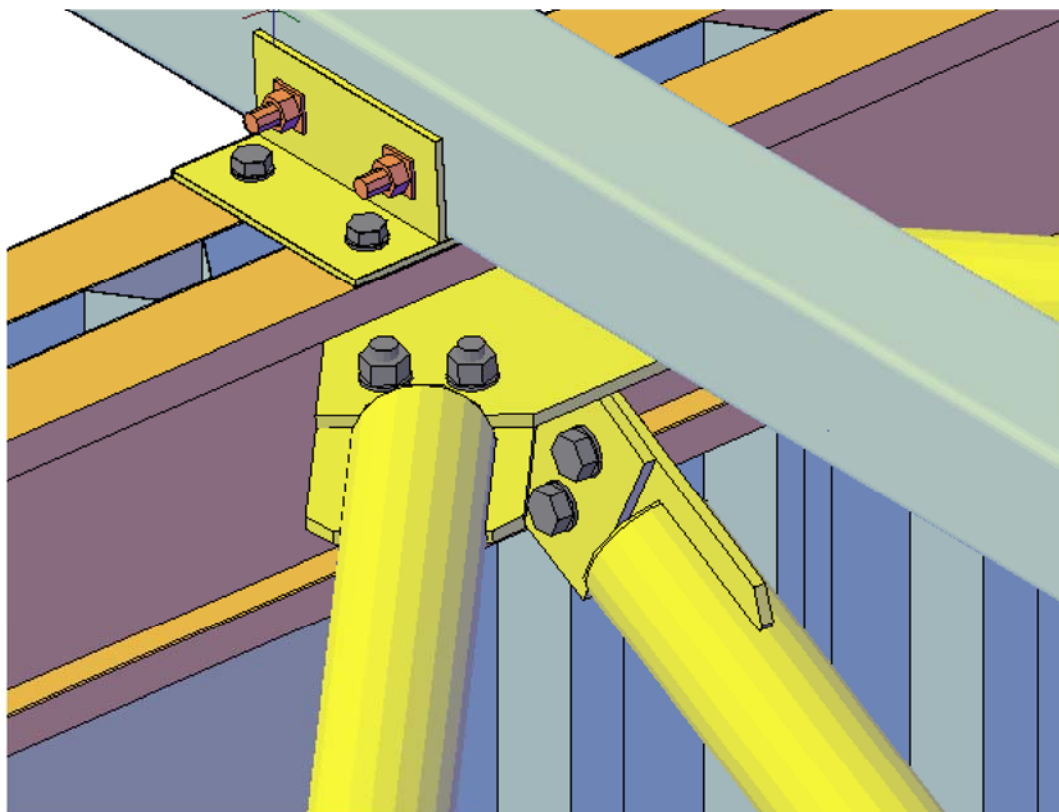


Figure 80. Connection of the main and secondary beams in assembly with bracings

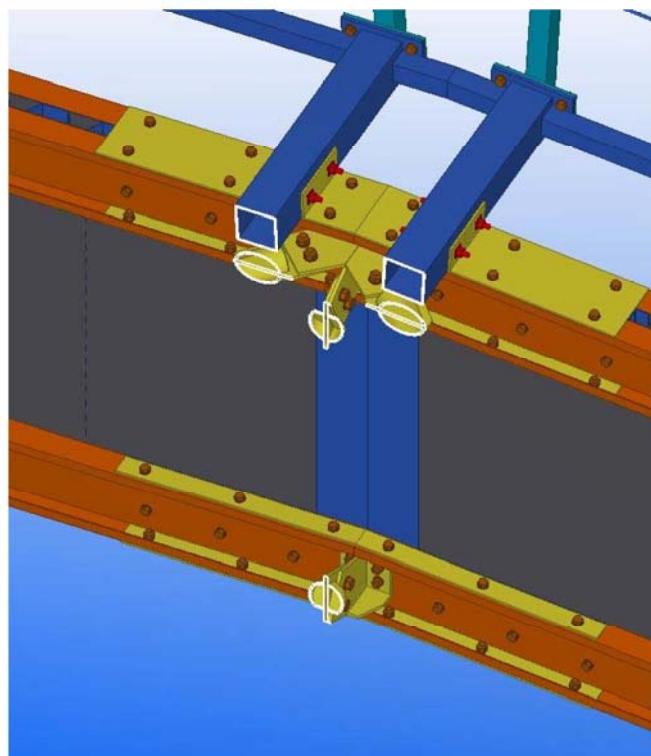


Figure 81. Cross-section of the midspan connection

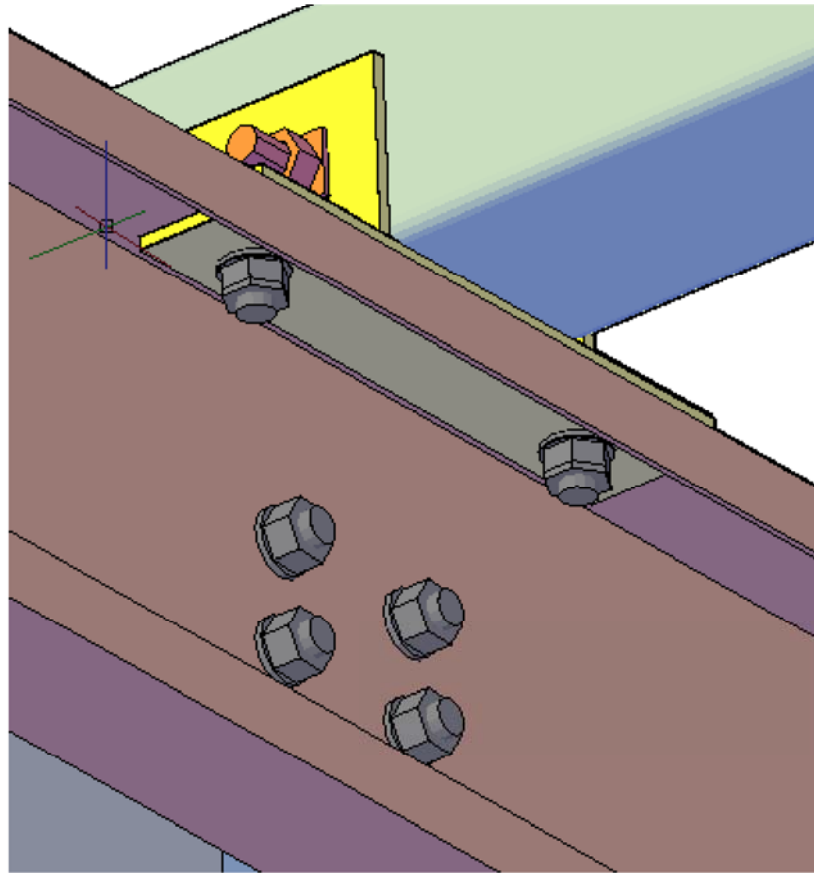


Figure 82. Connection of the bracings to the top flange

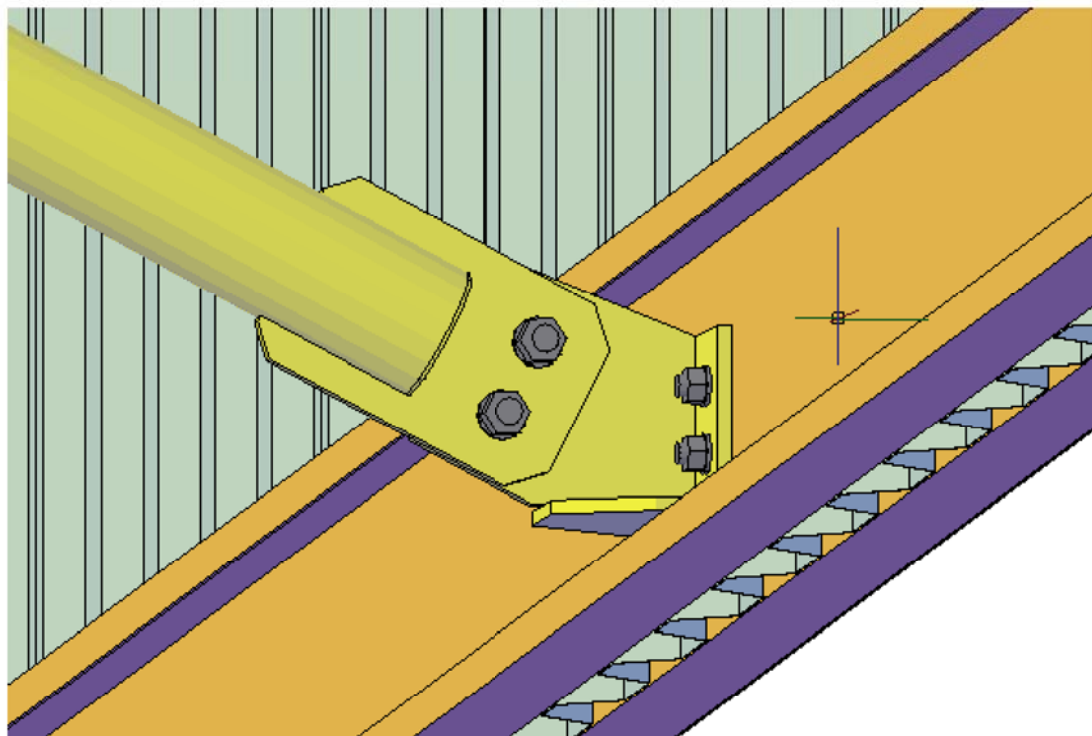


Figure 83. Connection of the transversal bracing element and bottom flange

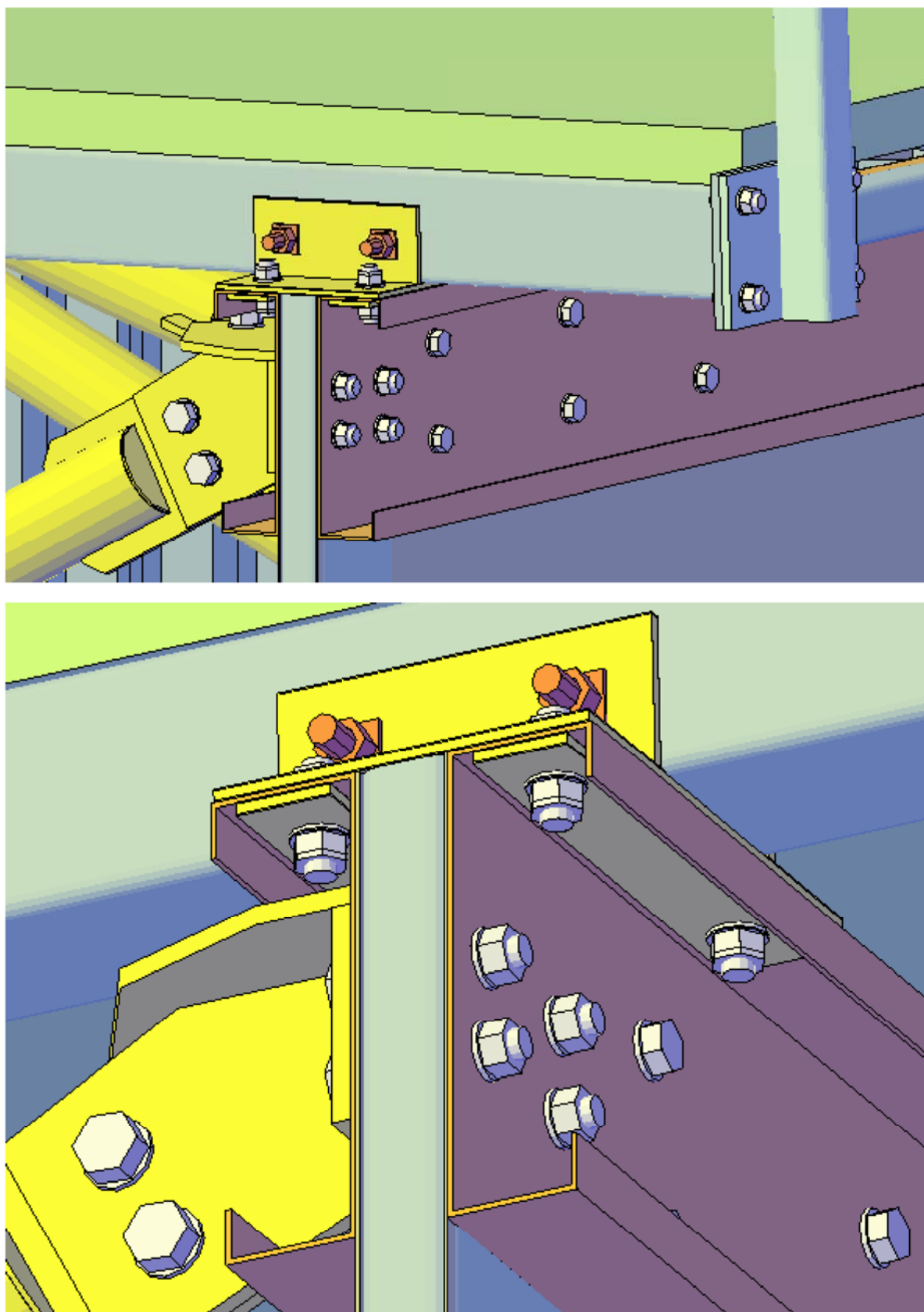


Figure 84. Connection of the secondary beam to the top flange at the support

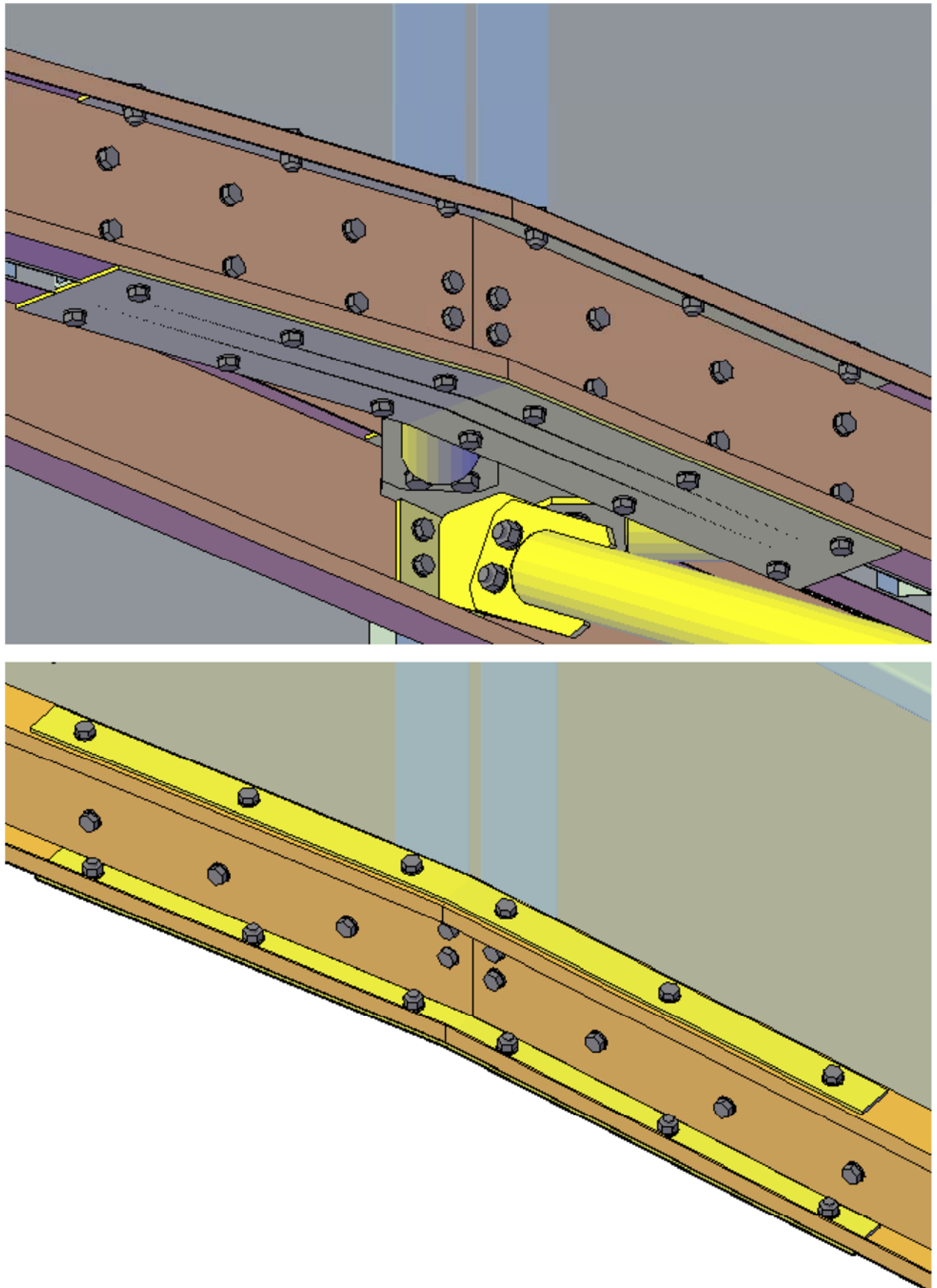


Figure 85. Connection of the bottom flanges at the midspan

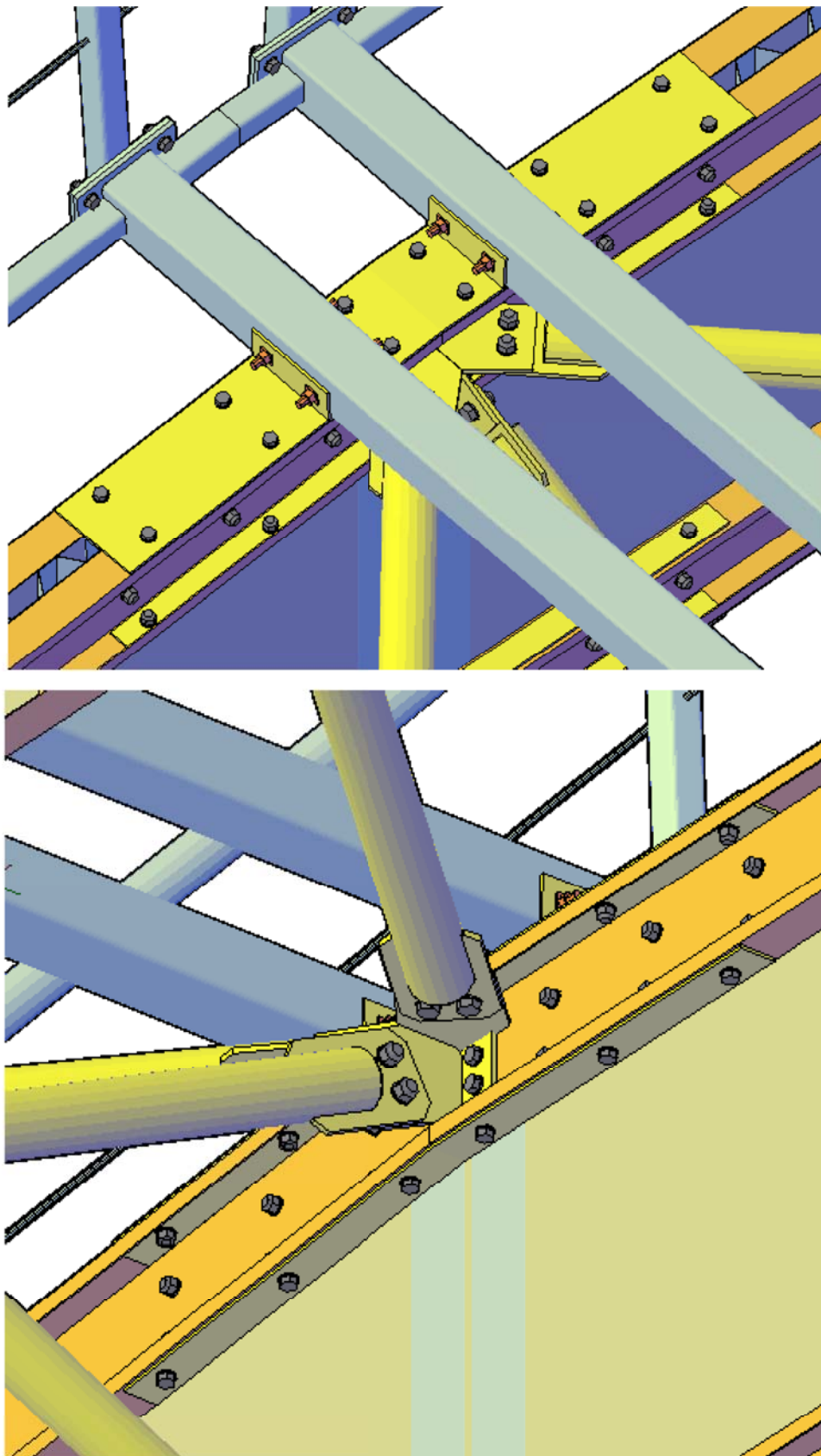


Figure 86. Connection of the top flanges at the midspan

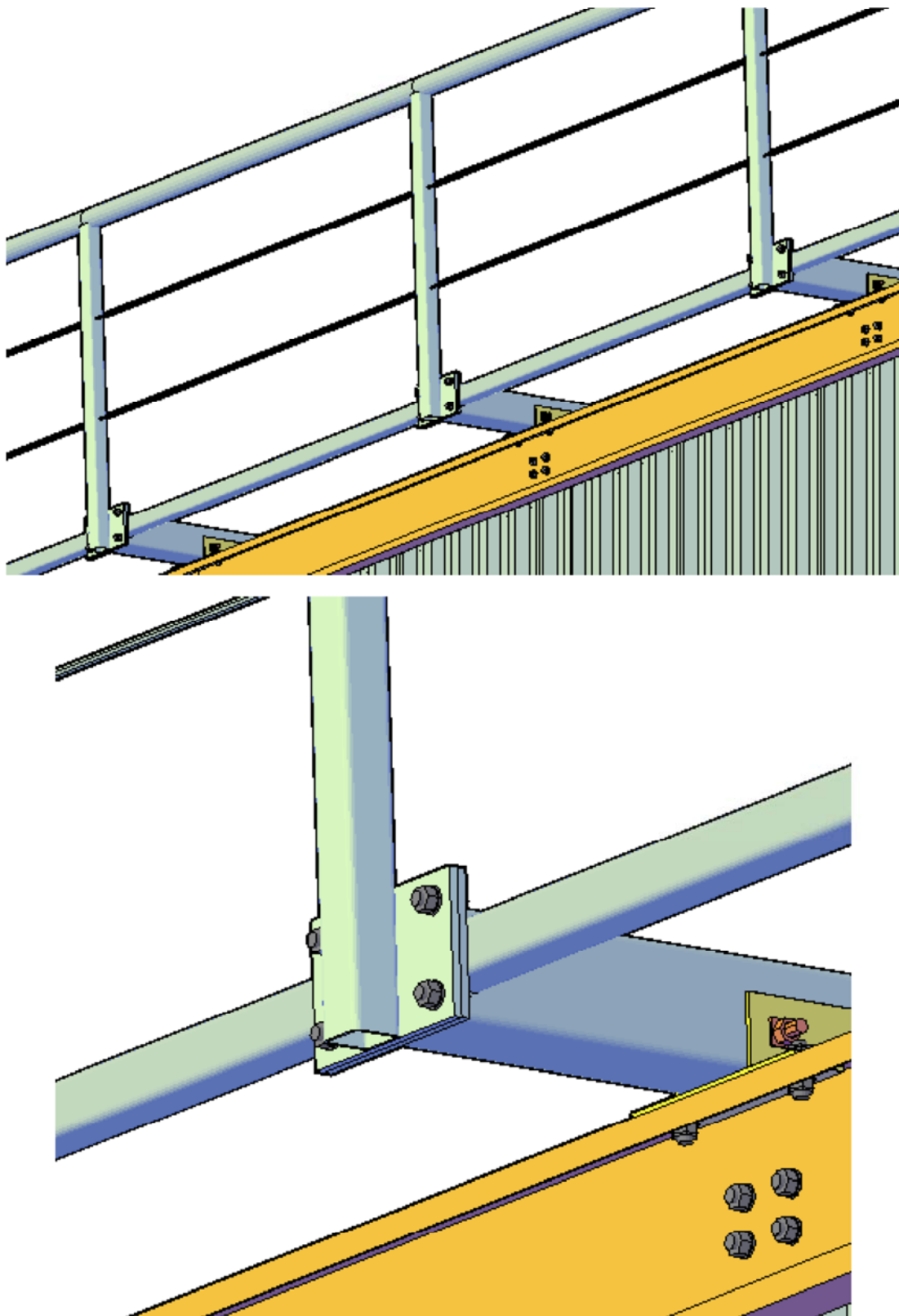


Figure 87. Handrail connection to the secondary beams and safety barriers

7. Economic effect

As a criterion of economical comparison of two solutions – bridge made with truss main beams and bridge with corrugated web main beams I take the volume of steel that is necessary for production and approximate cost of labor work related to welding.

The deck structure and railings remain the same and have the mass of 2.19 tons.

The mass of secondary equipment (lighting, decking, safety wire panels etc.) remain the same and their mass is not included into comparison.

In the first solution, the total mass of each steel truss beam calculated in SAP2000 is 4.8 tons. For two beams respectively 9.6 tons. For transversal bracings, we need 0.94 tons of steel. In total, we have 10.54 tons of steel for the main beams and bracings.

At the same time, each corrugated web beam has the mass of 2.24 tons. Therefore, for two main beams and transversal bracings we use 4.48 and 0.77 tons respectively. So, 5.25 tons in sum.

The price for one ton of steel as an approximate value and depends on many factors, but if we want to have a comparative survey we can use the weight as a relative value. We have the steel usage excess of 70% in the case of truss.

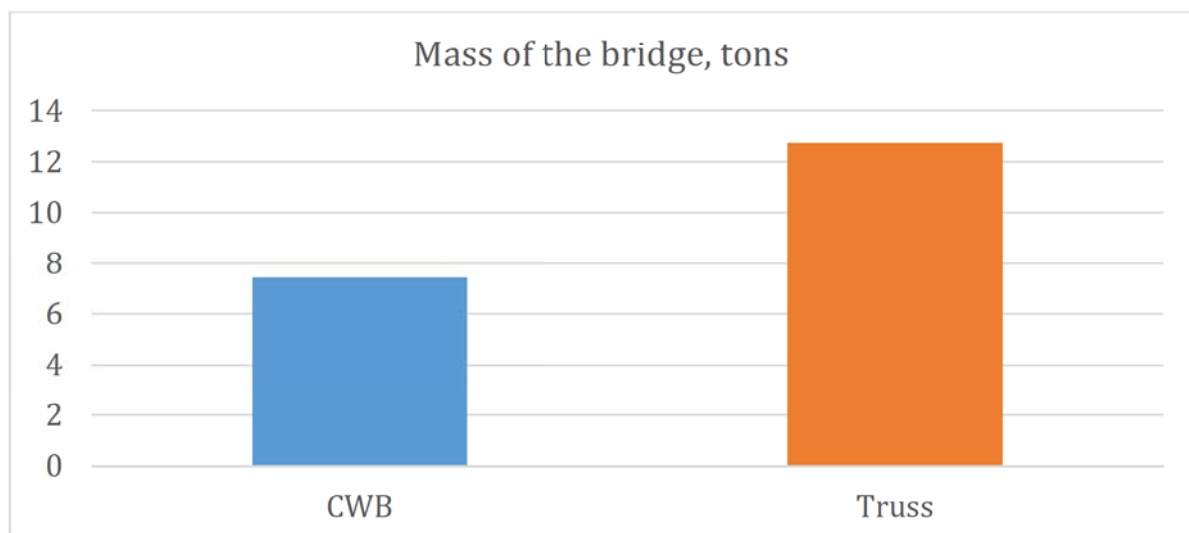


Figure 88. The comparison in steel consumption

Cost of materials is calculated in compliance with the commercial offer from the steel supplier.

List of materials for the truss construction of the pedestrian bridge:

No	Position	Quantity	Price per unit, €	Cost, €
1	Tube $\varnothing 139.7 \times 4$ mm	74 m	9.36	693
2	Tube $\square 200 \times 8$ mm	198 m	31.97	6330
3	Additional costs (painting, assembling, fasteners etc.)	-	-	350
TOTAL				7373

List of materials for the CWB construction of the pedestrian bridge:

No	Position	Quantity	Price per 1 m/kg, €	Cost, €
1	Tube $\varnothing 139.7 \times 4$ mm	64 m	9.36	600
2	C250/3 mm	352 m	8.05	2834
3	Trapezoidal sheeting T50-250 0.7mm	56 mp	7,45	417
4	Steel sheets	908 kg	0.54	490
TOTAL				4341

The results of the comparison are presented on Figure 89.

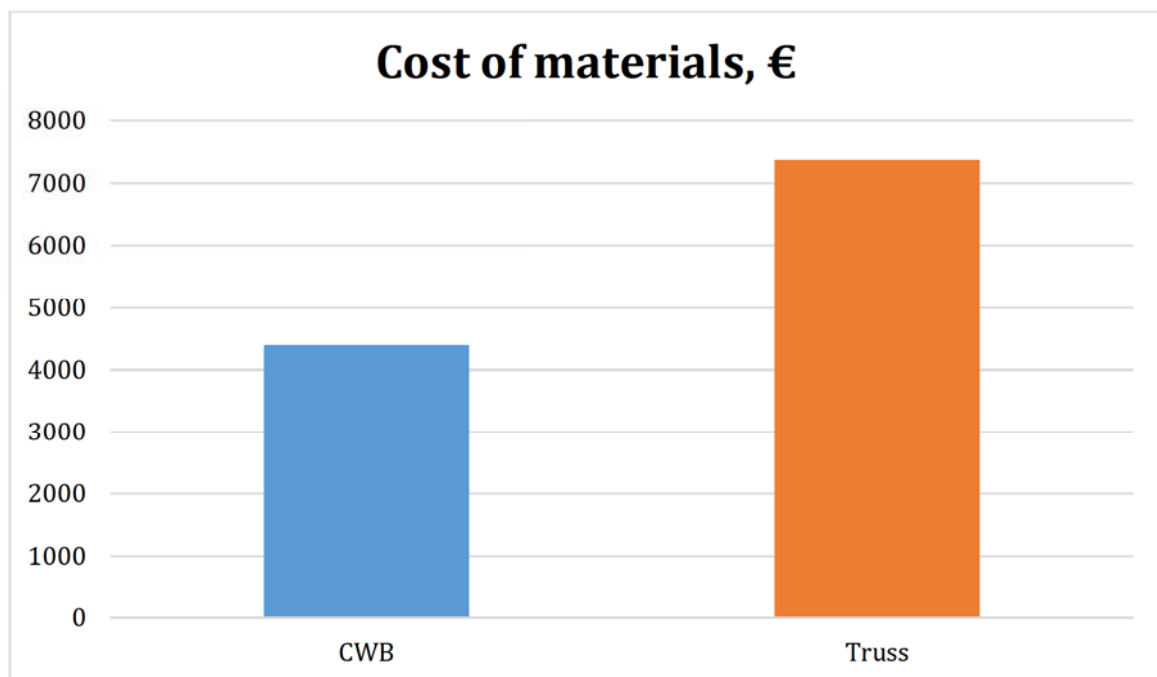


Figure 89. Comparison of the costs for materials depending on a type of bridge

For the estimation of the labor works, I will use approximate evaluation based on Cost Per Length Method.

$$\text{Labor cost/length} = (\text{L\&O rate}) / \{(\text{travel speed}) \times (\text{operating factor})\} \\ = (30\text{€/hr}) \times (1 \text{ hr} / 60 \text{ min}) / \{(0,254\text{m/min.}) \times (0.40)\} = 5\text{€/m}$$

$$\text{Filler metal cost/length} = \{(\text{wire feed speed}) \times (\text{wt. of electrode/m}) \times (\text{cost of electrode/Kg})\} / (\text{travel speed}) = \{(5\text{m/min}) \times (0,0201\text{Kg/m}) \times (2,53\text{€/Kg})\} / (0,254\text{m/min}) = 1\text{€/m}$$

$$\text{Shielding cost/length (flux)} = (\text{wt. of weld metal/length}) \times (\text{ratio of flux to weld metal}) \times (\text{cost of flux/Kg}) = (0,36\text{Kg/m}) \times (1,5) \times (\text{€}1.7/\text{Kg}) = 0,918\text{€/m}$$

$$\text{Cost/length} = (\text{Labor cost/length}) + (\text{filler metal and shielding cost/length}) \\ = 5\text{€/m} + 1\text{€/m} + 0,918\text{€/m} = 6,918\text{€/m}$$

In this case we have a total price for 1 meter of welding - 7€. With the total welding length of 24 meters for each truss beam we have $24\text{m} \times 2 \times 7\text{€} = 336\text{€}$.

For the CWB beam we do not use welding and need to establish two types of connection: using bolts and screws. Price for such an operation is a very crude data and based on quantity of bolts and screws, operating time and quantity of workers. For a reference I took the average value of 300€ as a sum of materials and work.

The results of analysis are presented at the Figure 90.

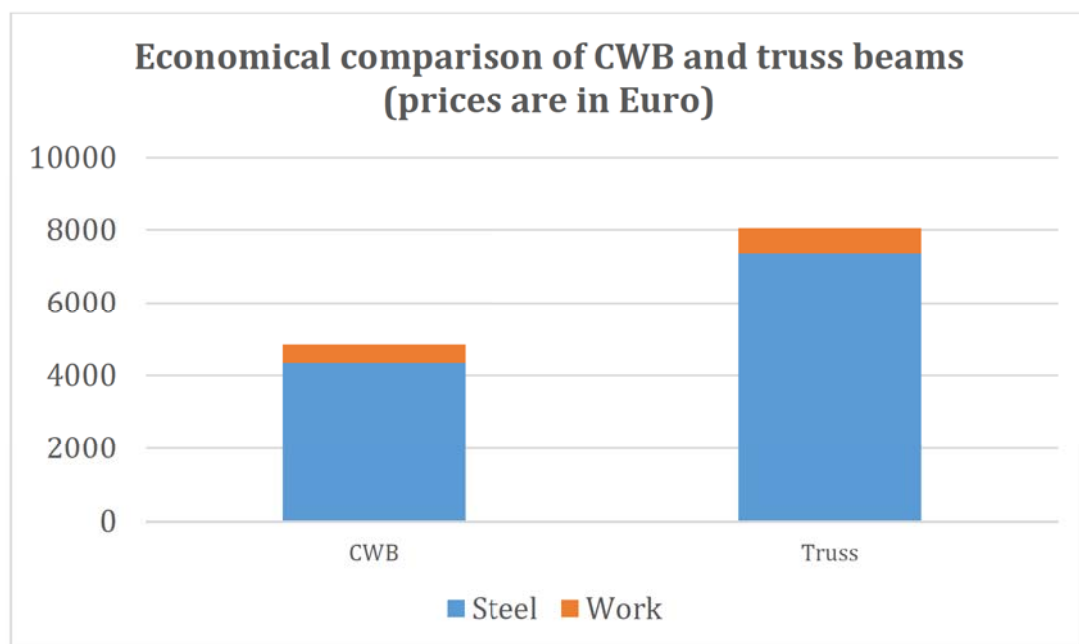


Figure 90. Economical comparison of CWB and truss beams with the prices indicated in Euro

Summing it up, we can see the significant economic advantage of the corrugated web application for beams. Observed difference in prices of 65% can figure prominently at the stage of projecting.

8. Conclusions

Finally, even the results look promising at the domain of structural response and the economic aspect, significant work has to be done in order to investigate, validate and optimize such a solution for mass production, i.e.:

- numerical models for calibration and validation of experimental models;
- to optimize the number of self-drilling screws used for connections;
- to optimize the dynamic response of the structure;
- tests using spot welding are the next step of research; there are no differences expected at the level of global behavior, but some are estimated in terms of strength and stiffness.

Based on that, standardized beams can be designed, calibrated for series of vertical loading intensities, accounting or not for lateral-torsional effects and the potential of this solution for industrialized fabrication has to be, once more, emphasized.

9. References

1. Abbas H.H. Analysis and design of corrugated web I-girders for bridges using high performance steel: Ph.D. dissertation. – Lehigh University, Bethlehem, USA, 2003. – 425 p.
2. Abbas H.H., Sause R., Driver R.G. Behavior of Corrugated Web I-Girders under In-Plane Loads // Journal of Engineering Mechanics. – 2006. – Vol. 132. – №8. – pp. 806-814.
3. Abbas H.H., Sause R., Driver R.G. Analysis of Flange Transverse Bending of Corrugated Web I-Girders under In-Plane Loads // Journal of Structural Engineering. – 2007. – Volume 133. – Issue 3. – pp. 347-355.
4. Chan C.L., Khalid Y.A., Sahari B.B., Hamouda A.M.S. Finite element analysis of corrugated web beams under bending // Journal of constructional steel research. – 2002. – Vol. 58. – pp. 1391-1406.
5. Chen B., Wang Y., Huang Q. New type of concrete arch bridge with corrugated steel webs // Proceedings of the 5th International conference on Arch Bridges. – 2007. – pp. 807-814.
6. Chung K.F., Liu T.C.H., Ko A.C.H. Investigation on Vierendeel mechanism in steel beams with circular web openings // Journal of constructional steel research. – 2001. – Vol. 57. – pp. 467-490.
7. Chung K.F., Liu T.C.H., Ko A.C.H. Steel beams with large web openings of various shapes and sizes: an empirical design method using a generalized moment-shear interaction curve // Journal of constructional steel research. – 2003. – Vol. 59. – pp. 1177-1200.
8. Commentary and worked examples to EN 1993-1-5 “Plated structural elements”. – Luxembourg: European Commission. Joint research centre, 2007. – 242 p.
9. Darwin D. Design of steel and composite beams with web openings. – American institute of steel construction, USA. – 1990. – 65 p.
10. Driver R.G., Abbas H.H., Sause R. Shear Behavior of Corrugated Web Bridge Girders // Journal of Structural Engineering. – 2006. – Vol. 132. – №2. – pp. 195-203.
11. Dubina D., Ungureanu V., Gîlia L.: Cold-formed steel beams of corrugated web and built-up section chords. Proceedings of the 7th European Conference on Steel and Composite Structures - EUROSTEEL 2014, September 10-12, 2014, Naples, Italy, ISBN 978-92-9147-121-8, 429-430.

12. Dubina D., Ungureanu V., Gîlia L.: *Cold-formed steel beams with corrugated web and discrete web-to-Flange Fasteners*. Steel Construction, Vol. 6, May 2013, 74-81.
13. Dubina D., Ungureanu V., Landolfo R. (2012): Design of Cold-formed Steel Structures. Eurocode 3: Design of Steel Structures. Part 1-3 Design of cold-formed Steel Structures. ISBN-13: 978-3-433-02979-4, Ernst & Sohn, A Wiley Company, Berlin, 654 pp
14. Dubina D., Ungureanu V. (2014): Cold-formed steel beams of corrugated web: Influence of lateral restraining and economic considerations (paper no. ICTWS2014-0210). Proceedings of the 7th International Conference on Thin-Walled Structures - ICTWS2014. ISBN: 979-11-953088-0-4. 28 September – 2 October 2014, Busan, Korea (9 pagini CD).
15. Easley. Buckling Formulas for Corrugated Metal Shear Diaphragms. Journal of the Structural Division, ASCE, No. ST 7, July 1975, pp. 1403-1417
16. Elgaaly M., Hamilton R.W., Seshadri A. Shear Strength of Beams with Corrugated Webs // Journal of Structural Engineering. – 1996. – Vol. 122. – №4. – pp. 390-398.
17. Elgaaly M., Seshadri A., Hamilton R.W. Bending Strength of Steel Beams with Corrugated Webs//Journal of Structural Engineering. – 1997. – Vol. 123. – №6 – pp. 772-782.
18. Elgaaly M., Seshadri A. Girders with Corrugated Webs under Partial Compressive Edge Loading // Journal of Structural Engineering. – 1997. – Vol. 123. – №6. – pp. 783-791.
19. Elgaaly M., Seshadri A. Depicting the behavior of girders with corrugated webs up to failure using non-linear finite element analysis // Advances in engineering software. – 1998. – Vol. 29. – № 3-6. – pp. 195-208.
20. Elgaaly M., Sheshadri A., Rodriquez R., Ibrahim S. Bridge girders with corrugated webs // Transportation Research Record. – 2000. – Vol. 1696. – pp. 162-170.
21. EN 1993-1-1: 2005. Eurocode 3: Design of Steel Structures - Part 1-1: General Rules and Rules for Buildings, CEN, Brussels, 2005.
22. EN 1993-1-5: 2005. Eurocode 3: Design of Steel Structures - Part 1-5: Plated structural elements, CEN, Brussels, 2005.
23. EN 1991-1-4, Eurocode 1 - Actions on structures, Part 1.4: General actions – Wind actions, 2005.
24. EN 1991-2, Eurocode 1 - Actions on structures, Part 2: Traffic loads on bridges, 2003.

25. EN 1993-2, Eurocode 3 – Design of steel bridges – Steel bridges, 2006.
26. EN 1998-2:2005, Design of structures for earthquake resistance — Bridges, 2005
27. Guidelines for the design of footbridges, 2005, 160 p.
28. Fraiser A.F. Experimental investigation of the strength of multiweb beams with corrugated webs. Technical note №3801. – Washington D.C., USA: National advisory committee for aeronautics, 1956. – 17 p.
29. Fülöp L.A., Dubina D.: *Design criteria for seam and sheeting-to-framing connections of cold-formed steel shear panels*. Journal of Structural Engineering, ASCE, vol. 132, 2006, no. 4, 582-590.
30. Gîlia, L.: Structural performances of steel beams with back-to-back cold-formed lipped channel sections for flanges and corrugated web. PhD Thesis (Promoters: Kiss Zs. and Dubina D.), Technical University of Cluj-Napoca, Romania, 2012 (in Romanian).
31. Guo S.J. Stress concentration and buckling behavior of shear loaded composite panels with reinforced cutouts // Composite Structures. – 2007. – Vol. 80. – pp. 1-9.
32. Guo S.J., Morishima R., Zhang X., Mills A. Cutout shape and reinforcement design for composite C-section beams under shear load //Composite structures. – 2009. – Vol. 88. – pp. 179-187.
33. Hagen N.C., Larsen P.K., Aalberg A. Shear capacity of steel plate girders with large web openings, Part 1: Modeling and simulations // Journal of constructional steel research. – 2009. – Vol. 65. – pp. 142-150.
34. Hagen N.C., Larsen P.K. Shear capacity of steel plate girders with large web openings, Part 2: Design guidelines // Journal of constructional steel research. – 2009. – Vol. 65. – pp. 151-158.
35. Human induced Vibrations of Steel Structures): Design of Footbridges – Background document, September 2008.
36. Human induced Vibrations of Steel Structures): Design of Footbridges – Guidelines, September 2008.
37. Höglund T. Strength of thin plate girders with circular or rectangular web holes without stiffeners. Stockholm, Sweden: Royal Institute of Technology; 1970.
38. Hsiao C., Libove C. Theoretical study of corrugated plates: Shear stiffness of a trapezoidally corrugated plate with discrete attachments to a rigid flange at the ends of the corrugations. Technical note № CR-1966. – Washington D.C., USA: National aeronautics and space administration, 1972. – 71 p.

39. Hoop H.G. Girders with corrugated webs. Literature study: Master thesis. – Technische Universiteit Delft, Netherlands, 2003. – 48 p.
40. Huang L., Hikosaka H., Komine K. Simulation of accordion effect in corrugated steel web with concrete flanges // Computers and structures. – 2004. – Vol. 82. – pp. 2061-2069.
41. Ibrahim S.A., El-Dakhakhni W.W., Elgaaly M. Fatigue of Corrugated-Web Plate Girders: Analytical Study // Journal of Structural Engineering. – 2006. – Vol. 132. – №9. – pp. 1381-1392.
42. Ibrahim S.A., El-Dakhakhni W.W., Elgaaly M. Behavior of bridge girders with corrugated webs under monotonic and cyclic loading // Engineering Structures. – 2006. – Vol. 28. – pp. 1941-1955.
43. Imanpour, Mirghaderi, Keshavarzi, Khafaf. Seismic design procedure and detailing of new reduced beam section moment connection with corrugated web in beam plastic hinge zone // Proceedings of International earthquake symposium. – Kocaeli. – 2007. – pp. 405-413.
44. Johnson R.P., Cafolla J. Local flange buckling in plate girders with corrugated webs // ICE Proceedings. Structures and Buildings. – 1997. – Vol. 123. – pp. 148-156.
45. Johnson R.P., Cafolla J. Corrugated webs in plate girders for bridges // ICE Proceedings. Structures and Buildings. – 1997. – Vol. 123. – pp. 157-164.
46. Kakuta T., Fujioka A. Development of corrugated steel web T-shaped prestressed concrete girder bridges // 7th International Conference on short and medium span bridges. – 2006. – Montreal, Canada. – 10 p.
47. Khalid Y.A., Chan C.L., Sahari B.B., Hamouda A.M.S. Bending behavior of corrugated web beams // Journal of materials processing technology. – 2004. – Vol. 150. – pp. 242-254.
48. Kurita A., Ohyama O. Recent steel-concrete hybrid bridges in Japan // Steel Structures. – 2003. – Vol. 3. – pp. 271-279.
49. Large web openings for service integration in composite floors. State of the art and special cases of the design of cellular beams. – Research fund for coal and steel, 2006. – 86 p.
50. Large web openings for service integration in composite floors. Final report. – Research programme of the Research fund of coal and steel, 2006. – 288 p.
51. Luo R., Edlund B. Ultimate strength of girders with trapezoidally corrugated webs under patch loading // Thin-walled structures. – 1996. – Vol. 24. – pp. 135-156.

52. Luo R., Edlund B. Shear capacity of plate girders with trapezoidally corrugated webs // Thin-walled structures. – 1996. – Vol. 26. – pp. 19-44.
53. Machacek J., Tuma M. Fatigue life of girders with undulating webs // Journal of constructional steel research. – 2006. – Vol. 62. – pp. 168-177.
54. McKenzie K.I. The shear stiffness of a corrugated web. Reports and Memoranda №3342. – London, UK: Ministry of Aviation. Aeronautical research council, 1963. – 13 p.
55. Metwally A.E. Prestressed composite girders with corrugated steel webs: A thesis submitted to the faculty of graduate studies in partial fulfillment of the requirements for the degree of master of science. – The University of Calgary, Canada, 1998. – 212 p.
56. Metwally A.E., Loov R.E. Corrugated steel webs for prestressed concrete girders // Materials and Structures. – 2003. – Vol. 36. – pp. 127-134.
57. Mo Y.L., Jeng C.H., Krawinkler H. Experimental and analytical studies of innovative prestressed concrete box-girder bridges // Materials and Structures. – 2003. – Vol. 36. – pp. 99-107.
58. Moon J., Yi J., Choi B.H., Lee H. Lateral-torsional buckling of I-girder with corrugated webs under uniform bending // Thin-Walled Structures. – 2009. – Vol. 47. – pp. 21-30.
59. Moon J., Yi J., Choi B.H., Lee H. Shear strength and design of trapezoidally corrugated steel webs // Journal of Constructional Steel Research. – 2009. – Vol. 65. – pp. 1198-1205.
60. Mori S., Miyoshi T., Katoh H., Nishimura N., Nara S. A study on local stresses of corrugated steel webs in PC bridges under prestressing. – Osaka, Japan: Incorporated Administrative Agency Public Works Research Institute, 2004. – 10 p.
61. Narayanan R., Chow F.Y. Experiments on perforated plates subjected to shear // Journal of strain analysis. – Vol. 20. – 1985. – pp. 23-34.
62. Neagoie B., Ungureanu V., Dubina D.: *Beams with cold-formed steel sections for flanges and corrugated web*. In: Stability and Ductility of Steel Structures – Recent research. Academic Days, 27 May 2005, Timisoara, Romania, ISBN: 978-973-661-977-9, 57-70 (in Romanian).
63. Niwa J. World's first PC-steel composite cable-stayed bridge using corrugated steel plate webs for PC girders. Yahagigawa Bridge on the Second Tomei Expressway. Project Report. – Tokyo, Japan: Tokyo Institute of Technology, 2005. – 6 p.

64. Pellegrino C., Maiorana E., Modena C. Linear and non-linear behavior of steel plates with circular and rectangular holes under shear loading // Thin-walled structures. – 2009. – Vol. 47. – pp. 607-616.
65. Peterson's stress concentration factors / Walter D. Pilkey – 2nd ed. – New York : John Wiley & Sons, 1997. – 524 p.
66. Peterson J.P., Card M.F. Investigation of the buckling strength of corrugated webs in shear. Technical note № D-424. – Washington, USA: National aeronautics and space administration, 1960. – 30 p.
67. Petersen C.: Dynamik der Baukonstruktion, Vieweg, 1996 (in German).
68. Petersen C.: Schwingungsdämpfer im Ingenieurbau, Vieweg, 1996 (in German).
69. Petersen C.: Stahlbau, Vieweg, 2nd edition, 1990 (in German).
70. Romeijn A., Sarkhosh R., Hoop H. Basic parametric study on corrugated web girders with cut outs // Journal of Constructional Steel Research. – 2009. – Vol. 65. – pp. 395-407.
71. Sause R., Abbas H.H., Driver R.G., Anami K., Fisher J.W. Fatigue Life of Girders with Trapezoidal Corrugated Webs // Journal of Structural Engineering. – 2006. – Vol. 132. – №7 – pp. 1070-1078.
72. Sayed-Ahmed E.Y. Behaviour of steel and (or) composite girders with corrugated steel webs // Canadian journal of civil engineering. – 2001. – Vol. 28. – pp. 656-672.
73. Sayed-Ahmed E.Y. Lateral torsion-flexure buckling of corrugated web steel girders // Proceedings of the Institution of Civil Engineers. Structures & Buildings. – 2005. – Vol. 158. – pp. 53-69.
74. Sayed-Ahmed E.Y. Design aspects of steel I-girders with corrugated steel webs // Electronic Journal of Structural Engineering. – 2007. – Vol. 7. – pp. 27-40.
75. Shanmugan N.E., Lian V.T., Thevendran V. Finite element modeling of plate girders with web openings // Thin-walled structures. – 2002. – Vol. 40. – pp. 443-464.
76. Siokola W., Poeter H. Fabrication tools for corrugated web I-beams // Modern Steel Construction. – 1999. – №7.
77. Tahir M.M., Sulaiman A., Saggaff A. Structural behaviour of trapezoidal web profiled steel beam section using partial strength connection // Electronic Journal of Structural Engineering. – 2008. – Vol. 8 – pp. 55-66.
78. Tuma M. Fatigue resistance of girders with undulating web: Pisemna prace ke statni doktorske zkousce. – Ceske Vysoke Ucení Technické v Praze, Czech Republic, 2003. – 47 p.

79. Virčík J. Skúšky nosníků z tenkých plechov (Tests of CWB) // Stavebnícky časopis. Bratislava. ČSSR – 1983. – Vol. 9 – pp. 711-724.
80. Wang X. Behavior of Steel Members with Trapezoidally Corrugated Webs and Tubular Flanges under Static Loading.: Ph.D. dissertation. – Drexel University, USA, 2003. – 192 p.
81. Yang Z., Kim C.B., Cho C., Beom H.G. The concentration of stress and strain in finite thickness elastic plate containing a circular hole // International journal of solids and structures. – 2008. – Vol. 45. – pp. 713-731.
82. Yi J., Gil H., Youm K., Lee H. Interactive shear buckling behavior of trapezoidally corrugated steel webs // Engineering Structures. – 2008. – Vol. 30. – pp. 1659-1666.
83. Yu D. The lateral torsional buckling strength of steel I-girders with corrugated webs: Ph.D. dissertation. – Lehigh University, Bethlehem, USA, 2006. – 364 p.
84. Zhang W., Zhou Q., Li Y., Cai Z., Wedera G.E.O. Hot rolling technique and profile design of tooth-shape rolls. Part 1. Development and research on H-beams with wholly corrugated webs // Journal of materials processing technology. – 2000. – Vol. 101. – pp. 110-114.
85. Zhang W., Zhou Q., Li Y., Qi X., Wedera G.E.O. Buckling strength analysis of the web of a WCW H-beam: Part 2. Development and research on H-beams with wholly corrugated webs (WCW) // Journal of materials processing technology. – 2000. – Vol. 101. – pp. 115-118.
86. Zhang W., Zhou Q., Li Y., Qi X., Wedera G.E.O. Optimization of the structure of an H-beam with either a flat or a corrugated web. Part 3. Development and research on H-beams with wholly corrugated webs // Journal of materials processing technology. – 2000. – Vol. 101. – pp. 119-123.
87. Zeman & Co Gesellschaft mbH. SIN Beams. Technical documentstion, 1993. – 13 p.

ANNEX 1. The calculation of the steel plate thickness for the Plate model in SAP2000.

Initial Data

For flanges, I use two pairs of cold-formed C-profiles C250 with the thickness of 3 mm. The characteristics of the cross-section if presented on Figure 91.

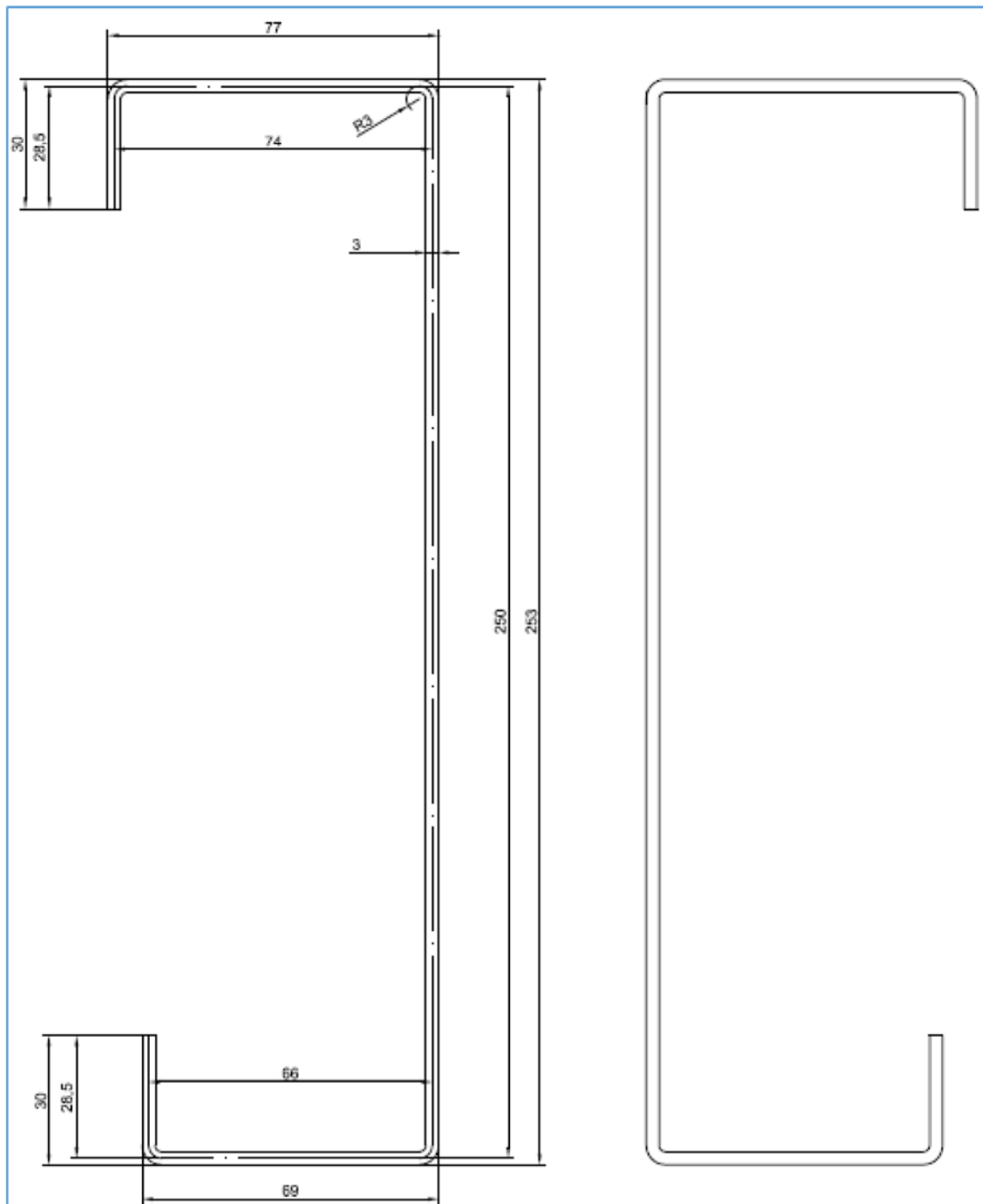


Figure 91. Geometrical characteristics for the flange

Total are of the flange – $A = 2526 \text{ mm}^2$

$$b_f = y_G + \frac{t}{2} + \frac{f}{2} = 20.17 + \frac{3}{2} + \frac{48.5}{2} = 46 \text{ mm}$$

$$h_f = \frac{h_w - z_{G1}}{2} = 639 \text{ mm}$$

Moments of inertia for C250-3mm:

$$I_z = 857566 \text{ mm}^4$$

$$I_y = 11489396 \text{ mm}^4$$

Having the C250-3 profiles as flanges we obtain the required thickness of the web from the equation:

$$4 \cdot \left(A \cdot \left(\frac{h_f}{2} \right)^2 \right) + 4 \cdot I_y + h_{web} \cdot \frac{b_{web}^3}{12} = I_{y.tot}$$

where

$$\begin{aligned} I_{y.tot} &= 4 \cdot \left(A \cdot \left(\frac{h_f}{2} \right)^2 \right) + 4 \cdot I_y + I_c = \\ &= 4 \cdot \left(2526 \cdot \left(\frac{639}{2} \right)^2 \right) + 4 \cdot 11489396 + 1.292 \cdot 10^6 = 1.077 \cdot 10^9 \text{ mm}^4 \end{aligned}$$

So, the thickness is $b_{web} = 22.291 \text{ mm}$. For the model, I use the thickness of 23 mm.

ANNEX 2. Results of section design.

Number of Element	Section of the Element	Ratio	Combination
47	Double C250-3mm TOP	0.9682	COMB19
45	Double C250-3mm TOP	0.9592	COMB19
25	Double C250-3mm TOP	0.949041	COMB19
42	Double C250-3mm TOP	0.920636	COMB19
10	Double C250-3mm TOP	0.914232	COMB19
64	TUBE-D139.7X4	0.890046	COMB20
48	Double C250-3mm TOP	0.868327	COMB19
63	TUBE-D139.7X4	0.850725	COMB20
43	Double C250-3mm TOP	0.826607	COMB19
44	Double C250-3mm TOP	0.81719	COMB19
46	Double C250-3mm TOP	0.812227	COMB19
162	Tube pinned 60x60x4mm	0.796713	COMB19
4	Double C250-3mm TOP	0.78986	COMB19
161	Tube pinned 60x60x4mm	0.785315	COMB19
163	Tube pinned 60x60x4mm	0.756534	COMB19
160	Tube pinned 60x60x4mm	0.728172	COMB19
164	Tube pinned 60x60x4mm	0.671276	COMB19
28	TUBE-D139.7X4	0.662178	COMB21
23	TUBE 120x120x4mm	0.653862	COMB19
156	TUBE-D139.7X4	0.622678	COMB20
62	TUBE-D139.7X4	0.612145	COMB20
159	Tube pinned 60x60x4mm	0.609137	COMB19
17	TUBE 120x120x4mm	0.603621	COMB19
57	Double C250-3mm TOP	0.598022	COMB5
14	TUBE 120x120x4mm	0.564797	COMB19
136	TUBE-D139.7X4	0.559201	COMB21
20	TUBE 120x120x4mm	0.540945	COMB19
155	TUBE-D139.7X4	0.533334	COMB20
105	TUBE60X60X4	0.530828	COMB10
66	TUBE-D139.7X4	0.526343	COMB21
165	Tube pinned 60x60x4mm	0.495943	COMB19
107	TUBE60X60X4	0.478188	COMB19
88	TUBE60X60X4	0.470277	COMB10
74	TUBE-D139.7X4	0.469582	COMB20
65	TUBE-D139.7X4	0.467556	COMB21
29	TUBE 120x120x4mm	0.452867	COMB19
26	TUBE 120x120x4mm	0.452768	COMB19
135	TUBE-D139.7X4	0.442625	COMB21
86	TUBE60X60X4	0.440378	COMB10
56	Double C250-3mm TOP	0.437953	COMB5
158	Tube pinned 60x60x4mm	0.43669	COMB19

97	TUBE60X60X4	0.434714	COMB7
102	TUBE60X60X4	0.431459	COMB11
19	TUBE 120x120x4mm	0.427944	COMB19
90	TUBE60X60X4	0.41571	COMB10
98	TUBE60X60X4	0.414114	COMB11
103	TUBE60X60X4	0.409237	COMB10
94	TUBE60X60X4	0.408485	COMB11
120	TUBE-D76.1X3.2	0.408026	COMB19
50	Double C250-3mm TOP	0.402103	COMB5
93	TUBE60X60X4	0.40059	COMB10
16	TUBE 120x120x4mm	0.399742	COMB19
51	Double C250-3mm TOP	0.398837	COMB5
91	TUBE60X60X4	0.396863	COMB12
95	TUBE60X60X4	0.394368	COMB11
92	TUBE60X60X4	0.39397	COMB11
96	TUBE60X60X4	0.393409	COMB15
104	TUBE60X60X4	0.393028	COMB15
106	TUBE60X60X4	0.392607	COMB10
101	TUBE60X60X4	0.391233	COMB15
99	TUBE60X60X4	0.38968	COMB11
89	TUBE60X60X4	0.38914	COMB1
79	Double C250 3mm BOTTOM	0.38628	COMB10
34	TUBE-D139.7X4	0.386011	COMB21
78	Double C250 3mm BOTTOM	0.381106	COMB10
81	Double C250 3mm BOTTOM	0.379459	COMB19
77	Double C250 3mm BOTTOM	0.376371	COMB10
172	Tube pinned 60x60x4mm	0.371957	COMB7
171	Tube pinned 60x60x4mm	0.371411	COMB7
80	Double C250 3mm BOTTOM	0.370505	COMB19
49	Double C250-3mm TOP	0.367487	COMB5
109	TUBE-D76.1X3.2	0.364962	COMB10
52	Double C250-3mm TOP	0.36475	COMB5
76	Double C250 3mm BOTTOM	0.363076	COMB10
58	Double C250-3mm TOP	0.349004	COMB5
173	Tube pinned 60x60x4mm	0.344554	COMB7
170	Tube pinned 60x60x4mm	0.343307	COMB7
31	TUBE-D139.7X4	0.341444	COMB21
113	Double C250 3mm BOTTOM	0.338801	COMB10
117	Double C250 3mm BOTTOM	0.336096	COMB10
71	TUBE-D139.7X4	0.334935	COMB20
55	Double C250-3mm TOP	0.334119	COMB7
119	TUBE-D76.1X3.2	0.321405	COMB10
54	Double C250-3mm TOP	0.318358	COMB5
53	Double C250-3mm TOP	0.315791	COMB5

32	TUBE 120x120x4mm	0.315291	COMB19
75	Double C250 3mm BOTTOM	0.314538	COMB10
110	TUBE-D76.1X3.2	0.313654	COMB10
100	Double C250 3mm BOTTOM	0.309949	COMB10
108	TUBE60X60X4	0.309534	COMB7
27	TUBE 120x120x4mm	0.304431	COMB5
21	TUBE 120x120x4mm	0.302548	COMB7
18	TUBE 120x120x4mm	0.297101	COMB1
87	TUBE60X60X4	0.295928	COMB1
111	TUBE-D76.1X3.2	0.291427	COMB10
131	Double C250 3mm BOTTOM	0.288397	COMB10
5	TUBE 120x120x4mm	0.286873	COMB7
6	TUBE 120x120x4mm	0.285664	COMB1
174	Tube pinned 60x60x4mm	0.281556	COMB7
169	Tube pinned 60x60x4mm	0.279747	COMB7
180	Double C250-3mm TOP	0.276981	COMB19
7	TUBE 120x120x4mm	0.27672	COMB1
82	Double C250 3mm BOTTOM	0.275993	COMB19
13	TUBE 120x120x4mm	0.27497	COMB1
11	TUBE 120x120x4mm	0.274538	COMB1
8	TUBE 120x120x4mm	0.274478	COMB7
118	TUBE-D76.1X3.2	0.266399	COMB10
132	Double C250 3mm BOTTOM	0.260977	COMB10
130	TUBE-D76.1X3.2	0.260756	COMB7
85	Double C250 3mm BOTTOM	0.259025	COMB10
121	TUBE-D76.1X3.2	0.253403	COMB1
116	TUBE-D76.1X3.2	0.253365	COMB10
12	TUBE 120x120x4mm	0.251977	COMB5
112	TUBE-D76.1X3.2	0.250676	COMB10
9	TUBE 120x120x4mm	0.250469	COMB7
68	TUBE-D139.7X4	0.244987	COMB21
24	TUBE 120x120x4mm	0.244474	COMB1
166	Tube pinned 60x60x4mm	0.243617	COMB19
129	TUBE-D76.1X3.2	0.242116	COMB7
122	TUBE-D76.1X3.2	0.23801	COMB1
73	Double C250 3mm BOTTOM	0.237666	COMB19
35	TUBE 120x120x4mm	0.235434	COMB10
157	Tube pinned 60x60x4mm	0.230935	COMB19
72	TUBE-D139.7X4	0.229726	COMB20
15	TUBE 120x120x4mm	0.226563	COMB7
33	TUBE 120x120x4mm	0.224631	COMB10
59	Double C250 3mm BOTTOM	0.222581	COMB5
67	TUBE-D139.7X4	0.221393	COMB21
123	TUBE-D76.1X3.2	0.219702	COMB1

128	TUBE-D76.1X3.2	0.218983	COMB7
30	TUBE 120x120x4mm	0.212855	COMB1
60	TUBE-D139.7X4	0.210148	COMB20
133	Double C250 3mm BOTTOM	0.209332	COMB10
177	Double C250-3mm TOP	0.207385	COMB5
84	Double C250 3mm BOTTOM	0.204901	COMB10
61	TUBE-D139.7X4	0.204249	COMB5
36	TUBE 120x120x4mm	0.203126	COMB12
1	TUBE 120x120x4mm	0.201396	COMB12
39	TUBE 120x120x4mm	0.201329	COMB12
127	TUBE-D76.1X3.2	0.198417	COMB7
178	Double C250-3mm TOP	0.196484	COMB19
124	TUBE-D76.1X3.2	0.195779	COMB1
83	Double C250 3mm BOTTOM	0.194426	COMB20
175	Tube pinned 60x60x4mm	0.193951	COMB1
168	Tube pinned 60x60x4mm	0.189694	COMB7
2	TUBE 120x120x4mm	0.185609	COMB10
41	TUBE 120x120x4mm	0.183369	COMB21
22	TUBE 120x120x4mm	0.182168	COMB10
114	TUBE-D76.1X3.2	0.182062	COMB10
115	TUBE-D76.1X3.2	0.174863	COMB10
125	TUBE-D76.1X3.2	0.16863	COMB7
126	TUBE-D76.1X3.2	0.168222	COMB1
38	TUBE 120x120x4mm	0.151887	COMB20
179	Double C250-3mm TOP	0.146882	COMB5
134	Double C250 3mm BOTTOM	0.122268	COMB19
3	TUBE 120x120x4mm	0.109806	COMB19
37	TUBE-D139.7X4	0.104373	COMB21
40	TUBE-D139.7X4	0.101122	COMB12
176	Tube pinned 60x60x4mm	0.084067	COMB1
70	TUBE-D139.7X4	0.081419	COMB5
167	Tube pinned 60x60x4mm	0.08046	COMB7
153	TUBE-D139.7X4	0.061688	COMB5
69	TUBE-D139.7X4	0.060415	COMB11
151	TUBE-D139.7X4	0.049154	COMB5
149	TUBE-D139.7X4	0.048721	COMB5
137	TUBE-D139.7X4	0.048627	COMB5
139	TUBE-D139.7X4	0.047279	COMB5
145	TUBE-D139.7X4	0.046487	COMB5
141	TUBE-D139.7X4	0.046454	COMB5
143	TUBE-D139.7X4	0.045766	COMB5
147	TUBE-D139.7X4	0.045373	COMB5
150	TUBE-D139.7X4	0.025001	COMB19
146	TUBE-D139.7X4	0.023727	COMB19

140	TUBE-D139.7X4	0.022444	COMB19
144	TUBE-D139.7X4	0.021995	COMB19
142	TUBE-D139.7X4	0.021952	COMB19
148	TUBE-D139.7X4	0.02133	COMB19
138	TUBE-D139.7X4	0.020376	COMB19
154	TUBE-D139.7X4	0.018072	COMB19
152	TUBE-D139.7X4	0.009928	COMB10

ANNEX 3. Verification of the most loaded cross-section.

Basic data

Dimensions of dual lipped channel C250 / 3.0 mm

$h = 250 \text{ mm}$	$f_{y,b} = 350 \text{ MPa}$	$\gamma_{M0} = 1$	EN1990
$t_{nom} = 3 \text{ mm}$	$E = 210 \text{ GPa}$	$\gamma_{M1} = 1$	
$t = 2.92 \text{ mm}$	$\nu = 0.3$	$\gamma_G = 1.35$	
$h_w = h - t_{nom} = 247 \text{ mm}$		$\gamma_Q = 1.5$	
$A_{eff,c} = 1.6061 \cdot 10^{-3} \text{ m}^2$	$A_{eff} = 2.5261 \cdot 10^{-3} \text{ m}^2$		T3701a
$W_{eff,y,c} = 1.7391 \cdot 10^{-4} \text{ m}^3$	$I_y = 2.2981 \cdot 10^{-5} \text{ m}^4$		
$W_{eff,y,t} = 1.6841 \cdot 10^{-4} \text{ m}^3$	$I_z = 8.5761 \cdot 10^{-7} \text{ m}^4$		
$W_{eff,y} = \min[W_{eff,y,c}, W_{eff,y,t}] = 1.6841 \cdot 10^{-4} \text{ m}^3$			

Applied loading on the joist at ULS

Maximum applied bending moment (at midspan) about the major axis y-y:

$$M_{y,ed} = 19.43 \text{ kNm}$$

Check of bending resistance at ULS

Design moment resistance of the cross-section for bending:

$$M_{c,Rd} = W_{eff,y} \cdot \frac{f_{y,b}}{\gamma_{M0}} = 58.94 \text{ kNm} \quad \text{EN1993-1-3 §6.1.4.1(1)}$$

Verification of bending resistance:

$$\frac{M_{y,ed}}{M_{c,Rd}} = 0.33 \quad \sqrt{0.33} \leq 1 \quad \text{OK} \quad \text{EN1993-1-1 §6.2.5(1)}$$

Check of shear resistance at ULS

Design to shear force

Maximum applied shear force

$$V_{Ed} = 34.23 \text{ kN} \approx 34.23 \text{ kN}$$

slope of the web relative to the flanges

$$\phi = 90^\circ$$

shear area

$$A_v = \frac{h_w \cdot t}{\sin(\phi)} = 1.4331 \cdot 10^{-3} \text{ m}^2$$

$$V_{pl,Rd} = \frac{A_v \cdot \left(\frac{f_{y,b}}{\sqrt{3}} \right)}{\gamma_{M0}} = 289.49 \text{ kN}$$

$$\text{EN1993-1-1 §6.2.6(2)}$$

Design shear buckling resistance

The relative slenderness λ_w for webs without longitudinal stiffeners:

$$\lambda_w = 0.346 \frac{h}{t} \sqrt{\frac{f_{y,b}}{E}} \leq 0.602$$

EN1993-1-3 §6.1.5

shear strength, considering buckling

$$f_{b,v} = \begin{cases} 0.58 f_{y,b} & \text{if } \lambda_w \leq 0.83 \\ 0.48 \frac{f_{y,b}}{\lambda_w} & \text{if } \lambda_w > 0.83 \end{cases} \quad f_{b,v} = 203 \text{ MPa}$$

$$V_{b,Rd} = A_v \frac{f_{b,v}}{\gamma_{M0}} = 290.82 \text{ kN}$$

Design shear resistance:

$$V_{c,Rd} = \min[V_{pl,Rd}, V_{b,Rd}] = 289.49 \text{ kN}$$

Verification of shear resistance

$$\frac{V_{Ed}}{V_{c,Rd}} = 0.12 \leq 1.0 \quad \text{OK}$$

EN1993-1-1 §6.2.6(1)

Check of local transverse resistance at ULS

Support reaction:

$$F_{ed} = 34.23 \text{ kN} \approx 34.23 \text{ kN}$$

To obtain the local transverse resistance of the web for a cross section with a single unstiffened web, the following criteria should be satisfied:

$$\frac{h_w}{t} = 42.586 \leq \frac{h_w}{t} \leq 200 \quad \text{OK}$$

EN1993-1-3 §6.1.7.2 (1)

$$\frac{r}{t} = 0.517 \leq \frac{r}{t} \leq 6 \quad \text{OK}$$

$$45^\circ \leq \alpha \leq 90^\circ \quad \text{OK}$$

The local transverse resistance of the web

bearing length $s_s = 200 \text{ mm}$

$$\frac{s_s}{t} = 34.483 \leq \frac{s_s}{t} \leq 60 \quad \text{OK}$$

EN1993-1-3
§6.1.7.2 (2)
Figure 6.7

$$k = \frac{f_{y,b}}{235 \text{ MPa}} = 1.535$$

EN1993-1-3 §6.1.7.2(3)

$$k_1 = 1.33 \leq k \leq 1.535 \quad \text{OK}$$

$$k_2 = 1.15 \leq k \leq 1.535 \quad \text{OK}$$

$$k_{2,v} = \begin{cases} 0.5 & \text{if } k_2 \leq 0.5 \\ k_2 & \text{if } 0.5 < k_2 \leq 1 \\ 1 & \text{if } k_2 > 1 \end{cases} \quad k_{2,v} = 1$$

$$k_3 = 0.7 + 0.3 \left(\frac{\phi}{90 \text{ deg}} \right)^2 \leq 1$$

For $s_s/t < 60$, the local transverse resistance of the web $R_{w,Rd}$ is:

$$R_{w,Rd} = \begin{cases} \frac{k_1 \cdot k_2 \cdot k_3 \cdot \left(5.92 + \frac{h_w}{132} \right) \cdot \left(1 + 0.01 \cdot \frac{s_s}{t} \right) \cdot t^2 \cdot f_{y,b}}{\gamma_{M1}} & \text{if } \frac{s_s}{t} \leq 60 \\ \frac{k_1 \cdot k_2 \cdot k_3 \cdot \left(5.92 + \frac{h_w}{132} \right) \cdot \left(0.71 + 0.015 \cdot \frac{s_s}{t} \right) \cdot t^2 \cdot f_{y,b}}{\gamma_{M1}} & \text{if } \frac{s_s}{t} > 60 \end{cases}$$

$$R_{w,Rd} = 72.979 \text{ kN}$$

Verification of local transverse force

$$F_{ed} \leq R_{w,Rd}$$

EN1993-1-3 §6.1.7.1(1)

$$\frac{F_{ed}}{R_{w,Rd}} \leq 0.5 \quad \sqrt{0.5} \leq \sqrt{OK}$$

ANNEX 4. The verification for the reversible serviceability.

It is important to check the comfort criteria of the construction for different scenario of the pedestrian loading (density). At least minimal comfort level should be guaranteed by the design.

The beam will be checked for two scenarios:

- A. Weak pedestrian traffic with the pedestrian density of 0.2 persons over m^2 . $n_A = 0.2 \cdot 22 \text{ m} \cdot 3.5 \text{ m} = 15.4$;
- B. Very dense pedestrian traffic (at the ceremony of the bridge opening, public events etc.) with the pedestrian density of 1.0 persons over m^2 . $n_B = 1.0 \cdot 22 \text{ m} \cdot 3.5 \text{ m} = 77$.

Comfort criteria are mentioned in Section 4.6.4.

1. Determination of the natural frequencies

$$f_{A \text{ vert}} = \frac{1}{2\pi} \cdot \frac{9.869}{L^2} \cdot \sqrt{\frac{E \cdot I_{\text{vert}}}{m}} = \frac{1}{2\pi} \cdot \frac{9.869}{(22 \text{ m})^2} \cdot \sqrt{\frac{5195 \text{ kN} \cdot \text{m}^2}{0.340 \frac{\text{t}}{\text{m}}}} = 0.401 \text{ Hz}$$

$$0.401 \text{ Hz} < 1.25 \text{ Hz} \quad \text{OK!}$$

$$f_{A \text{ lat}} = \frac{1}{2\pi} \cdot \frac{9.869}{L^2} \cdot \sqrt{\frac{E \cdot I_{\text{lat}}}{m}} = \frac{1}{2\pi} \cdot \frac{9.869}{(22 \text{ m})^2} \cdot \sqrt{\frac{37.38 \text{ kN} \cdot \text{m}^2}{0.340 \frac{\text{t}}{\text{m}}}} = 0.034 \text{ Hz}$$

$$0.034 \text{ Hz} < 0.5 \text{ Hz} \quad \text{OK!}$$

$$f_{B \text{ vert}} = \frac{1}{2\pi} \cdot \frac{39.478}{L^2} \cdot \sqrt{\frac{E \cdot I_{\text{vert}}}{m}} = \frac{1}{2\pi} \cdot \frac{39.478}{(22 \text{ m})^2} \cdot \sqrt{\frac{5195 \text{ kN} \cdot \text{m}^2}{0.340 \frac{\text{t}}{\text{m}}}} = 1.24 \text{ Hz}$$

$$1.24 \text{ Hz} < 1.25 \text{ Hz} \quad \text{OK!}$$

$$f_{B \text{ lat}} = \frac{1}{2\pi} \cdot \frac{39.478}{L^2} \cdot \sqrt{\frac{E \cdot I_{\text{lat}}}{m}} = \frac{1}{2\pi} \cdot \frac{39.478}{(22 \text{ m})^2} \cdot \sqrt{\frac{37.38 \text{ kN} \cdot \text{m}^2}{0.340 \frac{\text{t}}{\text{m}}}} = 0.136 \text{ Hz}$$

$$0.136 \text{ Hz} < 0.5 \text{ Hz} \quad \text{OK!}$$

The verification of the frequencies is OK. The frequencies are below the lower limit of the critical diapason.

2. Determination of the characteristic maximum accelerations

Using the data from References 31 and 32, we obtain the values of maximum accelerations for two scenarios of loading:

Case A

$$a_{A \max vert} = k_{a \ 95\%} \cdot \sqrt{\frac{C \cdot \sigma_F}{M_i^2} \cdot k_1 \cdot \zeta^{k_2}} = 2.278 \frac{m}{s^2}$$

$$a_{d \ vert} = \psi_1 \cdot a_{A \max vert} = 0.4 \cdot 2.278 = 0.911 \frac{m}{s^2}$$

with $C = 2.95$ $\sigma_F = 1.2 \cdot 10^{-4} \cdot 15.4 = 0.185 kN^2$ $k_{a \ 95\%} = 3.92$

$$k_1 = -0.08 \cdot 0.401^2 + 0.6 \cdot 0.401 + 0.075 = 0.3044 Hz^2$$

$$k_2 = 0.003 \cdot 0.401^2 - 0.04 \cdot 0.401 - 1.0 = -1.0156 Hz^2$$

$$a_{A \max lat} = k_{a \ 95\%} \cdot \sqrt{\frac{C \cdot \sigma_F}{M_i^2} \cdot k_1 \cdot \zeta^{k_2}} = 0.292 \frac{m}{s^2}$$

with $C = 6.8$ $\sigma_F = 2.85 \cdot 10^{-4} \cdot 15.4 = 4.389 \cdot 10^{-3} kN^2$ $k_{a \ 95\%} = 3.77$

$$k_1 = -0.08 \cdot 0.034^2 + 0.5 \cdot 0.034 + 0.085 = 0.102 Hz^2$$

$$k_2 = 0.005 \cdot 0.034^2 - 0.06 \cdot 0.034 - 1.005 = -1.007 Hz^2$$

Case B

$$a_{B \max vert} = k_{a \ 95\%} \cdot \sqrt{\frac{C \cdot \sigma_F}{M_i^2} \cdot k_1 \cdot \zeta^{k_2}} = 7.399 \frac{m}{s^2}$$

$$a_{B \ d \ vert} = \psi_1 \cdot a_{B \max vert} = 0.4 \cdot 6.807 = 2.96 \frac{m}{s^2}$$

with $C = 3.7$ $\sigma_F = 7 \cdot 10^{-3} \cdot 77 = 0.539 kN^2$ $k_{a \ 95\%} = 3.8$

$$k_1 = -0.07 \cdot 1.605^2 + 0.56 \cdot 1.605 + 0.084 = 0.802 Hz^2$$

$$k_2 = 0.004 \cdot 1.605^2 - 0.045 \cdot 1.605 - 1.0 = -1.062 Hz^2$$

$$a_{B \max lat} = k_{a \ 95\%} \cdot \sqrt{\frac{C \cdot \sigma_F}{M_i^2} \cdot k_1 \cdot \zeta^{k_2}} = 0.861 \frac{m}{s^2}$$

with $C = 7.9$ $\sigma_F = 2.85 \cdot 10^{-4} \cdot 77 = 0.022 kN^2$ $k_{a \ 95\%} = 3.73$

$$k_1 = -0.08 \cdot 0.136^2 + 0.44 \cdot 0.136 + 0.096 = 0.154 Hz^2$$

$$k_2 = 0.007 \cdot 0.136^2 - 0.071 \cdot 0.136 - 1.0 = -1.01 Hz^2$$

3. Analysis of the accelerations

Case	Vertical $a_{d\,vert}$	Comfort level			Lateral a_{lat}	Comfort level		
		Min	Med	Max		Min	Med	Max
A	0.911				0.292			
B	2.960	Light Discomfort			0.861	Light Discomfort		

From the table we observe the Medium comfort level guaranteed in both vertical and lateral directions for low density of pedestrians. The values of characteristic maximum accelerations are in the diapason of $[0.5 \dots 1.0 \text{ m/s}^2]$.

In Case B, when we expect high density of the people on the bridge the verification gives light discomfort level of accelerations due to not a big difference between the model accelerations and limits for:

- vertical acceleration $2.96 \frac{\text{m}}{\text{s}^2} > 2.5 \frac{\text{m}}{\text{s}^2}$
- lateral acceleration $0.861 \frac{\text{m}}{\text{s}^2} > 0.8 \frac{\text{m}}{\text{s}^2}$.

To control the vibration response. The non-compliance with required comfort limits implies the need to develop measures that improve the dynamic behavior of the footbridge. These measures include

- modification of the mass (using of heavier concrete deck slabs as an increasing of the modal mass),
- modification of frequency (in order to raise the frequency in both directions, applicable usually only at the design stage),
- modification of structural damping (additional damping devices such as tuned mass dampers, pendulum dampers, tuned liquid dampers etc.).